IOWA STATE UNIVERSITY
Digital Repository

1992

Fibercomposite and steel pavement dowels

Michael D. Albertson
Iowa State University

Recommended Citation

www.manaraa.com

Fibercomposite and steel pavement dowels

by

Michael D. Albertson

A Thesis Submitted to the

Graduate Faculty in Partial Fulfillment of the

Requirements for the Degree of

MASTER OF SCIENCE

Department: Civil and Construction Engineering
Major: Civil Engineering (Structural Engineering)

Iowa State University
Ames, Iowa
1992

TABLE OF CONTENTS

LIST OF FIGURES

LIST OF TABLES

SYMBOLS

A	cross-section area (in.^{2})
A_t	constant factor for general solution to differential Equation [1.1]
A_o	surface area for concrete shear cone failure (in.^{2})
B_t	constant factor for general solution to differential Equation [1.1]
b	width of the beam (in.)
C_t	constant factor for general solution to differential Equation [1.1]
c	distance to the extreme fiber from the centroidal axis of the member (in.)
con1	constant used to represent the solution for deflection of dowel
con2	constant used to represent the solution for deflection of dowel
con3	constant used to represent the solution for deflection of dowel
con4	constant used to represent the solution for deflection of dowel
con5	constant used to represent the solution for deflection of dowel
con6	constant used to represent the solution for deflection of dowel
D	diameter of the dowel (in.)

D_t constant factor for general solution to differential Equation [1.1]

D_{tors} diameter of bar used for torsion of a solid round bar shear test (in.)

E modulus of elasticity of the dowel bar (psi)

E_c modulus of elasticity for concrete (psi)

e base of Naperian logarithms

F form factor for shape of cross section

f maximum fiber stress (psi)

f_c peak load distribution value (psi)

f'_c compressive strength of the concrete (psi)

G shear modulus (psi)

h thickness of the concrete slab (in.)

I_z moment of inertia of beam about the z-axis of dowel bar (in.^{4})

k modulus of the foundation (psi)

k_o spring constant of elastic support (psi/in.)

k_r modulus of subgrade reaction (psi/in.)

L length of the dowel bar on one side of joint (in.)

L_{ASTM} length of short beam shear test specimen (in.)

L_{tors} length of bar used for torsion of a solid round bar shear test (in.)

L_r radius of relative stiffness (in.)

L_s shear span length (in.)

l_e dimension for concrete shear cone (in.)

M_b bending moment in the dowel at the face of the joint (lb-in.)

M_{max} maximum moment resistance of the dowel (lb-in.)

P concentrated load acting downward on the dowel at the center of the joint (lbs)

P_{ASTM} applied concentrated load for short beam shear test (lbs)

p peak load distribution value (psi)

Q Statical moment of area about neutral axis (in.^{3})

R radius of bar (in.)

T torque (lb-in.)

t width of the cross section (in.)

t_s shear stress (psi)

$t_{s\ max}$ maximum shear stress of dowel bar (psi)

V shear force on a cross section (lbs)

V_{max} ultimate shear capacity of dowel bar (lbs)

v_{cone} maximum shear cone stress (psi)

x distance along the dowel from the slab face at the joint (in.)

x_{pci}	dimension for concrete shear cone (in.)
y	deflection of the dowel (in.)
y_{pci}	dimension for concrete shear cone (in.)
Y_s	shear deflection (in.)
Z	width of joint (in.)
Z_c	maximum deflection for edge loadings (in.)
d^4y/dx^4	fourth derivative of the deflection of the dowel with respect to the position along the axis of the dowel
β	term used in the Timoshenko analysis method (in.$^{-1}$)
$\varnothing_{ACI}$	ACI strength reduction factor for bearing capacity
$\varnothing_{pci}$	PCI strength reduction factor for a shear cone
$\varnothing_{LRFD}$	LRFD strength reduction factor for bending
μ	Poisson's ratio for the concrete
$¥$	factor relating to the type of concrete used

1. INTRODUCTION

1.1. Needs for Alternative Concrete Reinforcement Materials

A considerable number of the nation's bridges, roads, parking structures and marine structures need repair or replacement because of deterioration resulting from the corrosion of the reinforcement. New construction methods and new materials are needed to protect the infrastructure so this type of deterioration can be avoided in the future. An obvious method of controlling the infrastructures' deterioration is by using materials that can extend their design lives by reducing or eliminating the corrosion of the reinforcement.

In the specific cases of bridges and highways, corrosion of the steel reinforcement used in concrete is a major cause of deterioration [1]. Epoxy-coated steel reinforcement was seen as the cure to this problem, but some reports of the performance of the epoxy-coated steel are less than encouraging [2]. Epoxy-coated steel reinforcement is not entirely corrosion resistant. This may be especially true when it is in a saltwater environment. This subject is not completely understood, but voids in the coverage of the epoxy on the reinforcement may be setting up a reaction between the exposed metal ions and the salt water. At the location of the void, corrosion would progress at a much faster rate than if the entire bar had not had an epoxy coating applied at all because of the cathode-

anode reaction being set up between the protected region of the bar and the uncovered area of the bar [3].

Epoxy-coated reinforcing steel can be expected to resist corrosion very effectively if no voids exist in the epoxy coating. Simply moving the bars to stock piles or stacking them on top of each other in the factories where the epoxy is applied can easily nick the coating. Additionally, construction workers commonly nick the coating in the placing of the steel reinforcement. Although careful handling of the bars and repairing of discovered nicks can reduce the number of nicks in the coating, nicks or pinholes cannot be entirely eliminated. A single nick is all that is needed to begin the corrosion process of a reinforcement bar. To expect that epoxy-coated steel bars are free of corrosion problems is not practical. To avoid corrosion of the reinforcement, a method other than epoxy coating should be used.

A logical choice is to use a material which is naturally resistant to the corrosive environments that it is placed in--thus eliminating the possibility of corrosion. Fibercomposites are a class of materials expected to be quite naturally corrosion resistant, and they may prove to be more corrosion resistant than epoxy-coated steel. Fibercomposites may degrade in wet and/or alkaline environments. Salty and/or acidic environments do not affect fibercomposite materials. Conversely, steel may corrode in salty and/or acidic environments. Steel and fibercomposite bars do

not degrade in a similar manner because they are not affected by the same types of corrosion agents.

1.2. Background on Fibercomposites

Fibercomposites are a class of materials composed of a combination of fibers and resin. Although there are many possible applications of fibercomposite materials, to date, most are of a specialty or exotic nature. Most of the applications for fibercomposites presently are in the aerospace and aeronautics industries. The space shuttles, stealth fighters and bombers, and the B-1 bomber are some of the aircraft made in part from fibercomposites [4]. Some other well-known applications for fibercomposites are car body panels, boats, tennis and racquetball rackets, and fishing poles [5].

Fibercomposites are made in many shapes and forms. Mats, resin combined with alternating angled layers of parallel fibers, are a common form of fibercomposites [6]. Rod stock, parallel fibers combined with a resin, are being researched as an alternative to steel reinforcement bars. In addition, W-shapes, channels, angles, square bars, round bars, and tubes are other commonly stocked cross sections carried by some manufacturers.

To date, the use of fibercomposites in structural applications is very limited. Unfamiliarity with the benefits of fibercomposites, a general lack of information on their design procedures, skepticism

associated with the use of a new material, and concerns over the behavior and failure methods of structures using these materials have kept most structural engineers from utilizing fibercomposite materials in their designs. However, research is currently being conducted at several universities that will aid in explaining the behavior of various structures utilizing fibercomposite materials [7, 8].

The research into fibercomposites is expanding, and as a result, technological advances resulting in better material properties are being developed rapidly [9]. More refined design procedures for structural applications of fibercomposite materials are expected to be developed in the near future. These factors will make fibercomposite materials more appealing to structural engineers.

Fibercomposites have some advantages in structural applications, as well as some disadvantages. Some of the advantageous characteristics of fibercomposite materials include:

1) High corrosion resistance,

2) High tensile strength,

3) High strength-to-weight ratio,

4) Good thermal insulation properties,

5) High electrical resistance properties, and

6) Architectural appearance easily controlled with the use of different colored resins.

Fibercomposite materials also have some significant disadvantages:

1) Low modulus of elasticity,

2) Brittle failures,

3) Material shape unalterable (bent) after initial manufacture,

4) Anisotropic material behavior,

5) Material's creep behavior unknown,

6) Poor bond characteristics compared to steel,

7) Generally poor fire resistance, and

8) Relatively low shear strengths.

Bars made of parallel fibers, instead of steel, have recently been used by some structural engineers as reinforcement in concrete. Fibercomposite concrete reinforcing bars generally have higher tensile strengths, much lower thermal and electrical conductivities, and lower weights than steel reinforcement bars [10].

The advantageous properties of the fibercomposites have sparked an interest in many areas of construction that could benefit by these characteristics. Higher corrosion, electrical and thermal resistance can benefit some types of structures.

Higher electrical resistance can be important in some instances. For example, some hospitals have equipment that is very sensitive to outside electrical currents. Currents can result in the building's steel reinforcement if large magnetic fields from the equipment exist around the reinforcement. Fibercomposite

reinforcement, on the other hand, has a much higher electrical resistance to these types of currents and may reduce them down to an acceptable level [11].

Fibercomposites' higher thermal resistance as compared to steel can also be an important factor. Concrete sandwich panels made from layers of concrete and insulation connected with fibercomposite ties instead of steel ties can significantly reduce thermal losses [12].

The higher corrosion resistance of fibercomposites as compared to steel is significant in pavement joint dowels, bridges, piers and other structures where corrosion of the reinforcement is a major problem. Many of these structures could benefit from the use of highly corrosion resistant fibercomposite reinforcing bars.

There are many other examples of structures that can benefit from the use of fibercomposites; the above examples are merely a few of the possible applications of this material.

1.3.   Experimental and Analytical Investigation

1.3.1.   Objective

The objective of the research project was to study the overall capacity and the load-deflection characteristics of specific fibercomposite and steel dowel systems. This objective was broken down into smaller tasks to explain the factors that contribute to the

behavior of dowels. The factors explained include material behavioral topics such as shear strength of fibercomposites, bearing strength of concrete, and shear cone strength of concrete. A dowel analysis method is also described in the following chapters. Finally, from the information learned, a new design procedure will be recommended for the dowel systems tested.

1.3.2. Scope

The scope of this research included the experimental testing of small, individual fibercomposite or steel dowels encased in concrete. For this research, a modified theoretical approach was used. The approach was developed based upon the Timoshenko theoretical model and the actual performance of these specimens.

Ten dowel specimens were tested. Five of the specimens had 1.25-inch fibercomposite dowels; the other five specimens had 1.5-inch steel dowels. The dowels' load-deflection characteristics, maximum load, failure modes, and associated behavior were determined by testing the specimens in shear.

1.4. Literature Review

The literature review for the pavement dowel portion of this research program was divided into several subtopics: analysis of dowels, shear capacity and testing methods for fibercomposites,

bearing capacity of concrete, and pavement dowel testing programs. Because the literature review of shear capacity and its testing methods is so extensive, it is not presented in this section, but rather the literature review of shear capacity is presented in Section 2.4.2.

1.4.1. Analysis of dowels

Five different analysis methods for pavement dowels were investigated. Four of these methods were theoretical, and one was empirical in nature. The four theoretical methods were originally developed by Timoshenko [13], Bradbury [14], Friberg [15], and Westergaard [16]. The theory developed by Timoshenko was determined to be the most logical approach to the analysis of the pavement dowels. The empirical approach was developed [1] for the Federal Highway Administration at the University of Illinois, Urbana-Champaign.

1.4.1.1. Timoshenko's theoretical model

The Timoshenko method of doweled joint analysis is explained in Part 2, Chapter 1 of his Strength of Materials textbook [13]. This chapter analyzes a prismatic beam supported by a continuous elastic foundation [13]. The Timoshenko method assumes that reaction at a point is directly proportional to the deflection at that point [13]. A constant, k_0, is the reaction per area per unit of deflection [13]. The

pressure per unit length may be expressed as $bk_o y$, where b is the width of the beam and y is the deflection of the dowel. The value of bk_o is set equal to k, which is the modulus of the foundation reaction. By definition, k is the reaction per unit length with a deflection of unity [13]. Thus, by definition, the load existing at a point is the deflection of that point multiplied by the modulus of the foundation reaction. This relationship for the load is then set equal to the general differential equation for load and solved [13]. The differential equation is [13]:

$$EI_z d^4 y/dx^4 = -ky \qquad (1.1)$$

where:

E = Modulus of elasticity of the dowel bar (psi)

I_z = Moment of inertia of beam about the z-axis (in.^{4})

$d^4 y/dx^4$ = Fourth derivative of the deflection of the dowel with respect to the position along the axis of the dowel

k = Modulus of the foundation (psi)

y = Deflection of the dowel (in.)

The term ß is then used to simplify the solution [13]:

$$\beta = \sqrt[4]{(k/4EI_z)}$$ (1.2)

where:

ß = Term used in Timoshenko analysis method (in.$^{-1}$)

The resulting general solution to the differential equation is [13]:

$$y = e^{\beta x}(A_t\cos\beta x + B_t\sin\beta x) + e^{-\beta x}(C_t\cos\beta x + D_t\sin\beta x)$$ (1.3)

where:

e = Base of Naperian logarithms

A_t, B_t, C_t, D_t = Constant factors for general solution to differential Equation [1.1]

To determine the constants $A_t, B_t, C_t,$ and D_t, boundary conditions are enforced [13]. The boundary conditions for a semi-infinitely long beam analysis approach include the following [13]:

1) The deflection approaches zero as the distance from the face of the joint approaches infinity,

2) The bending moment approaches zero as the distance from the face of the joint approaches infinity,

3) The bending moment at the face of the joint equals $-M_0$, and

4) The shear at the face of the joint equals -P.

Enforcing these boundary conditions and substituting them into the original solution to the differential equation and then simplifying results in [13]:

$$y = \frac{e^{-\beta x}(P\cos\beta x - \beta M_0(\cos\beta x - \sin\beta x))}{2\beta^3 EI_z} \qquad (1.4)$$

where:

x = Distance along the dowel from the slab face at the joint (in.)

P = Concentrated load acting downward on the dowel at the center of the joint (lbs)

M_0 = Bending moment in the dowel at the face of the joint (lb-in.)

After determining the four constants, the equations for the slope, moment, shear, and load can be determined by taking successive derivatives. The relationship between the load and the distance from the face of the joint is a sinusoidal wave function of

rapidly diminishing amplitude. According to the graph of this function, only the first cycle of the sinusoidal wave functions representing the transferring of the load from the dowel to the concrete is significant. This was the same conclusion that Bradbury made [14]. To illustrate the Timoshenko beam on an elastic foundation analysis method, Figures 1.1 through 1.4 show the load, moment, shear, and deflection diagrams for a 1.5-inch diameter steel specimen of average stiffness (which will be explained later in Section 3.4.2) for a 10,000-pound load.

The value that should be used for the modulus of subgrade reaction for specific situations, k, is not known. Throughout this analysis method, the development of the theory is straightforward, but information on how to apply the theory to actual situations is not given. The accuracy of the analysis method depends on how accurately k is known. Figure 1.5 illustrates the relationship of the deflection to the value of k assumed.

The Timoshenko model approach used in this research was a semi-infinitely long beam on an elastic foundation. Section 3.5 determines that for this solution to be accurate, the beam length multiplied by ß must be greater than 2. This value is determined in Section 3.5. For this research program, this was always true, as will be shown later. Significant modifications must be made to the theory to account for beams with ßL less than 2. These
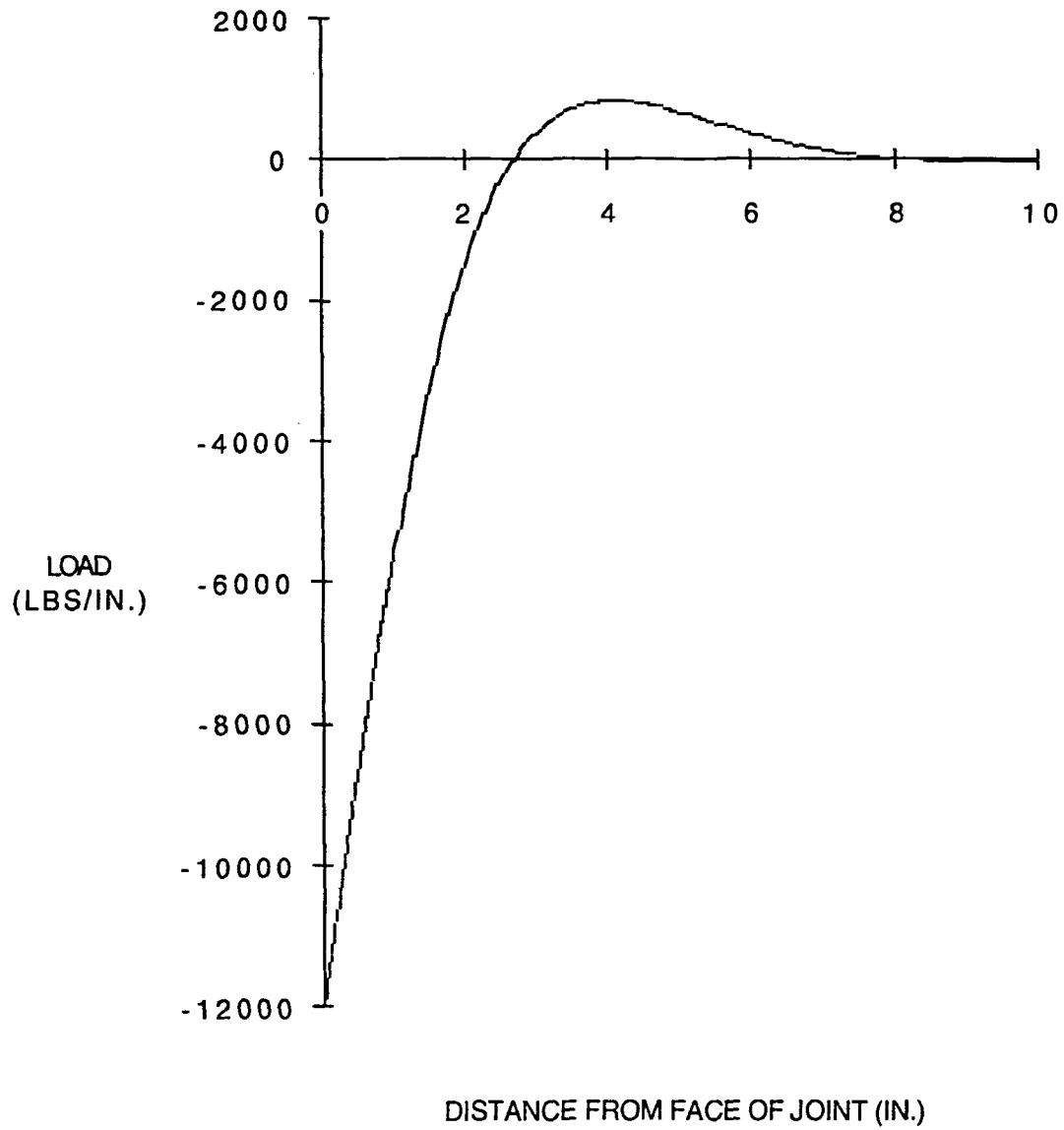
Figure 1.1. Load diagram for 1.50-inch steel dowel of average
stiffness using the Timoshenko analysis method
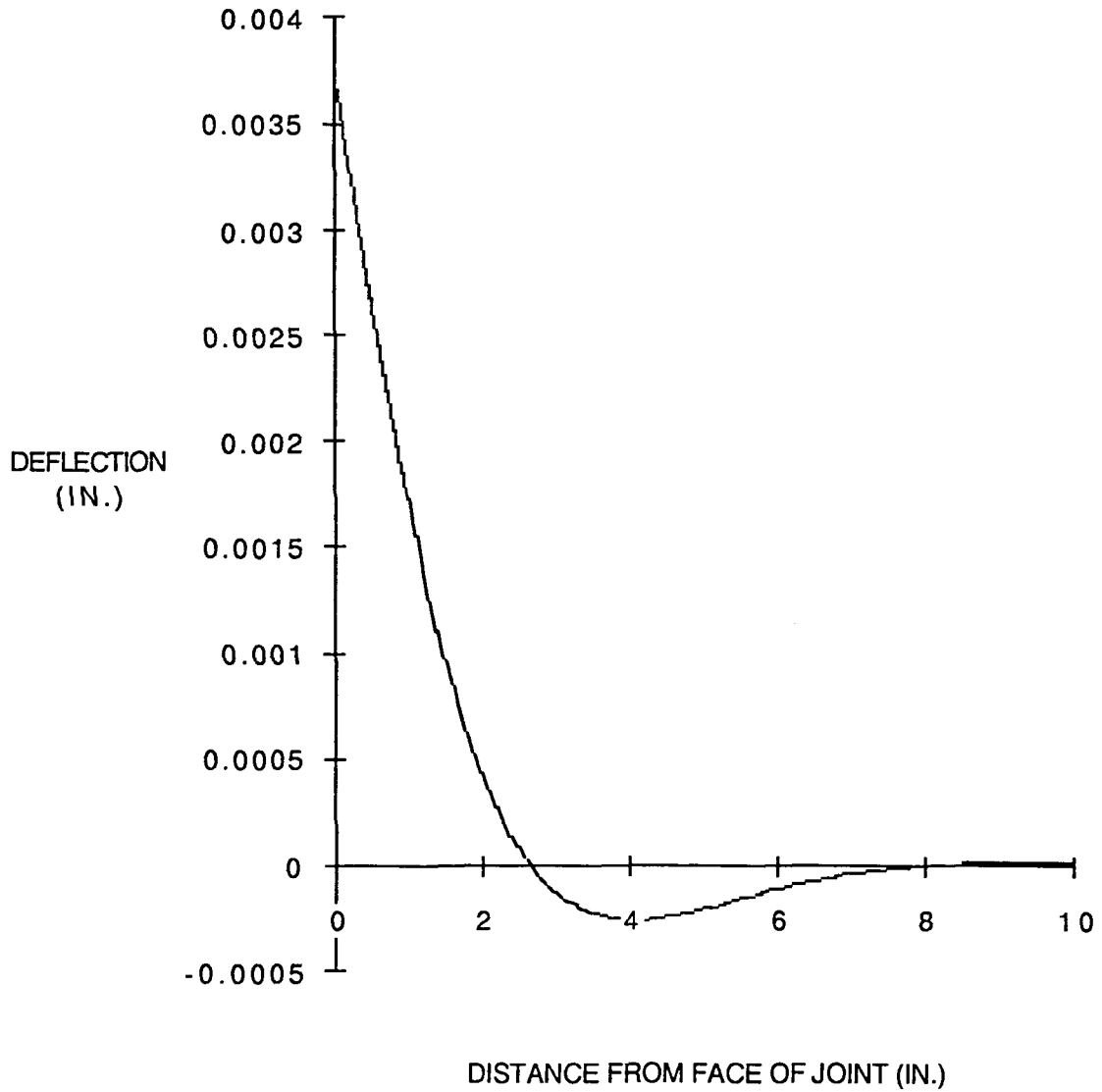
Figure 1.2. Deflection diagram for 1.50-inch steel dowel of average
stiffness using the Timoshenko analysis method
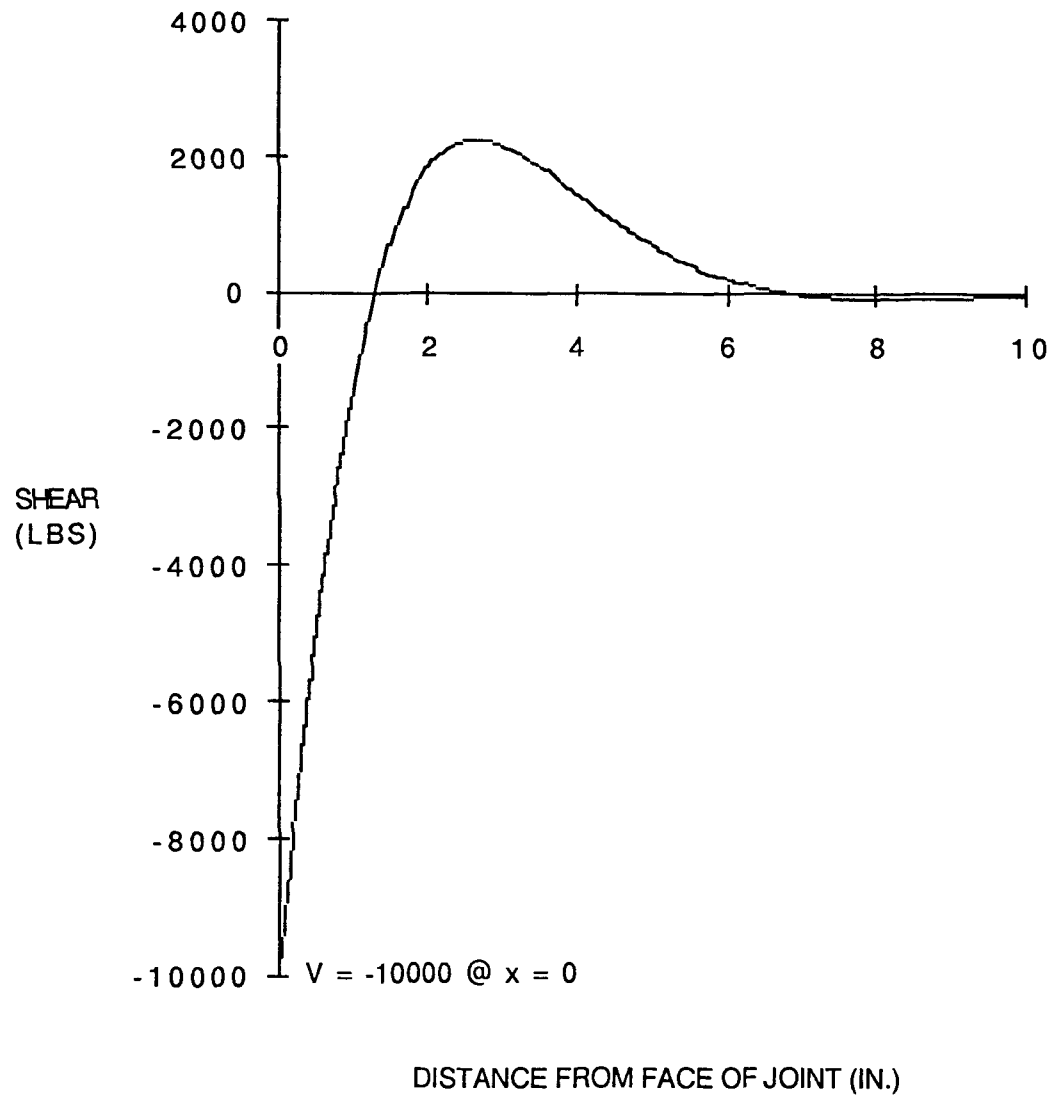
Figure 1.3. Shear diagram for 1.50-inch steel dowel of average stiffness using the Timoshenko analysis method
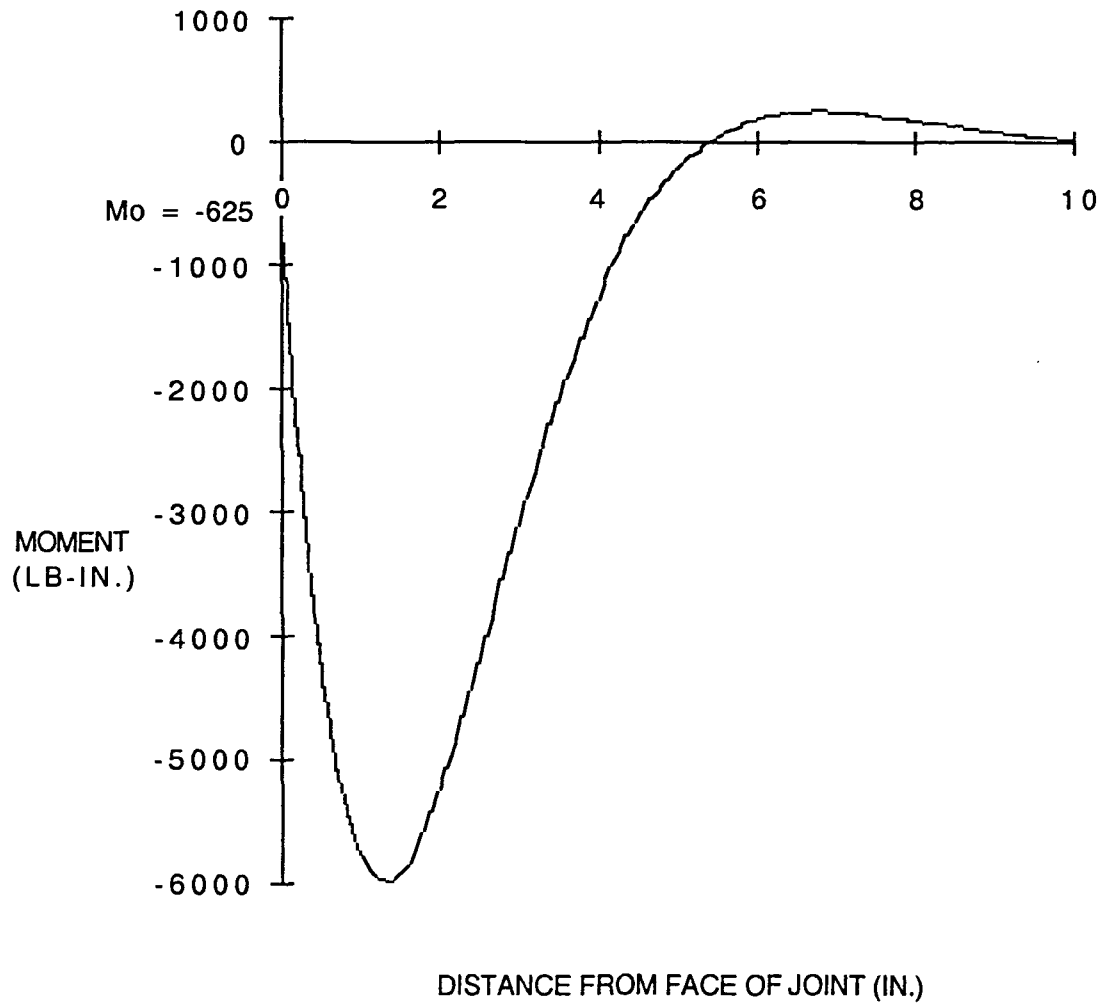
Figure 1.4. Moment diagram for 1.50-inch steel dowel of average stiffness using the Timoshenko analysis method
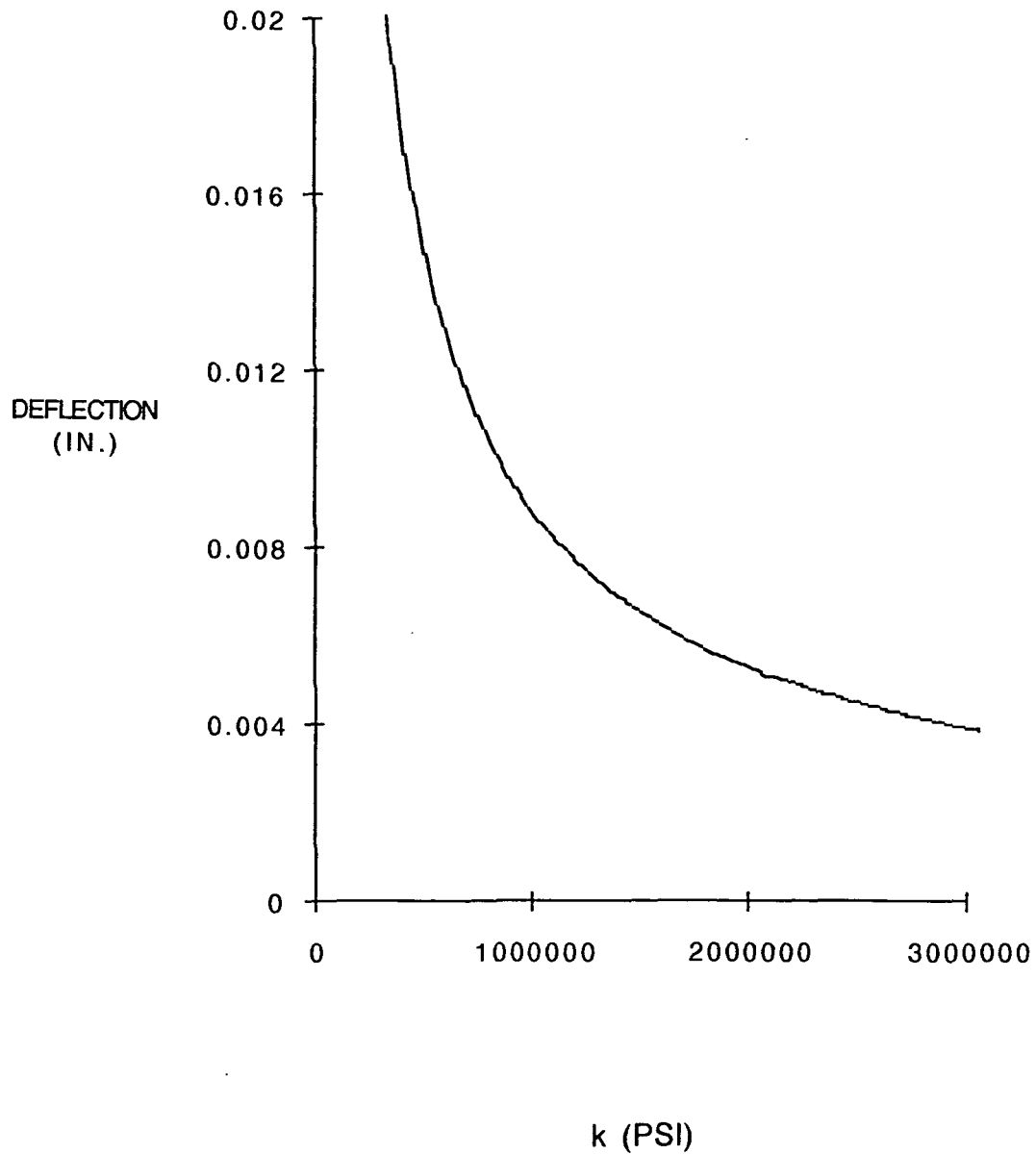
Figure 1.5. Deflection at the face of the joint versus k value for a 1.50-inch steel dowel using the Timoshenko analysis method

modifications result in equations that are significantly more complex.

1.4.1.2. Bradbury's theoretical model

In his 1932 book entitled <u>Design of Joints in Concrete Pavements</u> [14], R. D. Bradbury presented an approach to the determination of loads, shear, and moment in a doweled pavement joint. The approach used to analyze the dowel is the previously described Timoshenko method with a few modifications [14]. Bradbury gave the following reasons for the modifications to the Timoshenko analysis: A finite length bar rather than infinite length exists [14], and the modulus of foundation reaction for concrete-- being a function of the dowel flexural stiffness and the concrete bearing stiffness--cannot be easily determined [14].

To account for a bar of finite rather that infinite length, Bradbury assumes that the length of the bar covered by the first full cycle of positive and negative pressure on each side of the joint is assumed to be half of the length of the total dowel bar length [14]. The distribution of the load along the length of the dowel is based upon the distribution of force as determined by the Timoshenko model [14]. The load distribution is simplified, however, into a series of linear loads. The values of the peaks of the loads are a function of the length of the bar, the value of the force being transferred across the joint, the diameter of the bar, and the width

of the joint [14]. Figure 1.6 shows the assumed load distribution on the dowel.

The Bradbury method was not applied to the analysis of the dowels because the assumptions that Bradbury made in simplifying the Timoshenko analysis method are not known.

1.4.1.3.   Friberg's theoretical model

The Friberg pavement dowel analysis method is a simplified version of the Timoshenko model [15]. Five variables are included in the model: the load, the diameter of the dowel, the modulus of elasticity of the dowel, the relative flexural stiffness of the dowel compared to the surrounding concrete bearing stiffness, and the width of the joint [15]. Again, with this method as with the Timoshenko method, a term relating the relative flexural stiffness of the dowel compared to the bearing stiffness of the surrounding concrete is required.

The Friberg method was not used in this research project as an analysis method for accurately describing the behavior of the doweled joint system because the model was developed primarily for expansion joints where the width of the joint may be significant. Current design practices use contraction joints where the width of the joint is minimal.
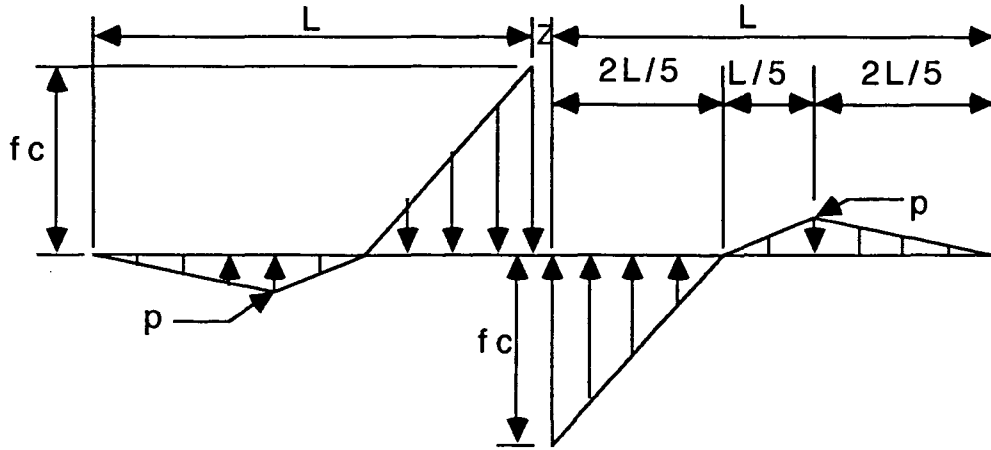
$$p = \frac{5P(L/2 + 7.5Z)}{3(L/2)^2 D}$$

where:

$$fc = \frac{25P(L/2 + 1.5Z)}{2(L/2)^2 D}$$

fc	=	Peak load distribution value (psi)
p	=	Peak load distribution value (psi)
P	=	Concentrate load acting downward on the center of the joint (lbs)
L	=	Length of dowel bar on one side of joint(in.)
Z	=	Width of joint (in.)
D	=	Diameter of dowel (in.)

Figure 1.6 Bradbury assumed load distribution on dowel bar

1.4.1.4.   Westergaard's theoretical model

The Westergaard analysis method requires the use of a term that is a measure of the stiffness of the subgrade [16]. An important development from the Westergaard analysis method was a term that determines how dowels adjacent to the concentrated load work together.

The following equations were given by Westergaard for the deflection of the interior portion of a slab at the face of the joint [16] :

$$Z_c = \frac{P}{8k_r L_r^2} \qquad (1.6)$$

where:

$$L_r = \frac{\sqrt[4]{E_c h^3}}{\sqrt[4]{12(1-\mu^2)k_r}} \qquad (1.7)$$

Z_c = Maximum deflection for edge loadings (in.)

L_r = Radius of relative stiffness (in.)

E_c = Modulus of elasticity for concrete (psi)

h = Thickness of the concrete slab (in.)

μ = Poisson's ratio for the concrete

k_r = Modulus of subgrade reaction (psi/in.)

P = Concentrated load acting downward on the dowel at the center of the joint (lbs)

The Westergaard method was not used in this research project as an analysis method that describes the behavior of the doweled joint system. There are several reasons for this decision, but the most important reason was that the assumptions made in developing the analysis method are not known. Therefore, the validity of applying this analysis method to the materials currently used is unknown.

1.4.1.5. Rehabilitation of concrete pavements FHWA-RD-88-071

The Federal Highway Administration sponsored a comprehensive research program at the University of Illinois Urbana-Champaign in the late 1980s [1]. Because this project was being performed to improve the methods for evaluating and repairing concrete pavements, the research encompassed field, laboratory and analytical studies [1]. This project's general procedure was to conduct very extensive surveys of actual field pavement conditions [1]. These surveys were combined with original design information and a history of loading to arrive at broad conclusions on pavement designs and suggestions to improve future designs and constructions of concrete pavements [1].

The performance of individual dowels was evaluated on a visual site inspection basis [1]. However, the dowels were located at the center of the pavement, and if the dowels had failed, the researchers would not have been able to directly identify the failure.

Only through the occurrence of related failure modes in the vicinity of the dowel would the failure have been detectable.

For the FHWA research, 515 round dowel bars were inspected in various locations around the United States [1]. Of these dowels, 98 percent were considered to be in good condition [1]. The average faulting (deflection) of the joints was 0.04 in. [1]. Other configurations of shear transfer devices were also inspected [1]. The FHWA researchers developed the following data about the percentage of transfer devices that were in good condition: double-vee shear, 72 percent; figure eight, 75 percent; and I-beam, 99 percent [1]. The I-beam shear had an average faulting distance of 0.13 inch, which is the maximum faulting distance for a joint [1]. At this amount of faulting, the rideability of the pavement was affected significantly [1]. As the faulting distance of a pavement joint was reduced, the pavement's potential for pumping, faulting, spalling, and cracking was greatly reduced, extending the life of the pavement [1].

The research conducted at the University of Illinois also developed an empirical relationship, which takes into account many variables, for the deflection of a doweled joint [1]. Accumulated equivalent 18-kip single axle loads, the age of the pavement, the presence of drainage, the material that the subbase and base was made from, the number of degree days below freezing, the thickness of the concrete slab, the presence of concrete shoulders, the spacing of contraction joints, and the type of dowel device used were all

included in their empirical statistical analysis [1]. This analysis method accounts for many conditions that affect the performance of the dowel.

Dowels in new jointed pavements often lose some of their effectiveness after a period of service [1]. This loss of effectiveness can be the result of any of several causes, including: poor consolidation of concrete, the effects of dowel/concrete bearing fatigue, or mechanical failure of the dowel caused by corrosion [1].

During the University of Illinois research, the deflection of the dowel decreased significantly as the diameter was increased from 1 to 1.5 inches [1]. A large reduction in dowel looseness as well as a large reduction in the additional deflection in the dowels caused by the oblonging of the holes surrounding them as a result of repeated loading occurred when the dowel diameter was increased from 1 inch to 1.5 inches [1]. For these reasons, the FHWA research report suggests that 1.5-inch diameter dowels be used in transverse joints, and that the effect of reduced faulting more than justifies the increase in cost for a larger dowel [1].

1.4.2. Bearing capacity of concrete

One of the most common failure modes for pavement dowel systems is a bearing failure of the concrete immediately above or below the dowel, adjacent to the face of the joint [15]. If steel

dowels with relatively large diameters (greater than 1 inch) are used, as is common practice, the limiting factor in the capacity of the joint is usually the bearing capacity of the concrete [17]. Because failures of dowel systems are usually bearing failures of concrete, a thorough literature review of the bearing capacity of concrete was made.

Many different theories for bearing failure of concrete exist, and the different approaches to the bearing strength of concrete have different results.

Research attempting to determine the bearing capacity of concrete concluded that, for the situations tested, the bearing capacity of the concrete is a function of the ratio of the concrete supporting area to the loading area, the ratio of the height to the width of the specimen, and the compressive strength of the concrete (cylinder strength) [18-22]. In all cases the load was applied in a uniform matter over either a square or circular area [18-22]. No research was found on what effects a varying load on the concrete has on the bearing capacity of the concrete.

In a bearing capacity type of failure, an inverted pyramid in the concrete occurs under the load [23]. This inverted pyramid acts as a wedge and eventually splits the concrete much in the same way that a wedge can split a log of wood, see Figure 1.7. The load at which failure occurs may be estimated with the internal friction theory of failure [21], but this would result in complex, cumbersome calculations beyond the scope of this research program at Iowa

State University. Instead of estimating the bearing capacity of the concrete through the use of the internal friction theory, the bearing capacity was estimated with factors relating the ratio of the maximum bearing stress to the cylinder strength to the ratio of the concrete area to the loading area. The width of the specimens was 10 inches in all cases, and the diameters of the bars were 1.5 inches and 1.25 inches.

1.4.3.   Shear cone development for concrete

Doweled pavement joints may experience a shear cone failure of the concrete above or below the dowel. A shear cone failure occurs when the shear stress on the surface area of the cone exceeds the maximum allowable shear stress [24]. The PCI Design Handbook describes the behavior of shear cones and gives a procedure for determining the design strength based upon shear cone failure. The remainder of this section is based upon information presented in the PCI Design Handbook [24].

The shear cone failure surface is assumed to be that of a 45° truncated cone for cases where no free edges are near the pullout cones [24]. For cases where free edges intersect the 45° truncated cone, the failure surface becomes more complex. The surface area for a pullout cone with one free edge as well as definitions for the x_{pci}, y_{pci}, l_e dimensions are shown in Figure 1.8. The equation for the surface area is [24]:
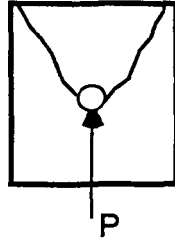
Figure 1.7. Bearing failure wedge
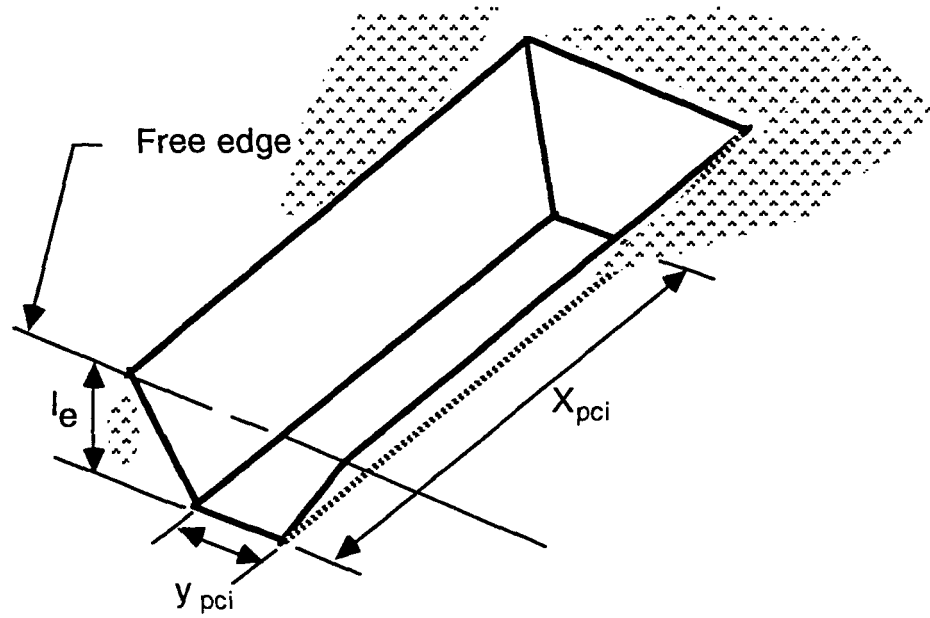
x_{pci}, y_{pci}, l_e = Dimensions for concrete shear cone

Note: All assumed failure surfaces are taken
to that of a 45° plane to the bearing surface

Figure 1.8. Surface area for a pullout cone with one free edge

$$A_o = \sqrt{2}(x_{pci}y_{pci} + l_e(2x_{pci} + y_{pci}) + 2l_e^2) \qquad (1.8)$$

where:

A_o = Surface area for concrete shear cone failure (in.^{2})

x_{pci}, y_{pci}, l_e = Dimensions for concrete shear cone as shown in Figure 1.8 (in.)

The surface area defined by Equation 1.8 includes the bottom surface of the truncated pyramid defined by the dimensions x_{pci} by y_{pci}. For the pavement dowel situation, the bottom surface of the truncated pyramid is occupied by the dowel. Therefore, the equation for the surface area of the shear cone must have the $x_{pci}y_{pci}$ term, representing the bottom of the truncated pyramid, removed. The resulting equation for the area of the shear cone is:

$$A_o = \sqrt{2}(l_e(2x_{pci} + y_{pci}) + 2l_e^2) \qquad (1.9)$$

The stress at which failure will occur is given as a function of the compressive strength of the concrete [24]. The maximum shear cone stress for a sloped face of a shear cone is given as [24]:

$$v_{cone} = 2.8 \sqrt{f_c'} \qquad (1.10)$$

where:

v_{cone} = Maximum shear cone stress (psi)

¥ = Factor relating to the type of concrete used (normal weight, sand-lightweight, all lightweight)

f'_c = Compressive strength of the concrete (psi)

The total capacity as governed by the shear cone capacity of the concrete is then the maximum stress times the surface area. This is given as:

$$P = A_o (2.8¥\sqrt{f'_c}) \qquad (1.11)$$

For the case of one free edge, the resulting equation is [24]:

$$P = \sqrt{2}(l_e(2x_{pci}+y_{pci}) + 2l_e^2)(2.8¥\sqrt{f'_c}) \qquad (1.12)$$

2.   MATERIALS

2.1.   Introduction

Fibercomposite materials were originally developed for NASA and the Department of Defense [4], who are interested in the material's high strength, high resilience, and lightweight [4].   The strength-to-weight ratios of many fibercomposite materials far surpass the strength-to-weight ratios of many metals [5].   This makes fibercomposites ideal for applications in aerospace and aeronautics where the overall weight of the structure is critical.

The fibercomposites used widely in the aerospace industry are composed of graphite fibers laid in layers of changing fiber orientations.   The F-117 stealth fighter/bombers and the B-2 long-range bombers--the state of the art in military aircraft--are primarily made of a shell of fibercomposite mats [25].

In the past, technology developed for military and space applications has been slowly transferred to the public domain.   If this trend continues, fibercomposites may become the material of the future for a wide range of applications.

Already some exotic applications for fibercomposite materials are developing.   Upscale sporting goods manufacturers are using fibercomposite materials for the construction of high-performance golf club shafts, tennis rackets, and bicycle frames.   In yachting, carbon fibercomposite mats--despite their cost of over $70 per

pound--are being used in the construction of some of the world's fastest yachts [25]. One of the most promising future uses of fibercomposites is in the automotive market where applications varying from drive shafts to body panels are already being developed and used [4].

The use of fibercomposite materials in civil engineering applications is presently extremely limited. When designers use fibercomposites, they usually are taking advantage of the material's high corrosion resistance (wastewater treatment plants, chemical plants), nonelectrical conductance properties (x-ray or imaging portions of hospitals), or low thermal conductivity (ties connecting wythes together in sandwich construction). These applications, important as they may be, represent only a small portion of the present construction in civil engineering. Future uses of fibercomposite materials could include any application in which steel is currently used, because fibercomposite materials can be formed into any shape that steel can be formed into. The limits to the applications of fibercomposite material lie in the material's properties and costs, as well as in the ability and willingness of structural engineers to use it.

Fibercomposite bars made of parallel fibers have recently become of interest to structural engineers. These bars can be used in place of steel as concrete reinforcement [26]. In comparison to steel, fibercomposites generally have higher tensile strengths, considerably higher resistance to corrosion, lower thermal and

electrical conductivities, and a much lighter weight [26]. Some of these properties, which could prove advantageous to many areas of construction, have drawn the industry's attention to fibercomposites. For example, fibercomposite bars, because of their corrosion resistance, may be an attractive solution for bridges, roads, parking structures and marine structures where corrosion of reinforcement steel is a major problem.

2.2. Engineering Properties

In the forming of fibercomposite bars, a low-strength resin is used to bind the long, high-strength filamentary fibers together in a parallel orientation. A large variation in the magnitude of material properties of fibercomposite bars occurs in different directions relative to the direction of the fibers. When compared to steel, fibercomposite bars can be expected to have higher tensile strengths, lower shear strengths, and much lower moduli of elasticity.

Fibercomposites are an anisotropic material. Anisotropic materials have different properties in different directions. Conversely, steel is nearly an isotropic material.

Many classical structural theory methods and relationships in mechanics of materials deal only with isotropic materials. Deviation from the isotropic behavior of materials requires that an exact theory include anisotropic material behavior. Some of the

major assumptions of "classical" methods are not met with the fibercomposite material. Examples of how assumptions made in the classical analysis of isotropic materials are violated with anisotropic materials include: some fibercomposite materials do not follow a linear stress versus strain relationship, plastic behavior does not exist in fibercomposites, and shear properties of anisotropic materials vary depending upon the direction of the shear relative to the direction of the fibers. Applying classical analysis methods while using anisotropic materials is at best an approximation. Because of the mathematical complexity of the analysis methods for anisotropic material behavior, classical theory methods were used throughout this research. For more information on anisotropic material behavior, refer to Ref. 27 [a general theory of strength for anisotropic materials].

The fibers give the fibercomposite materials high tensile strengths in the direction(s) that the fibers are placed [6]. If confined properly, the fibers provide the compressive strength of the fibercomposite material. The resin's primary uses are to resist shear forces, to transfer the stresses to the fibers, to protect the fibers, and to serve as a bracing material for small fibers.

Resins can be subdivided into two broad categories: thermosetting and thermoplastic. A thermosetting resin, once cured, will not soften upon the application of moderate heating [29]. Conversely, a thermoplastic resin will soften with the application of moderate heating [29]. To date, the resins used in structural

designs are all thermosetting resins such as polyester, vinyl ester and epoxy.

2.3.   Glass-fibercomposites

Fibercomposite bars are made of long, parallel glass fibers encapsulated with a resin. Presently, the resins most often utilized are either vinyl ester or polyester. Two different manufacturing methods often are used to produce fibercomposite bars--pultrusion and hand lay up. Pultrusion is a process in which glass fibers are taken off spools, combined with a resin, and then pulled through a heated die with the desired cross section [6]. Hand lay up is a manufacturing method in which glass fibers are laid out, coated with resin, and then hand rolled into the desired shape [26]. Both of these manufacturing methods can result in similar percentages of glass fibers in the bars [26, 6]. Percentage of glass fibers can be defined as the ratio, expressed in percent, of the volume or mass of glass fibers in a cross section of the bar to the total area of the cross section or total mass of the bar. The percentage of glass fibers is generally limited by the capability of the manufacturing process [6]. The higher the glass percentage is, the more difficult the manufacturing process is for that bar [6]. As the diameter of a bar increases, more resin must be added to the bar during the manufacturing process to arrive at a quality product. Therefore, as the diameter of the bar increases, the resin percentage also

increases, resulting in a lower percentage of glass. Typical glass fiber percentages range from 60 to 80 percent by volume, depending upon the diameter of the bars [6].

A limiting factor in the use of fibercomposite bars for concrete reinforcement is that presently fibercomposite bar manufacturers do not offer curved bars with thermosetting resins. These bars cannot be field bent and can only be used as straight reinforcement. Yet, in most construction projects where reinforced concrete is being used, straight, curved, and bent bars are needed. As a result, in order to use fibercomposite reinforcement currently, some steel reinforcement will also have to be used for the bent and curved bar applications. However, to benefit from the use of fibercomposite reinforcement, builders must use it exclusively throughout the structure. Protecting a structure from corrosion in most but not all areas leaves a weak link in the chain. If fiberglass is not used exclusively, the structure may be little more protected from corrosion-related problems than if steel was used throughout.

2.4. Mechanical Properties of Glass-fibercomposites

2.4.1. Tension

Fibercomposites, in general, have high tensile strengths in the direction of the fibers, commonly over 120 ksi, low shear strengths in all directions, and low bearing capacities in directions

perpendicular to the direction of the fibers. This unique combination of properties makes tensile testing by conventional methods with relatively short, high-pressure wedge grips impossible. When a fibercomposite bar is placed in the wedge grips, the pressure exerted by the grips easily crushes the fibercomposite bars. To successfully complete a tension test to failure of a fibercomposite bar, the load from the testing machine must be distributed over a greater area than the same size steel bar would require. The method used at Iowa State University was developed in prior research [28]. This method involves encasing the fibercomposite bar in epoxy inside of a copper tube--a copper tube much longer (12 inches) than the wedge grips of the tensile machine (4 inches) has been the most effective [28]. The epoxy between the copper tube and the fibercomposite bar distributes the load over the longer area [28]. By increasing the length to transfer the testing load, a tensile failure of the fibercomposite bar was observed in the center section of the tensile test specimen [28].

2.4.2. Shear

2.4.2.1. Shear test methods

2.4.2.1.1. Short beam test   The short beam shear test involves a short beam specimen supported at two points on the ends of the beam and a concentrated load applied at the center

specimen [29]. Figure 2.1 illustrates the short beam shear test geometry. The shear stress distribution across the cross section can be determined with the elementary beam theory equation:

$$\text{shear stress} = \frac{VQ}{I_z t} \tag{2.1}$$

where:

V = Shear force on a cross section (lbs)

Q = Statical moment of area about neutral axis (in.^{3})

t = Width of the cross section (in.)

I_z = Moment of inertia of beam about the z-axis (in.^{4})

The short beam test can be set up very easily, and as a result, this test method is often used to determine the shear strength of fibercomposites [29]. The short beam test, when used to test unidirectional fibercomposite materials, commonly does not produce interlaminar shear failures [29]. Often the failures of the specimens are associated with stress concentrations caused by the combination of the concentrated load at the center and the concentrated reaction points at the ends of the short beam [29]. These three point loads each cause stress concentrations around them, and the combination of three point loads in one very short beam causes significant stress concentration effects throughout the

$$P_{ASTM}$$

Specimen ——

—— 6.35 mm dia dowel

3.2 mm dia dowel

Span length

$$P_{ASTM}/2 \qquad L_{ASTM} \qquad P_{ASTM}/2$$

Horizontal shear load diagram
(flat laminate)
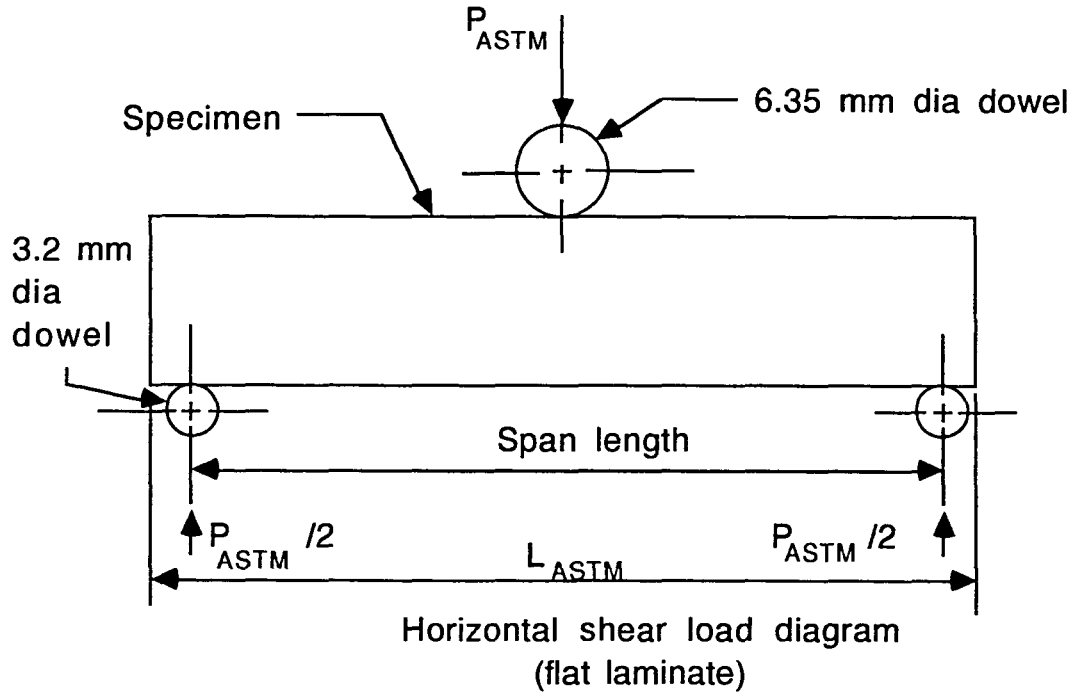
L_{ASTM} = Length of short beam shear test specimen (in.)
P_{ASTM} = Applied concentrated load for short beam shear test (lbs)

American Society for Testing and Materials (ASTM)
Recommended Ratio of Support Span to Thickness
and Ratio of Specimen Length to Thickness

Reinforcements	Span/Thickness	Length/Thickness
Glass fibers	4	7
Graphite fibers	4	6
Carbon fibers	4	6
Steel fibers	4	6

Figure 2.1. Short beam shear test geometry and specifications (ASTM) [30]

entire beam, questioning the validity of the test [29]. Many researchers have studied the stress distributions in an anisotropic short beam specimen using a finite element analysis technique [29]. The results from the finite element analysis, verified with photomicrographs of experimental tests, show that stress concentrations (with resulting maximum stresses on the top fibers up to three times the maximum shear stress on the centerline of the specimen) often can affect the results of the short beam test and that inaccurate results commonly occur while using this test procedure [29]. These findings, as well as the results from the photomicrographs for the fibercomposite specimens, conclude that the short beam test is not an accurate measure of the shear strength of fibercomposite materials because of the stress concentrations that are occurring throughout the beam specimen [29].

2.4.2.1.2. Torsion of a solid round bar

The torsion of a solid round bar involves a round bar with a torque applied to one end while the other end is torsionally simply supported. Figure 2.2 illustrates the torsion of a solid round bar. A simple equation can be used to determine the shear stress occurring on the surface of the round bar:

$$\text{shear stress}_{(maximum)} = \frac{2T}{\pi R^3} \qquad (2.2)$$

Figure 2.2. Illustration of the torsion of a solid round bar shear test
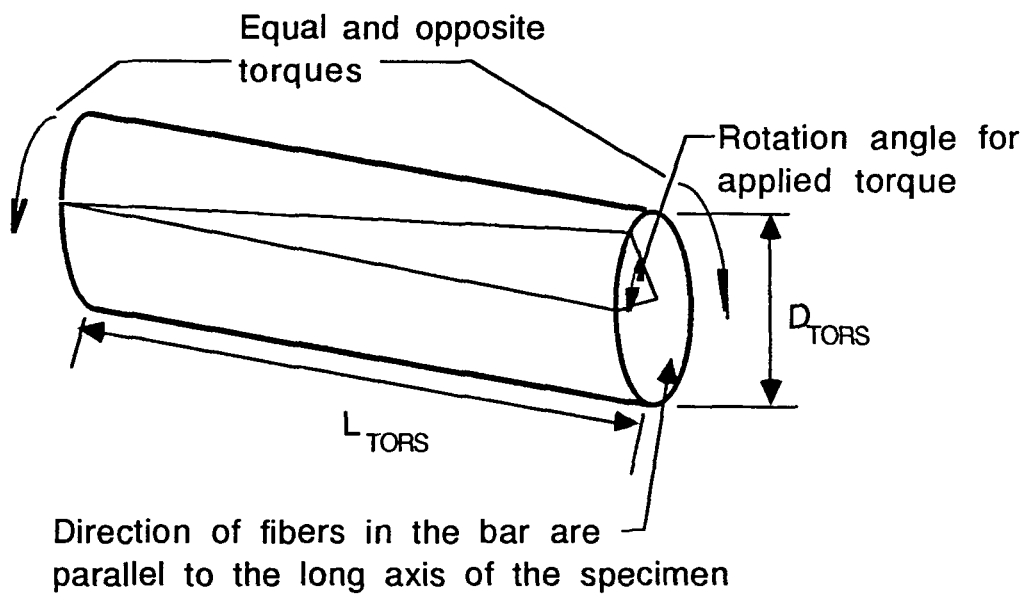
D_{TORS} = Diameter of bar used for torsion of a solid round bar shear test (in.)

L_{TORS} = Length of bar used for torsion of a solid round bar shear test (in.)

where:

T = Torque (lb-in.)

R = Radius of bar (in.)

This test can determine the stress occurring in the rod up to the proportionality limit if the fibers are parallel to the axis of the specimen [31]. For this research project, this test method does not accurately model the transverse loading situation occurring in the pavement dowel bar. Therefore, a torsion of a solid rod shear test was not developed for this research program.

2.4.2.1.3. Iosipescu shear test method

By design, the specimen in the Iosipescu shear test method is in constant shear at its centerline [32]. The load is applied in such a way that the shear is constant in the region at the centerline of the dowel and the moment is zero at the centerline of the specimen [32-34]. This is accomplished by rotationally restraining both ends of the speciment while thespecimen is being loaded in shear. Figure 2.3 illustrates the force, shear, and moment diagrams for the Iosipescu shear test method. The Iosipescu shear test method was chosen for the Iowa State research program for three main reasons:

1) The loading resulting from the test procedure is nearly identical to the loading situation that a pavement dowel would experience in the field.
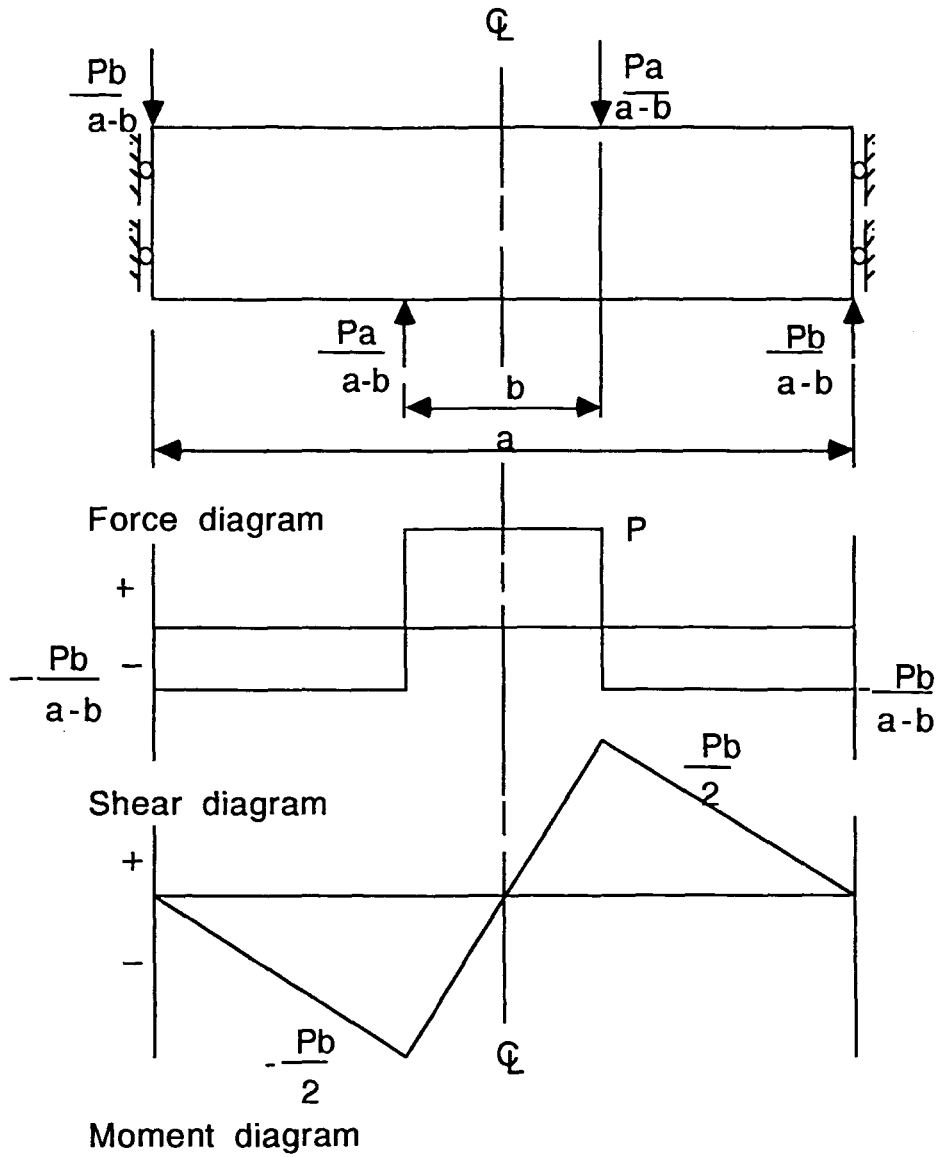
Figure 2.3. Force, shear, and moment diagrams for the Iosipescu shear test

2)   If the shear stress reaches the limiting value, the specimen will fail in shear. Shear tests that do not result in the shear failure of the specimen are not an accurate measure of the material's shear strength.

3)   The loading situation is such that large stress concentrations resulting from the application of required point loads is avoided. The load can be applied to the specimen over a relatively large area so that stress concentrations will not occur.

To utilize the Iosipescu shear test method, the test frame used for this research project was constructed based on the smaller Iosipescu test frames developed by Adams at the University of Wyoming [32]. The test fixture used by Adams was made for very small test specimens. This research project required a much larger frame; however, the geometry of the loading and support are the same. Figure 2.4 shows a schematic of the frame used by Adams at the University of Wyoming. Figure 2.5 shows a schematic of the frame developed in this research project for testing the relatively large dowel specimens.

The nominal shear stress for the Iosipescu shear test for a round bar (for unnotched specimens) is determined through the use of the following equation:

$$\text{shear stress}_{(nominal)} = \frac{V}{A} \qquad\qquad (2.3)$$
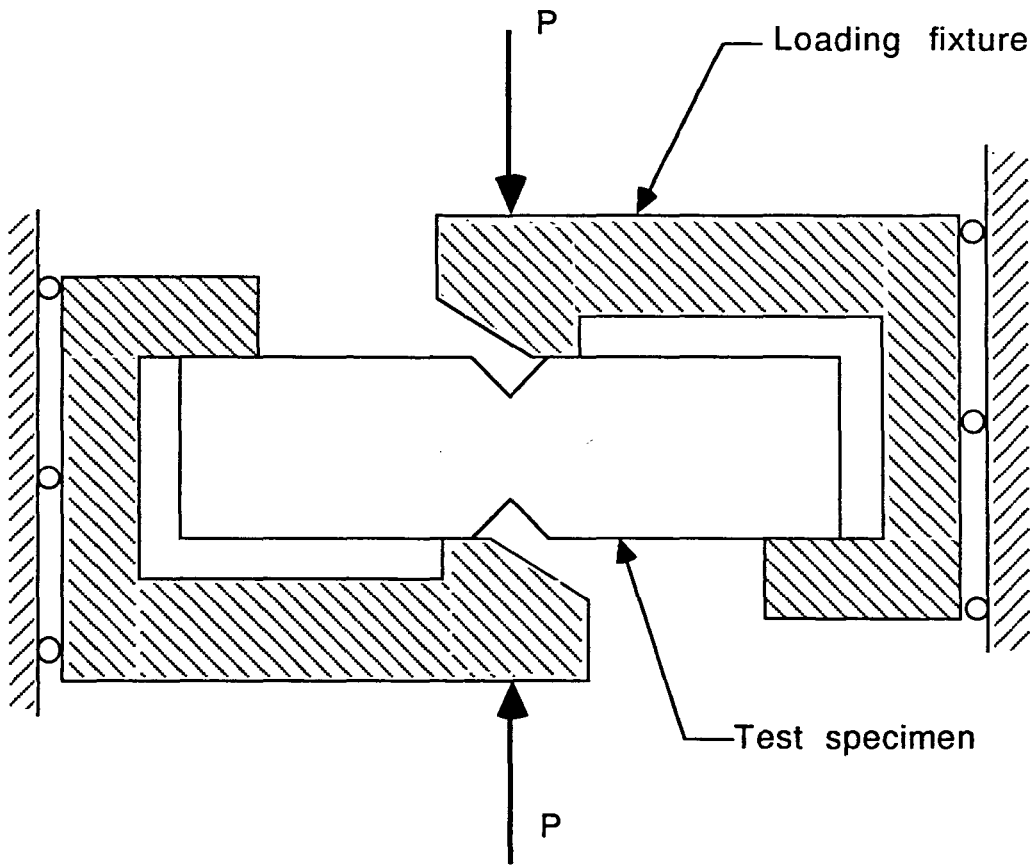
Figure 2.4.   Schematic of Adam's Iosipescu testing
frame [32]
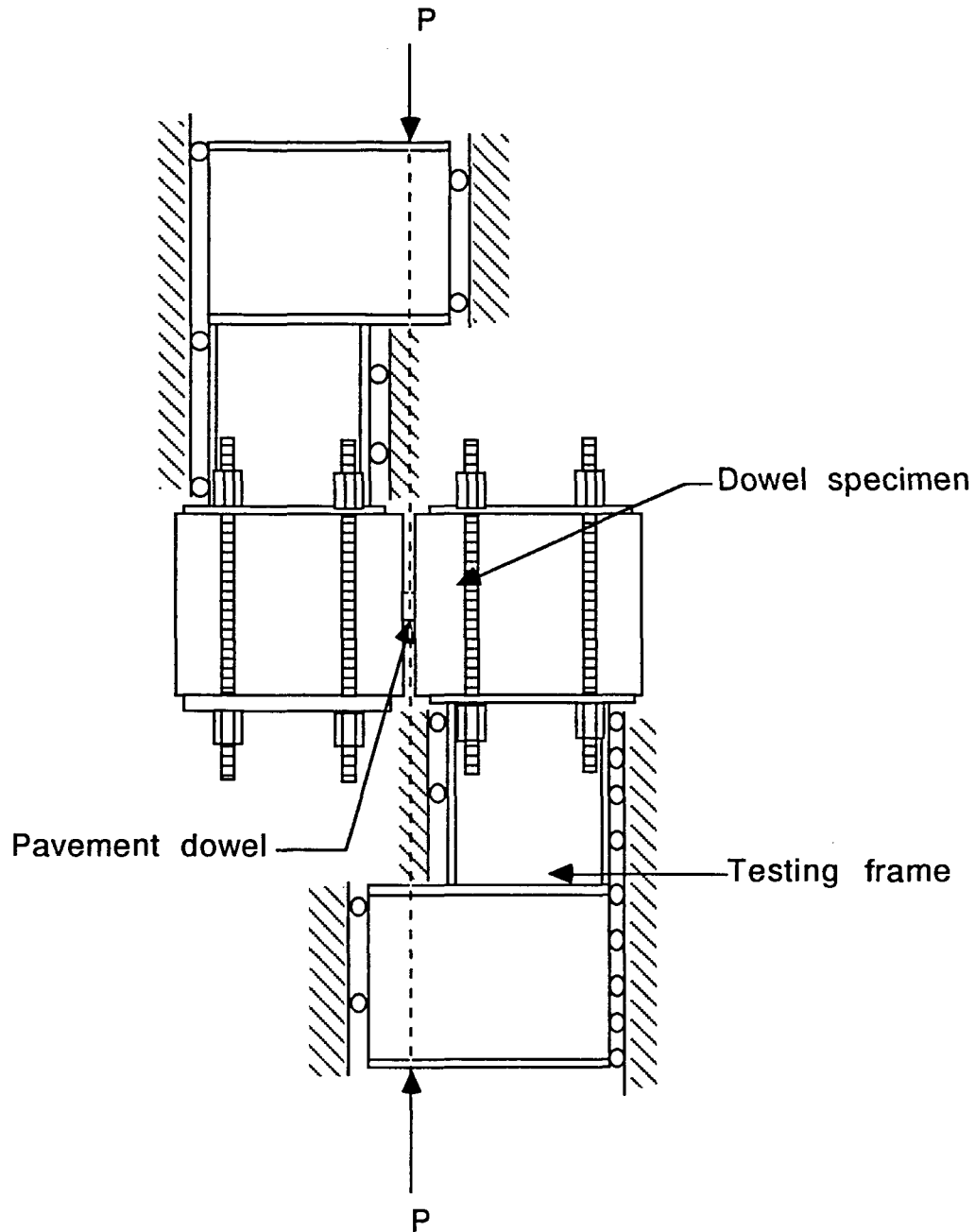
Figure 2.5. Schematic of frame developed in this research
project for Iosipescu shear testing of pavement
dowels

2.4.2.2. Shear strengths from previous research programs

Testing methods for determining the material properties of fibercomposite materials are different than the testing methods used for isotropic materials, like steel, because of the non-isotropic nature of the fibercomposite materials. Shear strength is one of the least understood properties of fibercomposite materials because many shear test methods used for isotropic materials do not give accurate results for fibercomposite materials. Testing of isotropic materials by common shear test methods often results in shear failures of the specimens if testing is allowed to reach ultimate conditions.

The shear test methods that gave the most accurate results for fibercomposite materials are the Iosipescu shear test method and the torsion of a round bar, based primarily on the suggestions from previous shear testing programs. An important item in this project's consideration was a test method that gave accurate results with a shear failure mode. Results published from various testing programs, including information on material type and shear strength, are shown in Table 2.1.

The materials shown in Table 2.1 are different than the fibercomposite material used in the research program.

Table 2.1. Fibercomposite shear strengths from other research programs

Author	[REF.]	Material	Shear strength (ksi)
Rosen	[35]	Boron/Epoxy	17.8
Lenoe	[36]	Boron/Epoxy	15.7-17.4
Walrath & Adams	[32]	SMC-R50	17.8
		XMC-3	19.1
		Graphite/Epoxy	11.7

2.5.   Shear Testing

2.5.1.   Test specimen preparation

Ten dowel specimens were tested in this portion of the research program. All of the specimens were 10 inches wide by 10 inches thick by 24 inches long. The 10-inch-thick dimension was chosen to represent a commonly used 10-inch-thick pavement. Specimens identical to those used in this part of the research program were used in the following part of the research program, in which the dowel specimens as well as other specimens were submersed in a water-based solution inside a set of tanks. Because a number of specimens were placed into each tank, clearance problems had to be considered, and as a result, minimum specimen sizes (i.e., specimens with a 10-inch width) were used. At the

center of the length there was a 1/8-inch gap. Five of the specimens had 18-inch long, 1.5-inch diameter steel dowels in their centers; the other five specimens had 18-inch long, 1.25-inch diameter fibercomposite dowels in their centers.

The specimens were constructed with steel prefabricated forms. Three sheet metal pieces were placed at the centerline of each dowel specimen to create a gap. A gap was required to transfer the force through the dowel, instead of through a combination of the dowel and aggregate interlock. The concrete used was the Iowa Department of Transportation's M-4 mix with a superplasticizer [17]. Cylinders also were cast and tested. The average strength of the concrete, determined through the testing of the cylinders, was 8,010 psi.

Eight Number 5 steel reinforcing bars were placed in each specimen to prevent a horizontal shear failure. The bars were placed on the side of the specimen opposite to the side where bearing and shear cone failures could occur so as to try not to influence their behavior. Figure 2.6 is a sketch of the dowel specimens that shows where the reinforcement was placed and the direction of the loading placed on the specimen.

2.5.2. Description of testing

All of the specimens were tested to failure using an Iosipescu shear test format. In this test, the center of the specimen, the

4-#5 steel reinforcement
bars on each side of joint
opposite of the side where
either the load or
reaction is applied

P*

P*

12"

1/8"

24"

12"

Dowel - either 1.50 in. steel or
1.25 in. fibercomposite
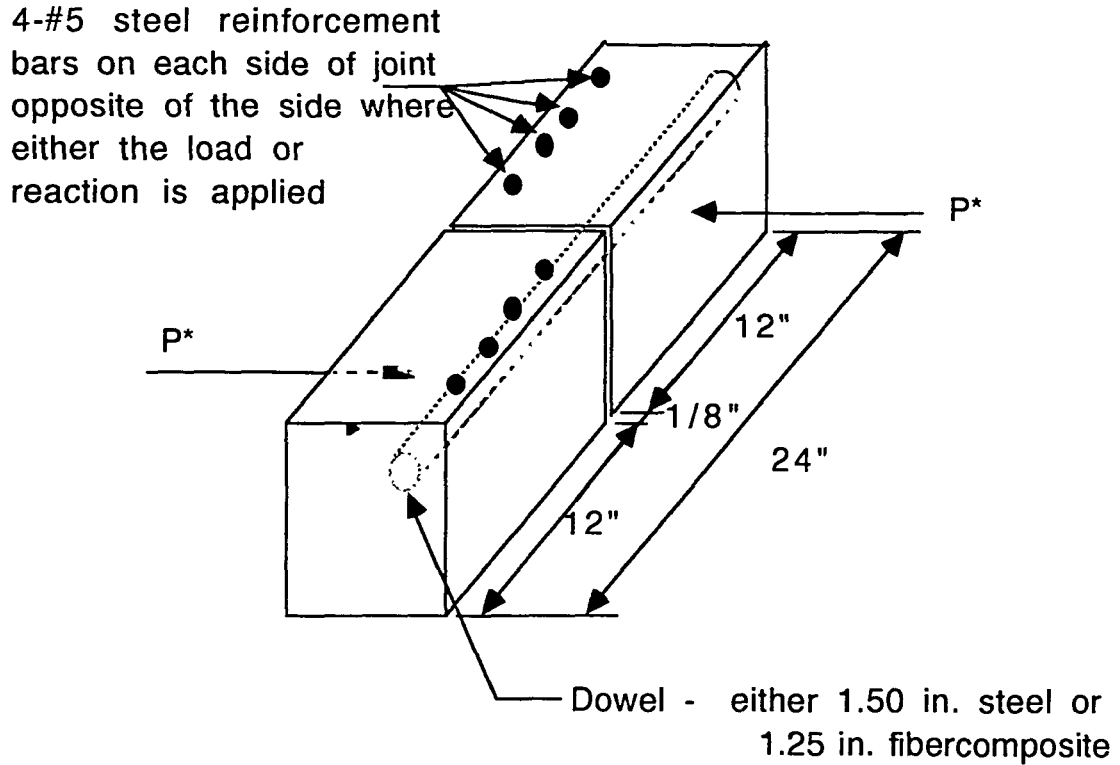
* See Sections 3.4.1 and 3.4.2 for assumed load distributions

Figure 2.6. Sketch of dowel specimen and where reinforcement
was placed

loading device (hydraulic ram), and the center of the reaction all lie on the same line [32]. (The Iosipescu shear test was more fully described in Section 2.4.2.1.3.) A pure shear at the center of the specimen results. This type of test format is not only the best type of shear test, but it is similar to the loading situation a dowel would experience in an actual pavement [32].

In the Iosipescu shear test, the testing frame must be constructed so neither side of the specimen can rotate during testing. To eliminate any rotation, rollers were placed between the inside pieces and the outside frame. The rollers were placed in such a way that the inside pieces could only move in the direction of the load. Figure 2.7 shows the testing frame, the rollers, and the hydraulic ram.

The relative deflection of two sides of the joint was measured with direct current displacement transducers (DCDTs). Figure 2.8 shows the relative deflection that was measured during the testing.

2.6. Testing Description and Results

To determine the shear strength of the fibercomposite material, only the value of the maximum load the fibercomposite bar carried prior to a shear failure is required. In this testing program, shear failures did not occur but rather shear cone failures of the concrete directly below the dowel occurred. Section 3.3 describes the failure mode of the specimens in greater detail. Because of the
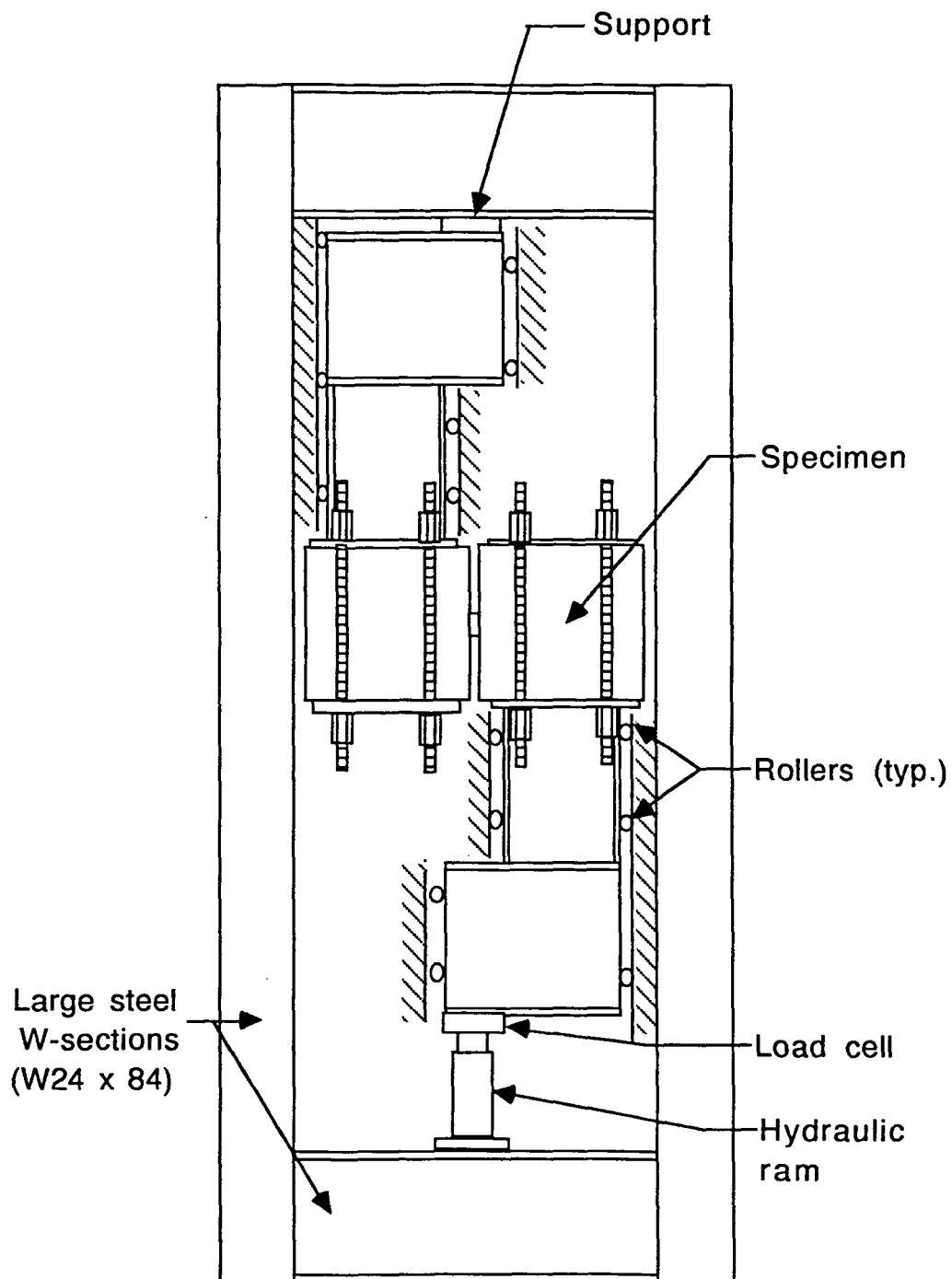
Figure 2.7. Illustration of testing frame with rollers and the hydraulic ram

Relative deflection
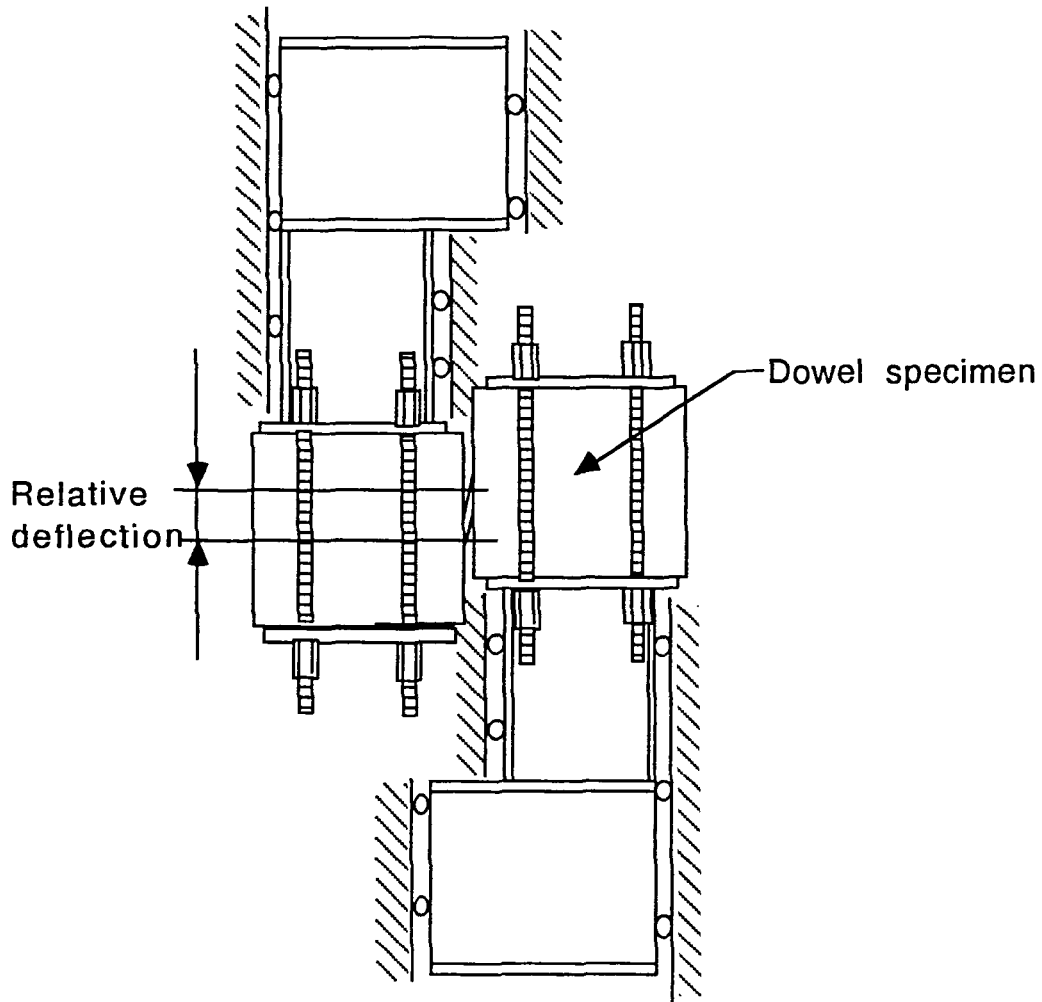
Dowel specimen

Figure 2.8. Illustration of the measurement of the relative deflection of the dowel specimen

absence of a shear failure of the bars, the shear strength of the bar could not be determined. The shear strength of the bar was based upon the load resisted by the dowel system prior to the shear cone failure of the concrete. This stress is below the maximum shear stress that the fibercomposite bars can resist, but, as will be shown shortly, the maximum shearing stress occurring in the bars is approximately the maximum shear stress that would be predicted based on the results of previous shear testing programs. Table 2.2 shows the maximum loads that the fibercomposite dowel samples carried prior to the shear cone failure of the concrete and the maximum dowel bar shear stresses calculated by Equation 2.3.

The maximum shearing stresses occurring in the fibercomposite dowel bars had an average of 13,090 psi. This is comparable to the maximum shearing stresses occurring in research programs shown in Table 2.1 that determined the shear capacity of several different types of fibercomposite materials. Different materials have different properties. The shear strength of one material by itself does not explain the strength of another material. However, an estimate of the range of the fibercomposite's shear strength can be made. This information suggests that the maximum shearing stress occurring in the bar may have been close to the maximum shearing stress of the bar. If the shear cone of the concrete surrounding the dowel bar would have occurred at a higher load, a shear failure of the dowel bar probably would have resulted. Of course, this point is pure speculation because a shear failure of

Table 2.2. Maximum loads and maximum shear stresses resulting in
the experimental specimens containing 1.25-inch
diameter fibercomposite dowels

Specimen No.	Experimental Max. Load Carried (lbs)	Theoretical (V/A) Shear Stress (psi)
FIB 1	17,067	13,907
FIB 2	20,552	16,747
FIB 3	14,015	11,420
FIB 4	16,071	13,096
FIB 5	12,613	10,288
	Average	= 13,090 psi

the bar did not occur, and consequently, the maximum shear strength
of the fibercomposite bar was not determined.

In the area of shear testing of fibercomposite materials,
information on the strength of the resin in shear could not be found.
This is perhaps the most important parameter in the determination
of the shear strength of the fibercomposite materials because the
shear strength of the material has been said to be a function of the
strength of the resin and not the shear strength of the fibers. The
fibercomposite materials with drastically different tensile
strengths have similar shear strengths. The best way to verify the
values determined in this research program is to compare them to
values determined from other research programs that studied the
shear strength of fibercomposites. A value for the shear strength of

vinyl ester, glass-fiber fibercomposite material was not found during the literature review for this research project; however, a comparable value, the shear strength of high-strength fiber encased in a resin, was found. Therefore, the values of the shear strength of the vinyl ester, glass-fiber fibercomposite material (determined during this research) were compared to the shear strengths of high-strength fibers encased in a resin (determined in other fibercomposite shear strength research programs).

3. PAVEMENT DOWELS

3.1.   Introduction

Transverse joints allow pavements to expand and contract. Pavement dowels and/or aggregate interlock transfer a load across a joint.   Many pavements have deteriorated significantly despite the use of standard practices in their design.   Faulting, spalling, lockup of joints, and corner cracking can result from joint problems [1]. The costs incurred to repair pavements that have joint problems can be quite high and could constitute a large portion of an agency's repair budget.

Transverse pavement joints with and without dowel bars are used in rigid pavements.   Dowel bars are included in the construction of transverse joints if aggregate interlock cannot be relied upon solely for the transfer of the load across the joint.   This is commonly the case and especially true when large wheel loads are expected or large temperature ranges can be experienced by the pavements from season to season [37].   Large temperature changes cause significant changes in the length of pavements.   If the change in length is substantial, the opposite sides of the joint may no longer be in contact with each other, thus making aggregate interlock across the joint impossible.   For these types of cases, dowel bars must be used in the joints [37].

The most common type of dowel bar is a round steel bar placed horizontally at the slab transverse joint [1]. Figure 3.1 shows a typical doweled contraction joint. The dowel is cast in concrete on one side of the joint and greased or fitted with sleeves on the other side of the joint to allow the slab to expand or contract freely. Some other types of dowel bars that have been used include epoxy-coated, round steel bars, double-vee steel bars, small I-beams, and concrete-filled steel tubes [1].

Pavement dowels used in different situations may experience drastically different stresses [1]. Regional climatic and geologic conditions can vary tremendously. Because there are varying conditions throughout the country, and the world, no uniform design method exists for the pavement dowels. Instead, engineers typically rely upon past experience when designing a doweled joint [38]. In some instances, designs based upon previous experience have worked well, but based upon the failure of many joints, this is not always true. Instead of relying upon this "black box" type of design method where the behavior of the resulting system is not known, this report will help design engineers understand the behavior of the dowel systems.

The design of effective dowels must result in joint systems that limit stresses, both in the dowel bar and in the concrete, to acceptable levels. Shear and bending stresses are of primary importance in the dowel bar. Bearing stresses and cone failures must be considered in the concrete.
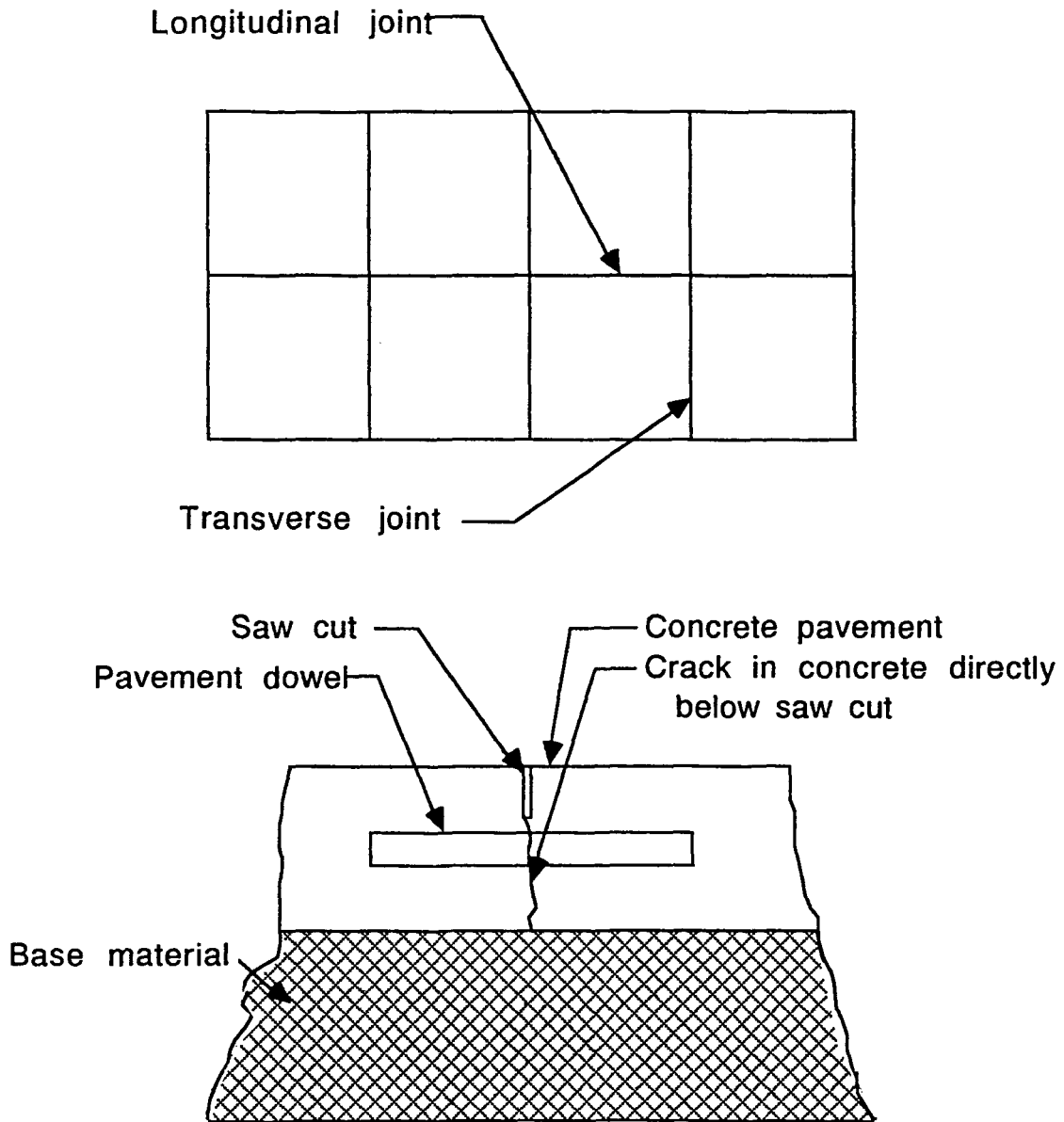
Figure 3.1. Pavement cross section

3.2. Background

Smooth, round steel bars across transverse joints in concrete pavements for the purpose of transferring load may first have been used in a pavement built in the winter of 1917-18 near Newport News, Virginia [39]. This pavement was constructed with four 3/4-inch diameter bars for every 20-foot-wide section [39].

Current design of doweled joints makes use of charts to determine dowel diameter, length, and spacing. There is no direct consideration of stresses occurring in the region surrounding the dowel because of the lack of credible data for the ratio of dowel flexural stiffness to concrete bearing stiffness. Typical designers use a rule that calls for dowel diameters equal to the pavement thickness divided by eight. This method is based on experience of the past performance of dowels in pavements. This "trial and error" design approach has performed well in some situations and poorly in others [1].

3.3. Dowel Testing Results

The trial and error design approach was not used to select the sizes of the dowels used during the research performed at Iowa State. For the fibercomposite dowels, a 1 1/4-inch diameter dowel was selected because it was the largest diameter vinyl ester resin bar available. For the steel dowels, 1 1/2-inch diameter dowels,

which are commonly used by the Iowa Department of Transportation, were used. During the testing, all of the specimens experienced a shear cone failure in the concrete. Three cracks occurred, initiating from the dowel at the face of the joint. In all of the specimens, the deflection of the dowel was small until the formation of the cracks. Immediately following the formation of the cracks, the specimens underwent much larger deflections. Figure 3.2 presents a sketch of the cracks that formed in the specimens during testing. The peak load was recorded just prior to the formation of the cracks.

The load-deflection graphs for individual specimens can be found in the Appendix of this thesis. The initial portions of the load-deflection graphs have essentially a linear relationship. Following the initial portion, a nonlinear behavior relationship was exhibited by the specimens for the remainder of the experiment. Figures 3.3 and 3.4 present the load-deflection curves for the steel and fibercomposite specimens, respectively. Table 3.1 summarizes the maximum loads and the dowel system stiffnesses for each of the fibercomposite specimens. The dowel system stiffness is defined as the best fitting line for the experimental load versus the experimental deflection for the initial portion of testing. This stiffness is composed of the stiffness of the dowel in the concrete and of the stiffness of the dowel in the gap between the two sides of the specimen. Table 3.2 summarizes the maximum loads and the dowel system stiffnesses for each of the steel specimens.
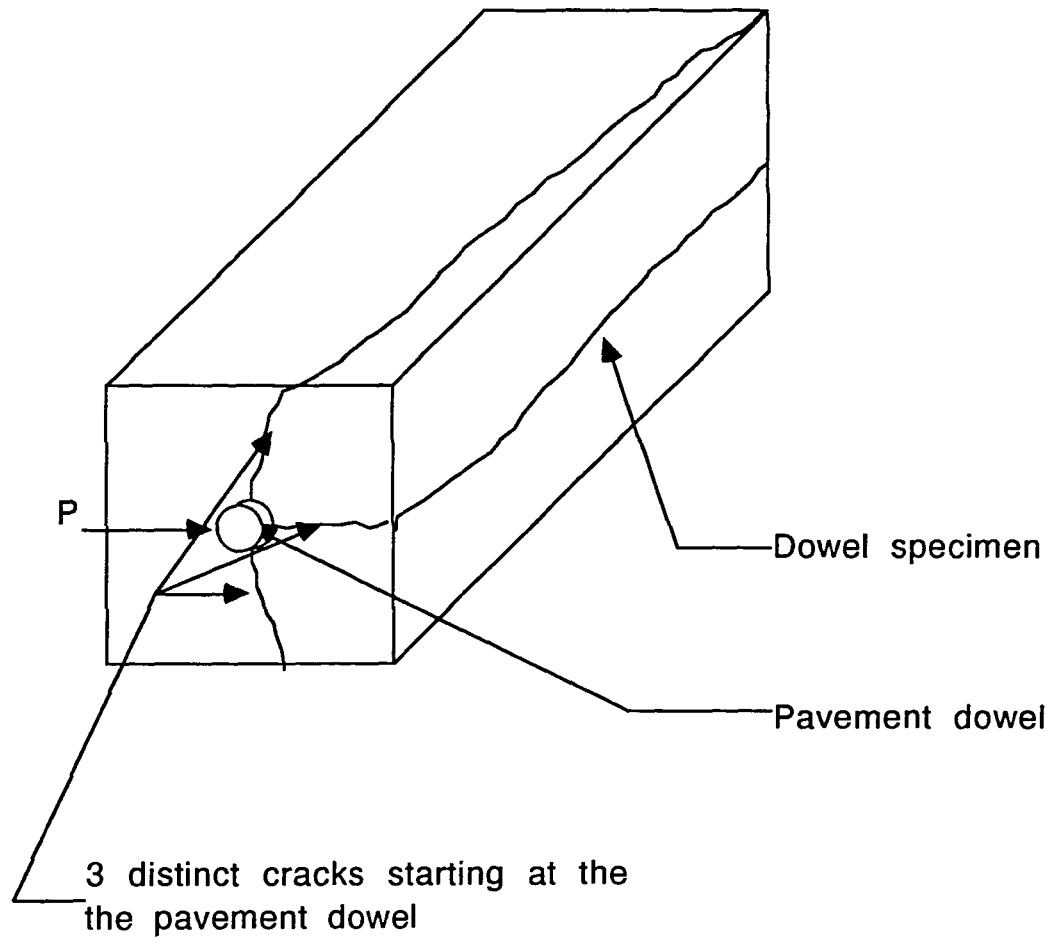
Figure 3.2. Sketch of the cracks which formed in the dowel specimens during testing
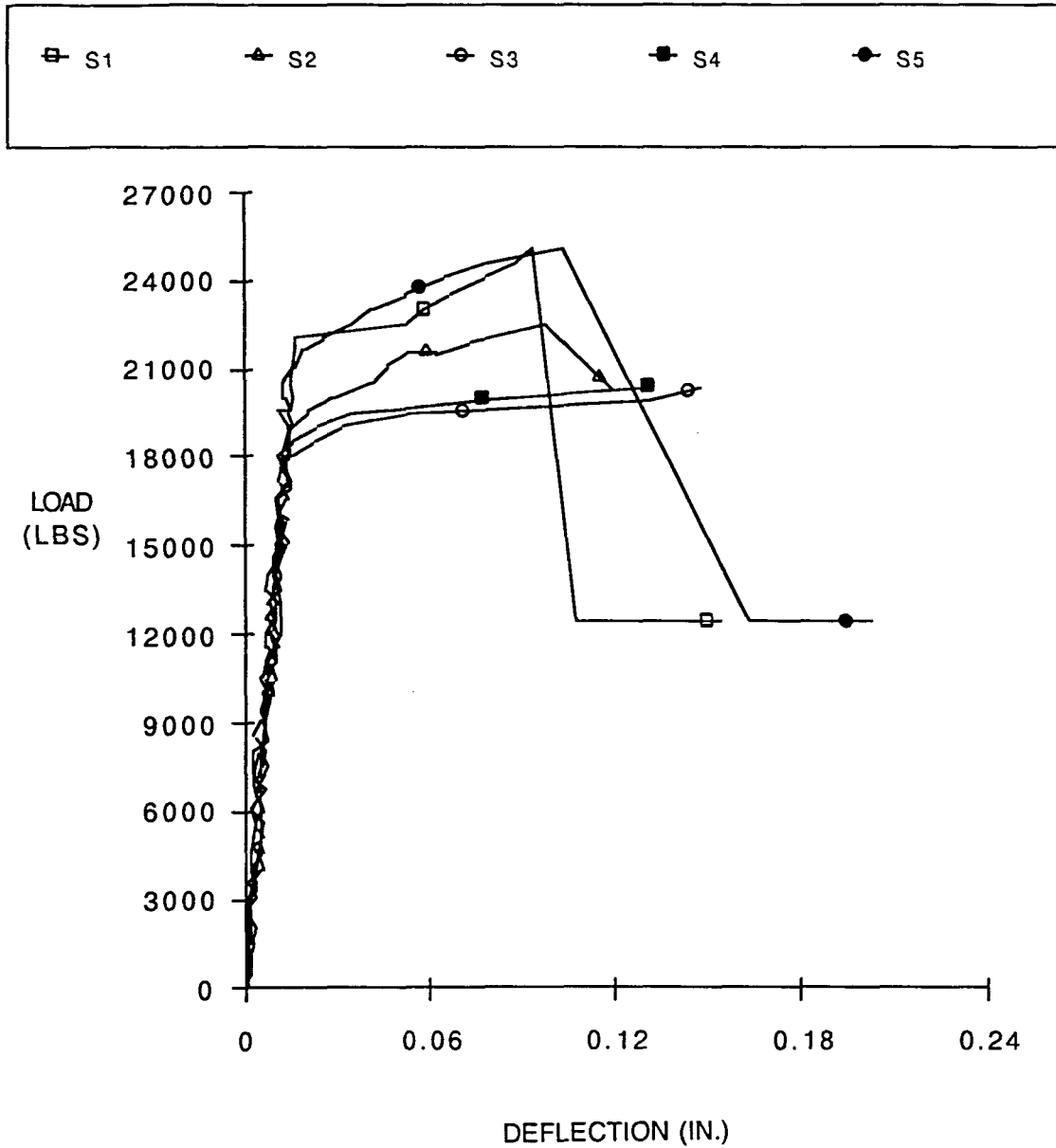
Figure 3.3. Load versus deflection for 1.50-inch steel dowel
Specimens S1-S5
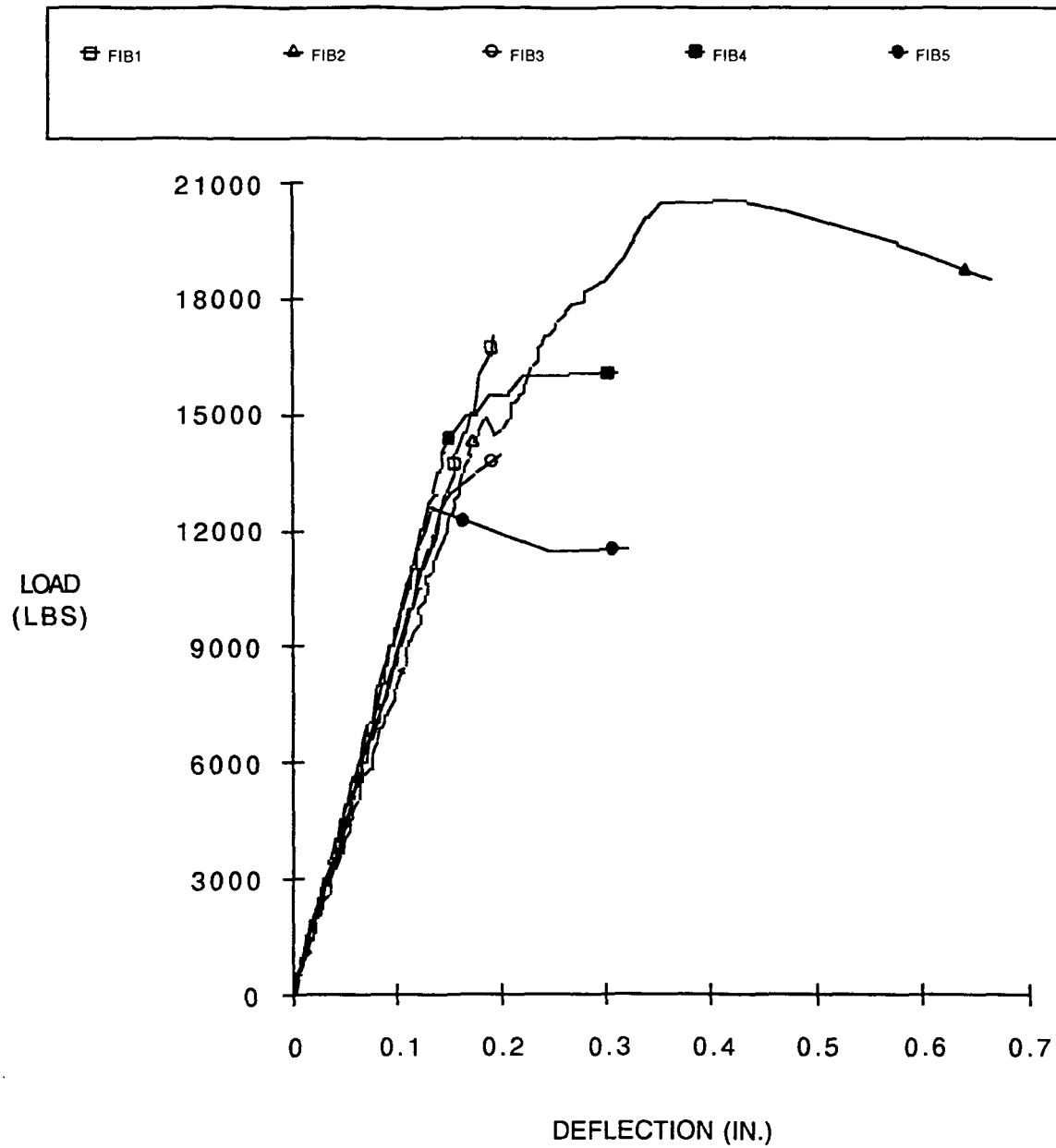
Figure 3.4. Load versus deflection for 1.25-inch fibercomposite
dowel Specimens FIB1-FIB5

The elastic limit loads given in Tables 3.1 and 3.2 are not the maximum loads recorded during the testing of the dowel specimens. Rather, they are the maximum loads recorded prior to the cracking of the dowel specimens. Following the cracking of the specimens, further concrete failures may have been prevented by a clamping force applied to the testing frame.

Table 3.1. Fibercomposite dowel specimen maximum experimental loads and dowel system stiffnesses

Specimen No.	Elastic Limit Load (lb)	Dowel System Stiffness (lb/in)
FIB1	17,100	86,100
FIB 2	14,900	81,300
FIB 3	12,000	87,500
FIB 4	12,700	94,700
FIB 5	12,600	95,000
Average	13,900	88,900

The ratio of the average dowel system stiffness for the steel and fibercomposite dowel specimens is equal to about 15. The ratio of the flexural rigidities for the steel and fibercomposite dowel specimens is approximately equal to 9. The difference between these two values suggests that there are size and/or material

Table 3.2. Steel dowel specimen maximum experimental loads and dowel system stiffnesses

Specimen No.	Elastic Limit Load (lb)	Dowel Shear Stiffness (lb/in)
S1	17,800	1,310,000
S2	19,000	1,410,000
S3	18,100	1,250,000
S4	18,400	1,280,000
S5	18,000	1,400,000
Average	18,300	1,330,000

effects beyond the simple ratio of the flexural rigidities for the specimens that contribute to the performance of the dowels.

3.4. Analysis of Pavement Dowels Using Timoshenko Theoretical Model

An objective of the research was to develop a preliminary design procedure for pavement dowels. One of the most important parameters that must be determined before developing a design procedure is an appropriate analysis method. The Timoshenko theoretical model was studied extensively, and information on the development of the method is given in Sections 1.4.1.1. The semi-infinitely long beam Timoshenko theoretical analysis approach is

assumed to be applicable to all of the dowels analyzed in this research program. The correctness of the assumption is proven in Section 3.5.

3.4.1. Calibration of the analytical method

A discussion of the Timoshenko theoretical model of a beam on an elastic foundation as applied to the pavement dowel was given in Section 1.4.1.1. The modulus of subgrade reaction, k, can be used to correlate the analysis method to the data determined in the experimental portion of the research project. The constant, k, relates the stiffness of the beam, or dowel, to the stiffness of the foundation, or concrete [13]. To correlate the analysis method to the experimental data, a graph was made of the resulting deflection at some arbitrary load for a wide range of assumed k values. After the actual deflection at the same arbitrary load has been determined experimentally, the k value correlating to that deflection can be determined graphically and verified numerically.

Once the k value has been determined, the equation for the deflection of the dowel at any point can be solved. After the equation for the deflection has been determined, the equations for the slope, moment, shear, and load along the dowel can be determined by taking successive derivatives as discussed in Section 1.4.1.1. The equation for the deflection of the dowel at any point was determined to be [13]:

$$y = \frac{e^{-\beta x}(P\cos\beta x - \beta M_0(\cos \beta x - \sin\beta x))}{2\beta^3 EI_z} \quad (1.4)$$

3.4.2. Results of Timoshenko's semi-infinitely long beam analysis approach

To determine k, the modulus of subgrade reaction, a graph was made of deflection determined by the Timoshenko analysis versus assumed k values at 10,000 pounds (an arbitrary load). The k value was determined by plotting the experimental deflection value on the graph and reading the corresponding k value.

The graph for the deflection, at an arbitrary load, versus the assumed k value must be developed for each type of dowel used. To develop the graph, the modulus of elasticity, the moment of inertia of the dowel and the width of the joint must be known initially. The resulting deflections are then graphed versus the assumed k values. Figure 3.5 shows the graph of the deflection versus the k value for the 1.5-inch diameter steel dowels. Figure 3.6 is a graph of the deflection at the face of the joint versus the k value for the 1.25-inch diameter fibercomposite dowels for a 10,000-pound load.

The value used for the experimental deflection was not the actual experimental deflection of the specimen at a load of 10,000 pounds. Instead, the deflection used was the stiffness of the
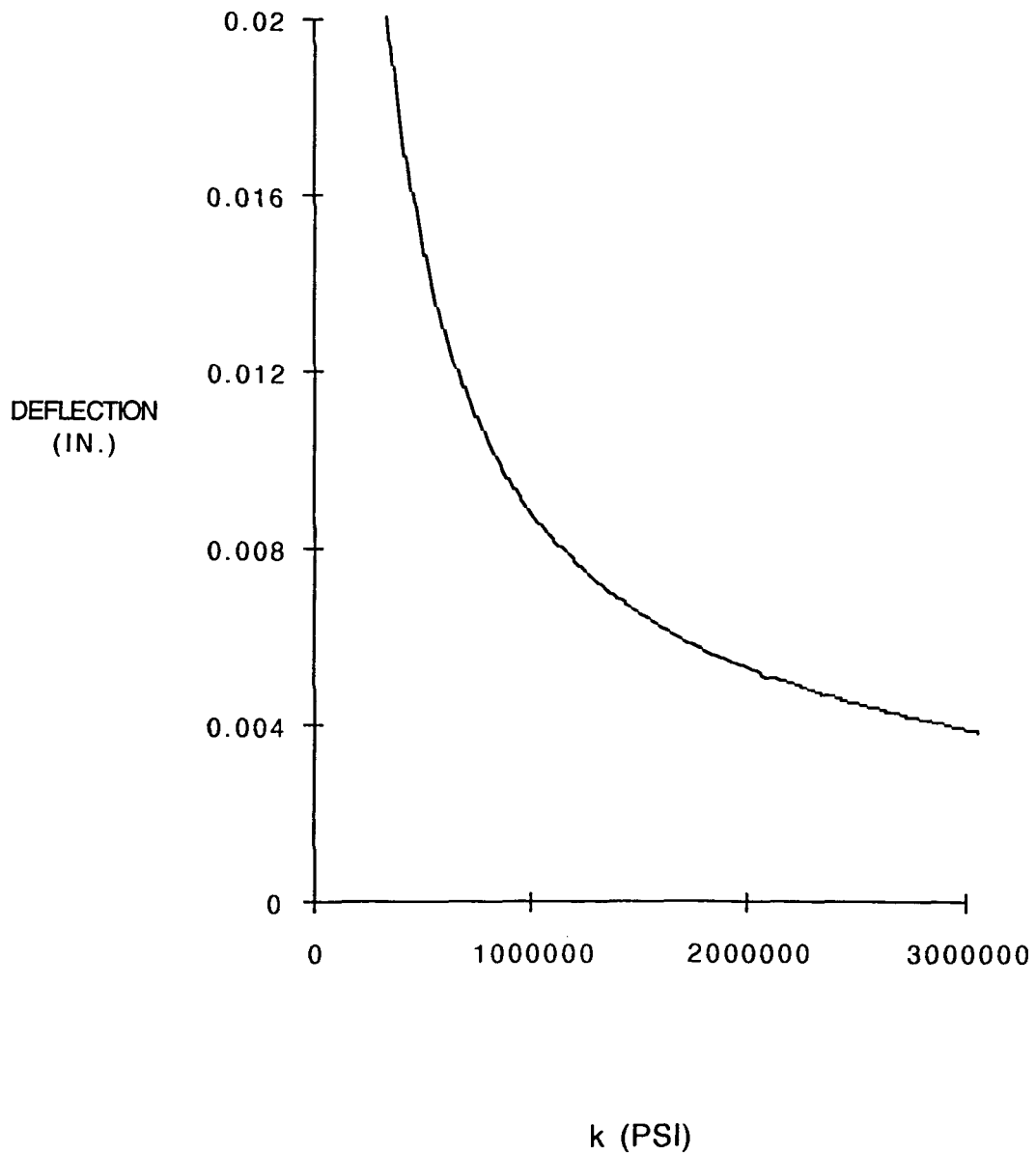
Figure 3.5. Deflection versus k value for 1.50-inch steel dowel using the Timoshenko analysis method
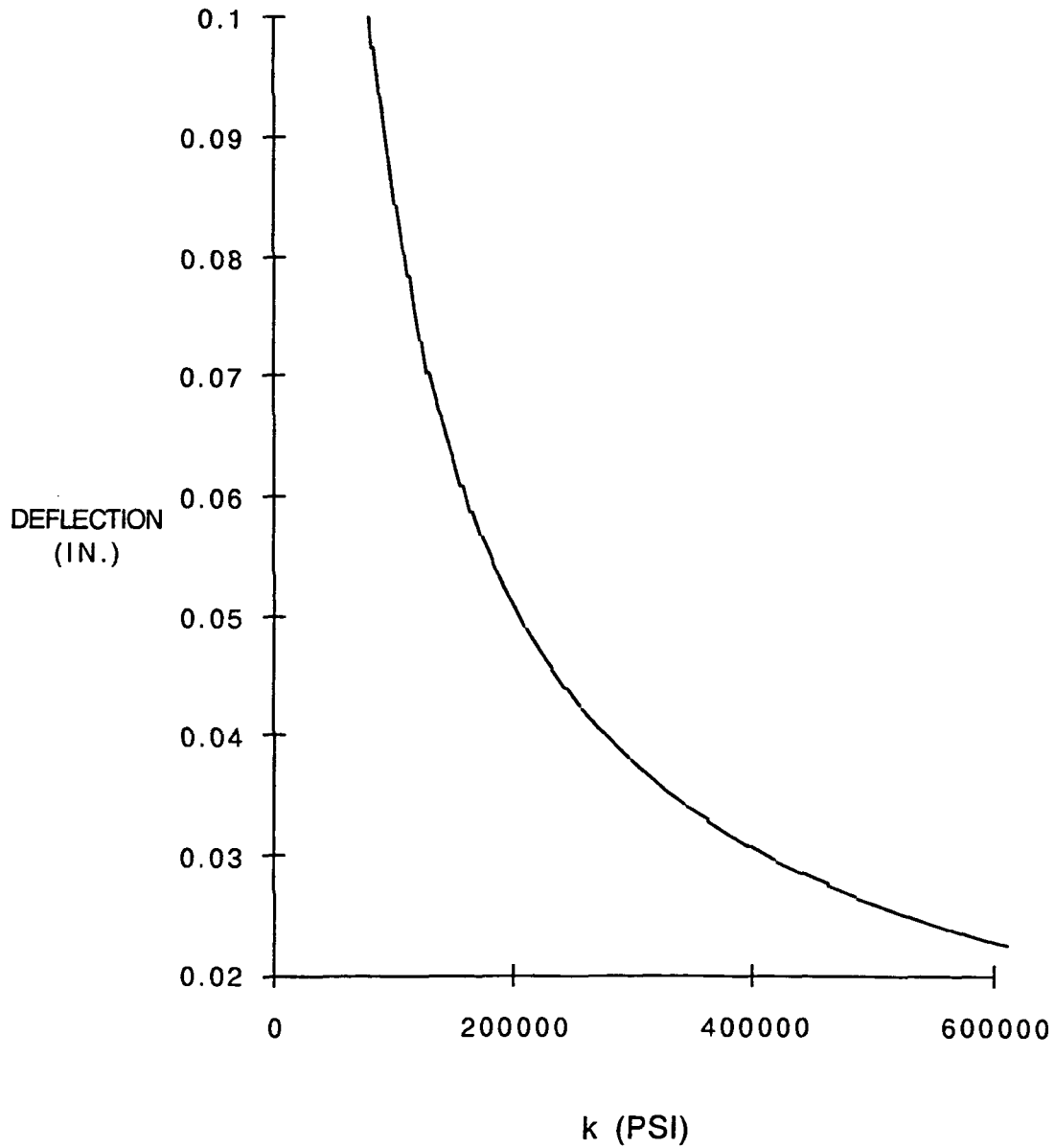
Figure 3.6. Deflection versus k value for 1.25-inch fibercomposite dowel using the Timoshenko analysis method

specimen determined experimentally multiplied by 10,000 pounds. This gives a better representation of the overall performance of the individual specimens compared to using the actual deflection at 10,000 pounds.

The experimental deflection includes the shear deflection occurring in the 1/8-inch gap between the two sides of the specimen. This deflection must be subtracted from the total experimental deflection. The shear deflection can be calculated using the equation [40]:

$$Y_s = \frac{FPL_s}{AG} \qquad (3.1)$$

where:

Y_s = Shear deflection (in)

F = Form factor for shape of cross section that is equal to 10/9 for a solid circular section [40]

P = Concentrated load acting downward on the dowel at the center of the joint (lbs)

L_s = Shear span length (in)

A = Cross-section area (in^2)

G = Shear modulus (psi)

For a 10,000-pound load on a 1.5-inch diameter steel dowel
with a 1/8-inch shear span and a shear modulus of 11,100,000 psi,
the following equation would be used:

$$Y_s = \frac{(10/9)(10,000 \text{ lbs})(1/8 \text{ inch})}{(\pi/4)(1.5)^2 \ (11,100,000)}$$

$$= 0.0000708 \text{ in}$$

Similarly, for a 10,000-pound load on a 1.25-inch diameter
fibercomposite dowel with a 1/8-inch shear span, a modulus of
elasticity of 6,900,000 psi [41], and a Poisson's ratio of 0.25, the
following equation would be applied:

$$Y_s = \frac{(10/9)(10,000 \text{ lbs})(1/8 \text{ inch})}{(\pi/4) \ (1.25)^2 \ (6,900,000/2(1+0.25))}$$

$$= 0.00041 \text{ in.}$$

Table 3.3 presents a deflection breakdown for the individual
steel specimens for a load of 10,000 pounds, and Table 3.4 gives a
summary of the k values for the individual steel specimens. For the
individual fibercomposite specimens, Table 3.5 presents a deflection
breakdown for a load of 10,000 pounds, and Table 3.6 gives a
summary of the k values.

After the k values are determined for the individual
specimens, the equation for the deflection along the dowel can be
solved. The equations for the slope, moment, shear, and load along
the dowel can be determined by taking successive derivatives of the
equation for the deflection. Figures 3.7 through 3.10 show the

Table 3.3. Deflection breakdown for individual steel specimens

Spec. No.	Total Rel. Defl. (in.)	1/2 Total Rel. Defl. (in.)	Shear Defl. (in.)	1/2 Shear Defl. (in.)
S1	0.0077	0.00383	0.0000708	0.000035
S2	0.0071	0.00355	0.0000708	0.000035
S3	0.0080	0.00400	0.0000708	0.000035
S4	0.0078	0.00391	0.0000708	0.000035
S5	0.0071	0.00357	0.0000708	0.000035
Specimen of Average Stiffness	0.0075	0.00377	0.0000708	0.000035

Table 3.4. k values for individual steel specimens

Spec. No.	1/2 Total Relative Defl - 1/2 Shear Defl. (in.)	k_o Value (lb/in.^{3})	k Value (psi)
S1	0.00379	1,930,000	3,140,000
S2	0.00351	2,130,000	3,480,000
S3	0.00396	1,820,000	2,960,000
S4	0.00387	1,870,000	3,050,000
S5	0.00353	2,110,000	3,460,000
Spec. of Avg. Stiffness	0.00373	1,970,000	3,210,000

Table 3.5. Deflection breakdown for individual fibercomposite specimens

Specimen No.	Total Rel. Defl. (in.)	1/2 Total Rel. Defl. @ (in.)	Shear Defl. (in.)	1/2 Shear Defl. (in.)
F1	0.116	0.0580	0.00041	0.00020
F2	0.123	0.0615	0.00041	0.00020
F3	0.114	0.0570	0.00041	0.00020
F4	0.106	0.0530	0.00041	0.00020
F5	0.105	0.0525	0.00041	0.00020
Spec. of Avg. Stiff.	0.113	0.0565	0.00041	0.00020

deflection, moment, shear, and load diagrams for the k value corresponding to the average stiffness of the steel dowel specimens. Figures 3.11 through 3.14 show the deflection, moment, shear, and load diagrams for the k value corresponding to the average stiffness of the fibercomposite specimens. These figures are the deflection, moment, shear, and load diagrams for the steel and fibercomposite dowel specimens of average stiffness using the Timoshenko analysis approach.

The applicability of the semi-infinite long beam Timoshenko analysis appraoch, which is determined by the dowel specimen's ßL value, must be checked. The applicability of the semi-infinitely long

beam approach developed by Timoshenko is the subject of Section 3.5. Table 3.7 gives the ß and ßL values for dowel specimens of average stiffness for both the 1.5-inch steel dowels and the 1.25-inch fibercomposite dowels.

Table 3.7 shows that the ßL values are greater than 2. Therefore, the Timoshenko analysis method, assuming an infinitely long beam, is applicable.

Table 3.6.   k values for individual fibercomposite specimens

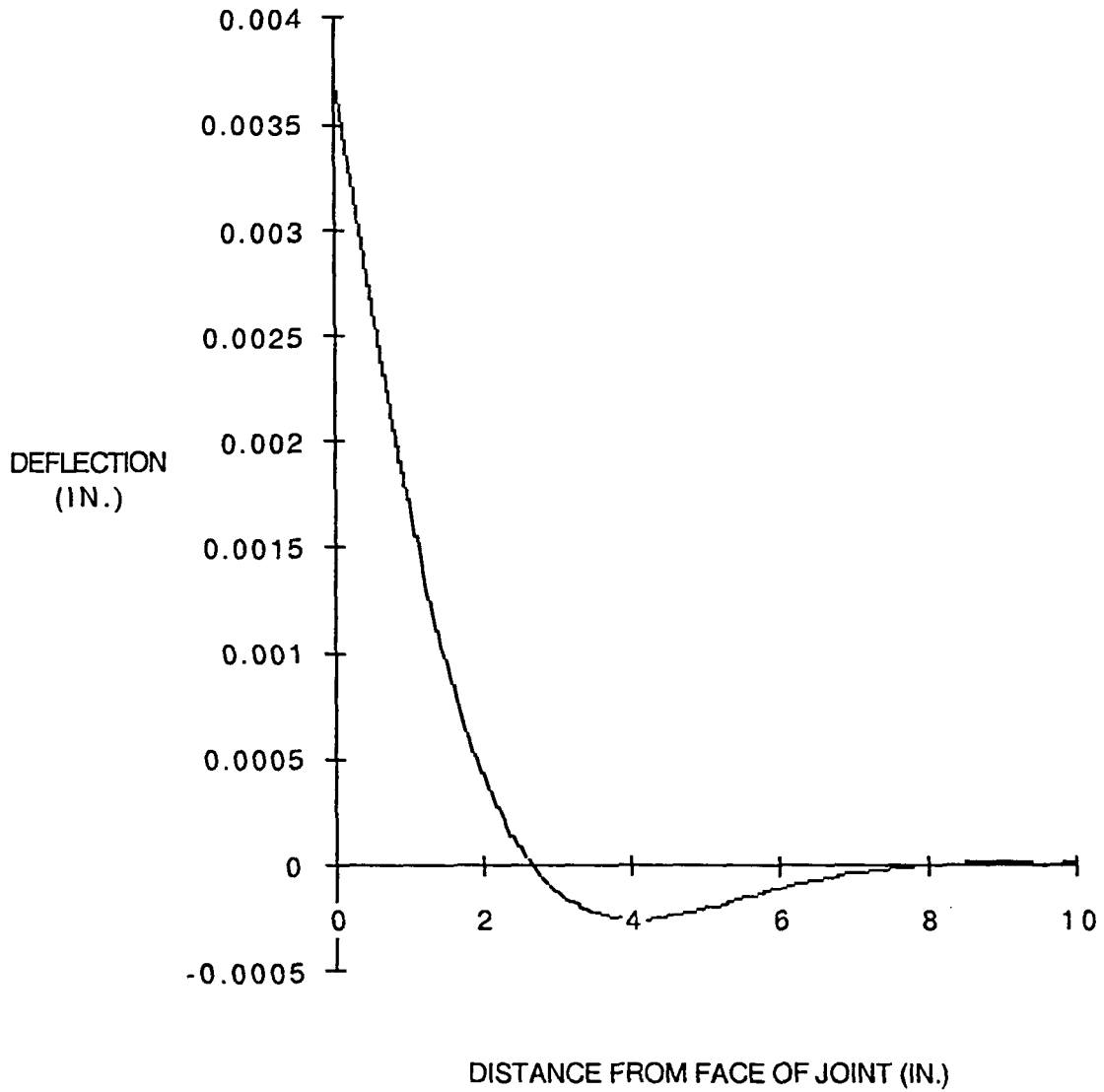| Spec. No.	1/2 Total Relative Defl - 1/2 Shear Defl. (in.)	k_0 Value (lb/in.^{3})	k Value (psi)
F1	0.0578	135,000	165,000
F2	0.0613	126,000	157,000
F3	0.0568	139,000	174,000
F4	0.0528	154,000	192,000
F5	0.0523	155,000	194,000
Specimen of Average Stiffness	0.0563	141,000	176,000

Figure 3.7. Deflection diagram for a 1.50-inch steel dowel of average stiffness of the specimens using the Timoshenko analysis method

Figure 3.8. Moment diagram for a 1.50-inch steel dowel of average stiffness of the specimens using the Timoshenko analysis method

4000

2000

0

-2000

SHEAR
(LBS)

-4000

-6000

-8000

-10000 — V = -10000 @ x = 0

0   2   4   6   8   10

DISTANCE FROM FACE OF JOINT (IN.)

Figure 3.9. Shear diagram for a 1.50-inch steel dowel of average
stiffness of the specimens using the Timoshenko
analysis method

Figure 3.10. Load diagram for a 1.50-inch steel dowel of average stiffness of the specimens using the Timoshenko analysis method

Figure 3.11. Deflection diagram for a 1.25-inch
fibercomposite dowel of average stiffness of the
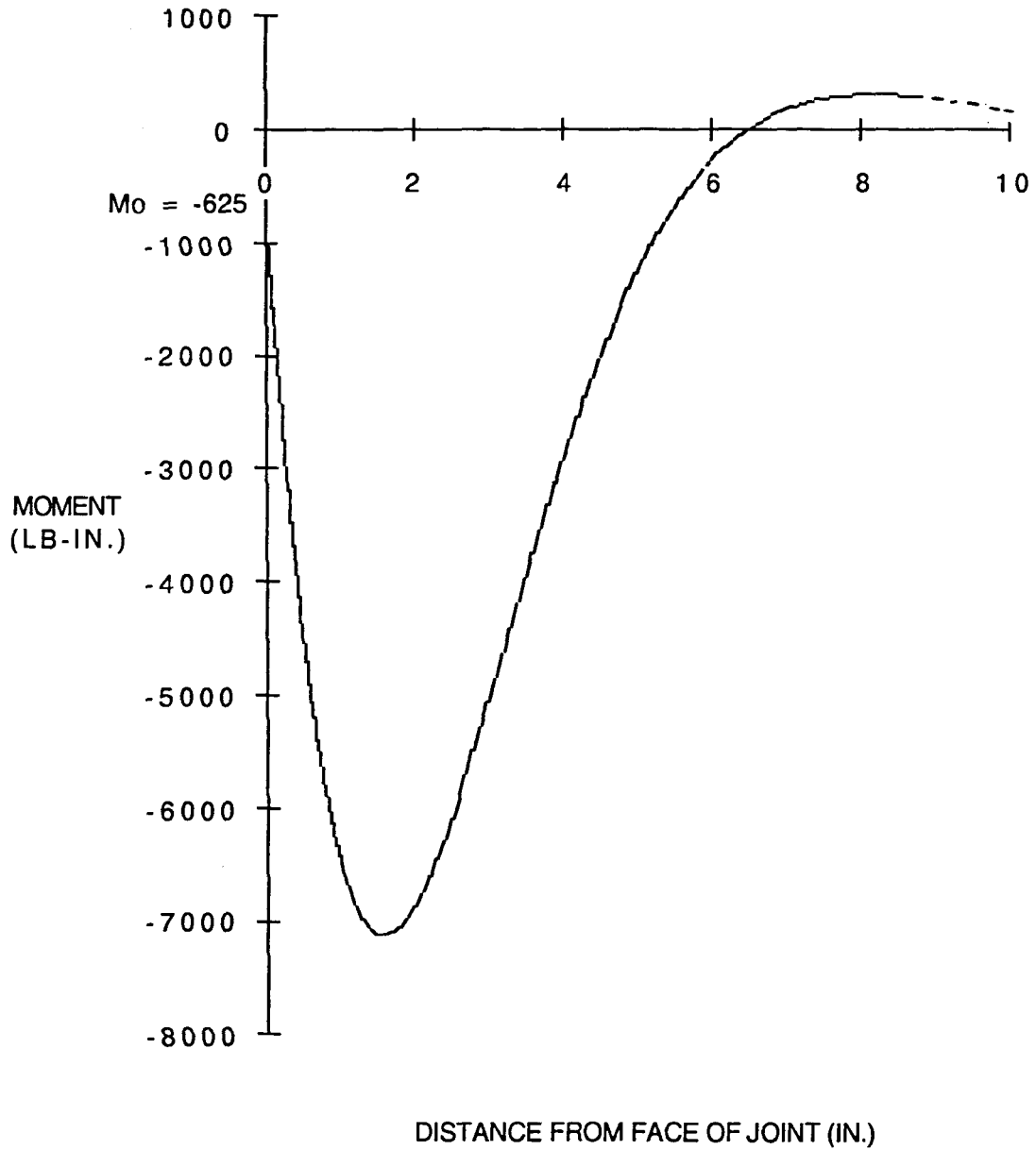specimens using the Timoshenko analysis method

Figure 3.12. Moment diagram for a 1.25-inch fibercomposite dowel
of average stiffness of the specimens using the
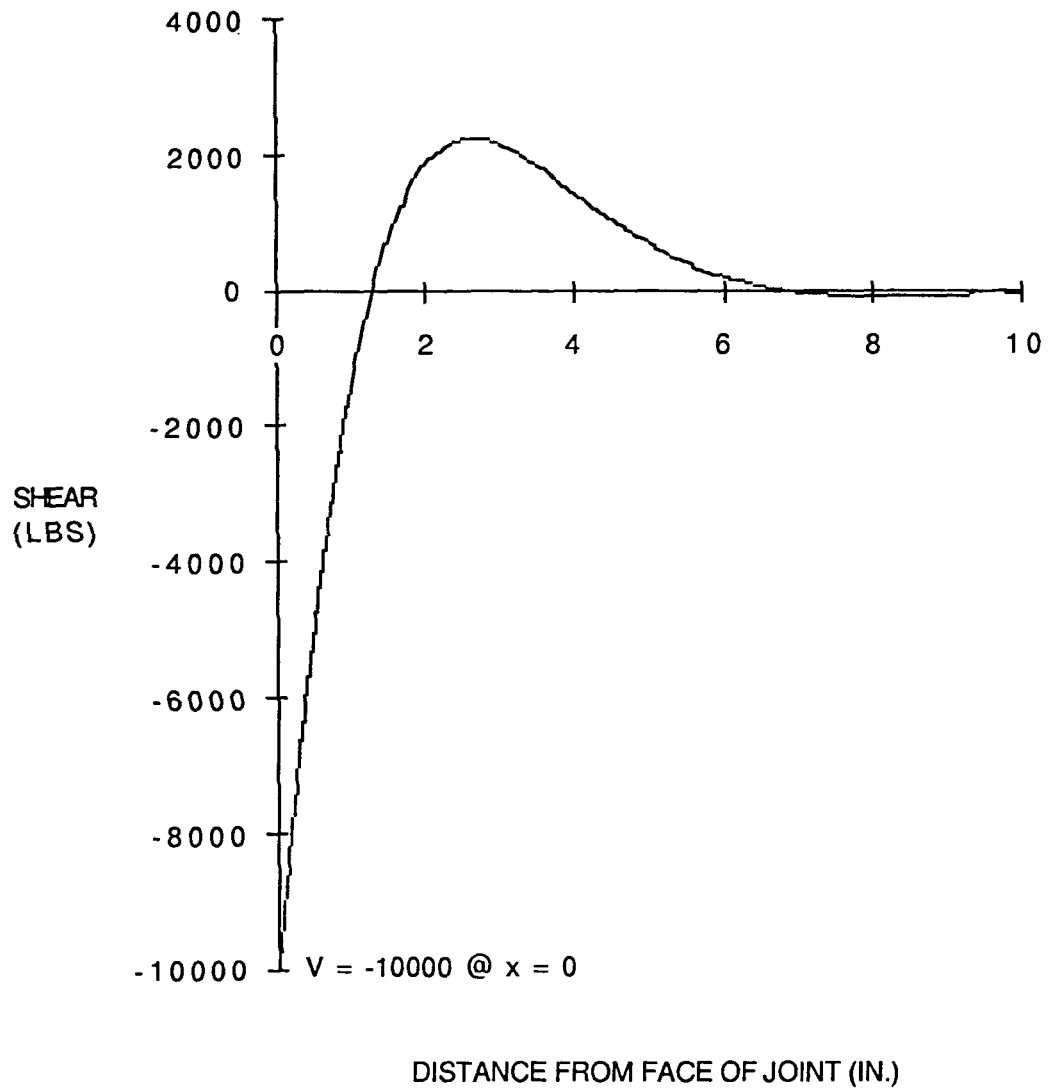Timoshenko analysis method

Figure 3.13. Shear diagram for a 1.25-inch fibercomposite dowel of average stiffness of the specimens using the Timoshenko analysis method
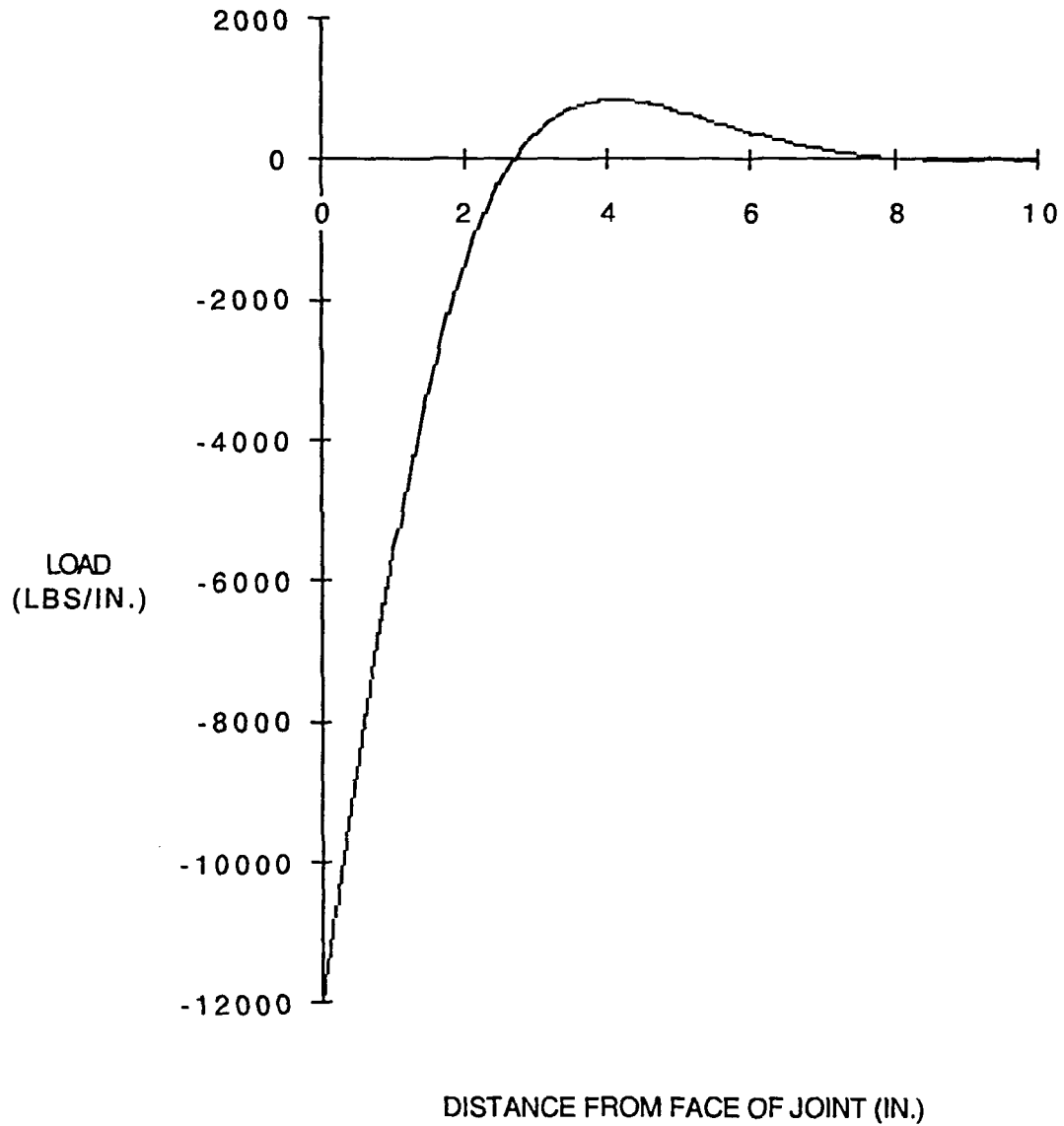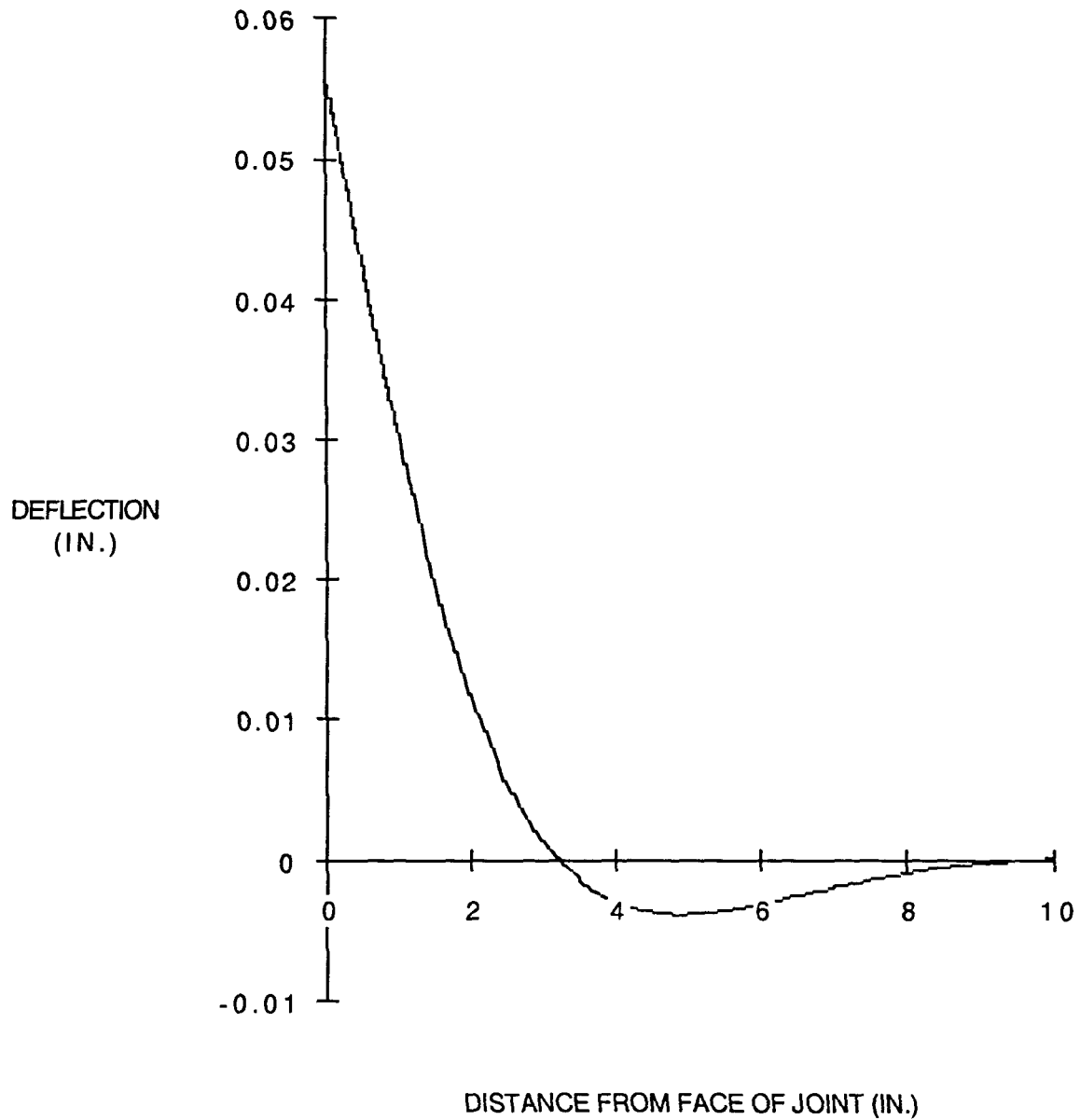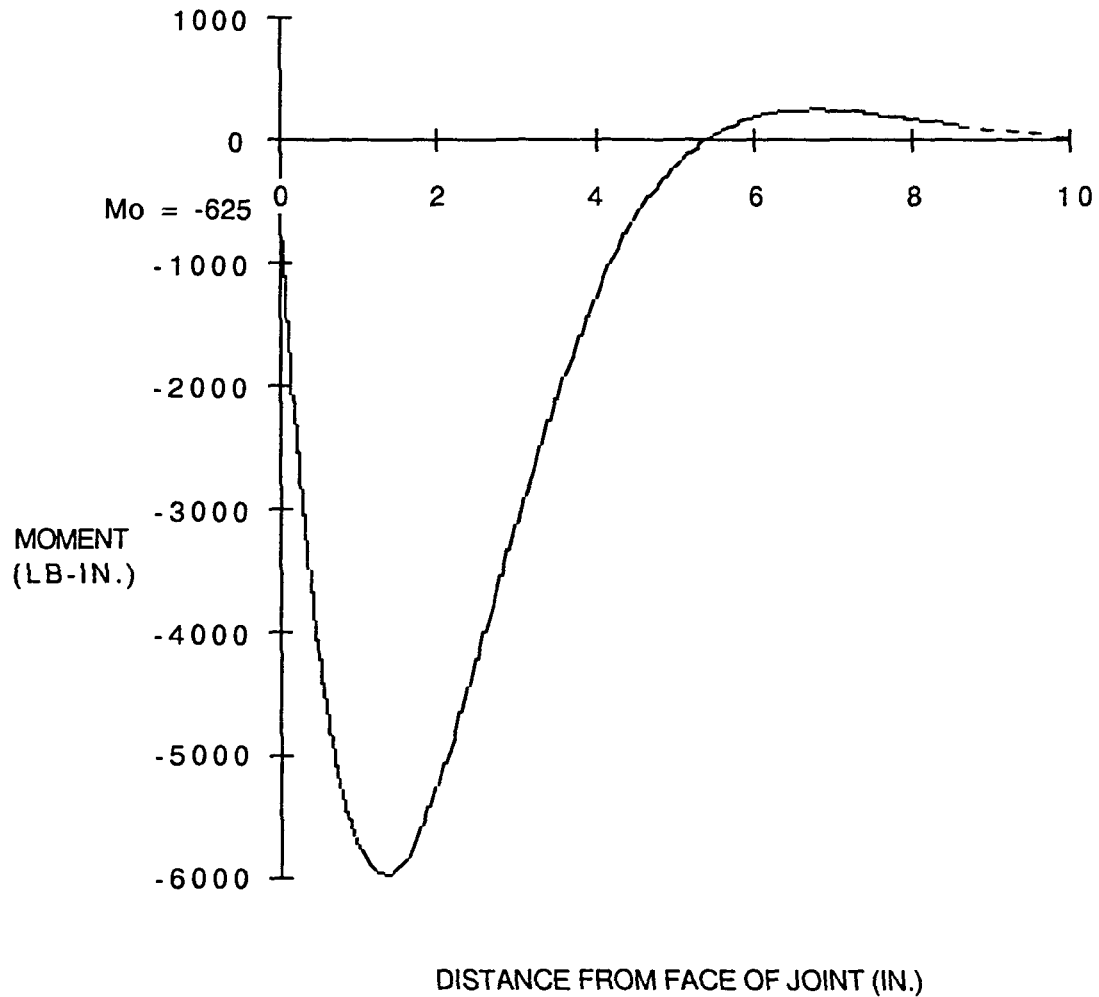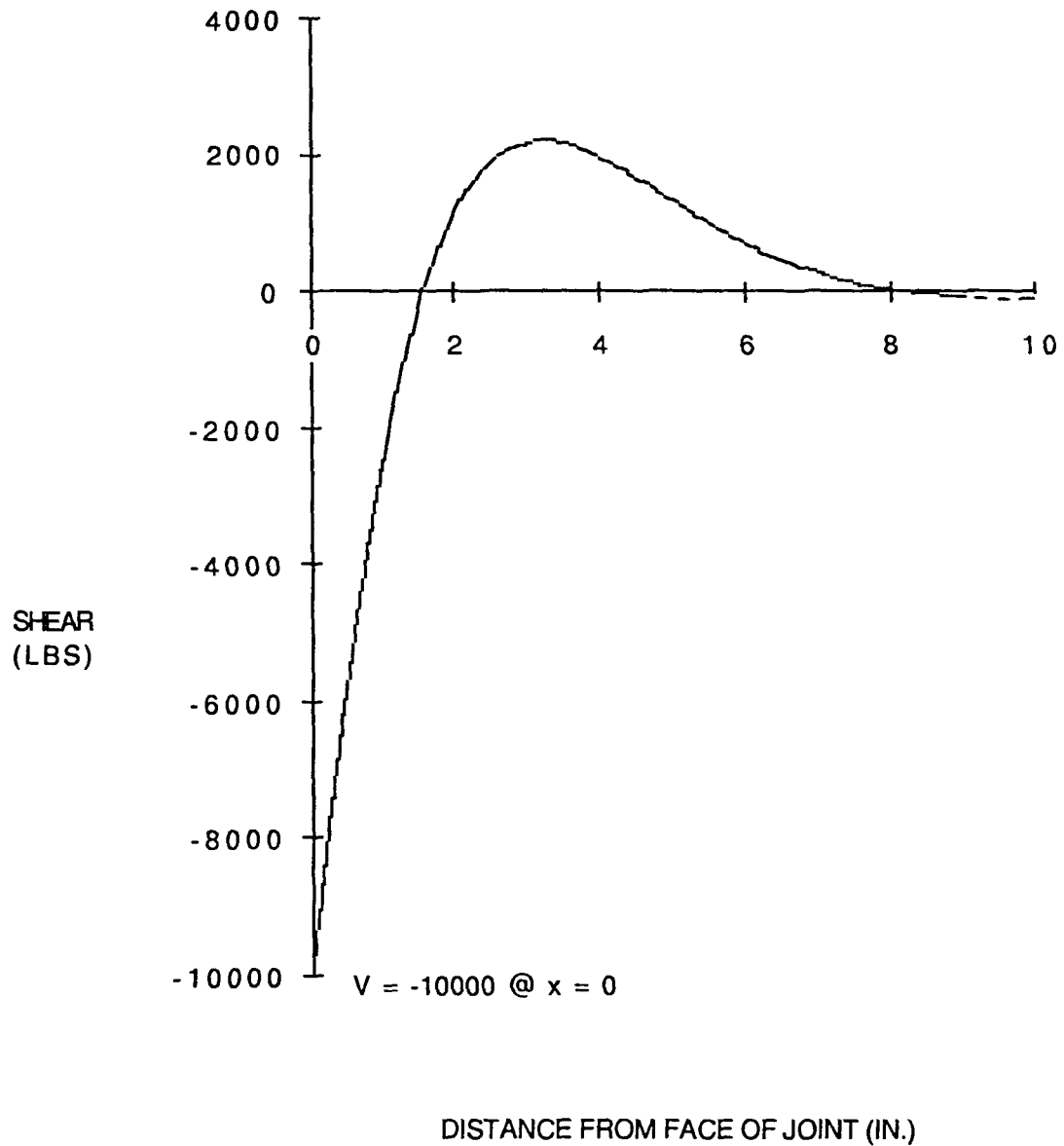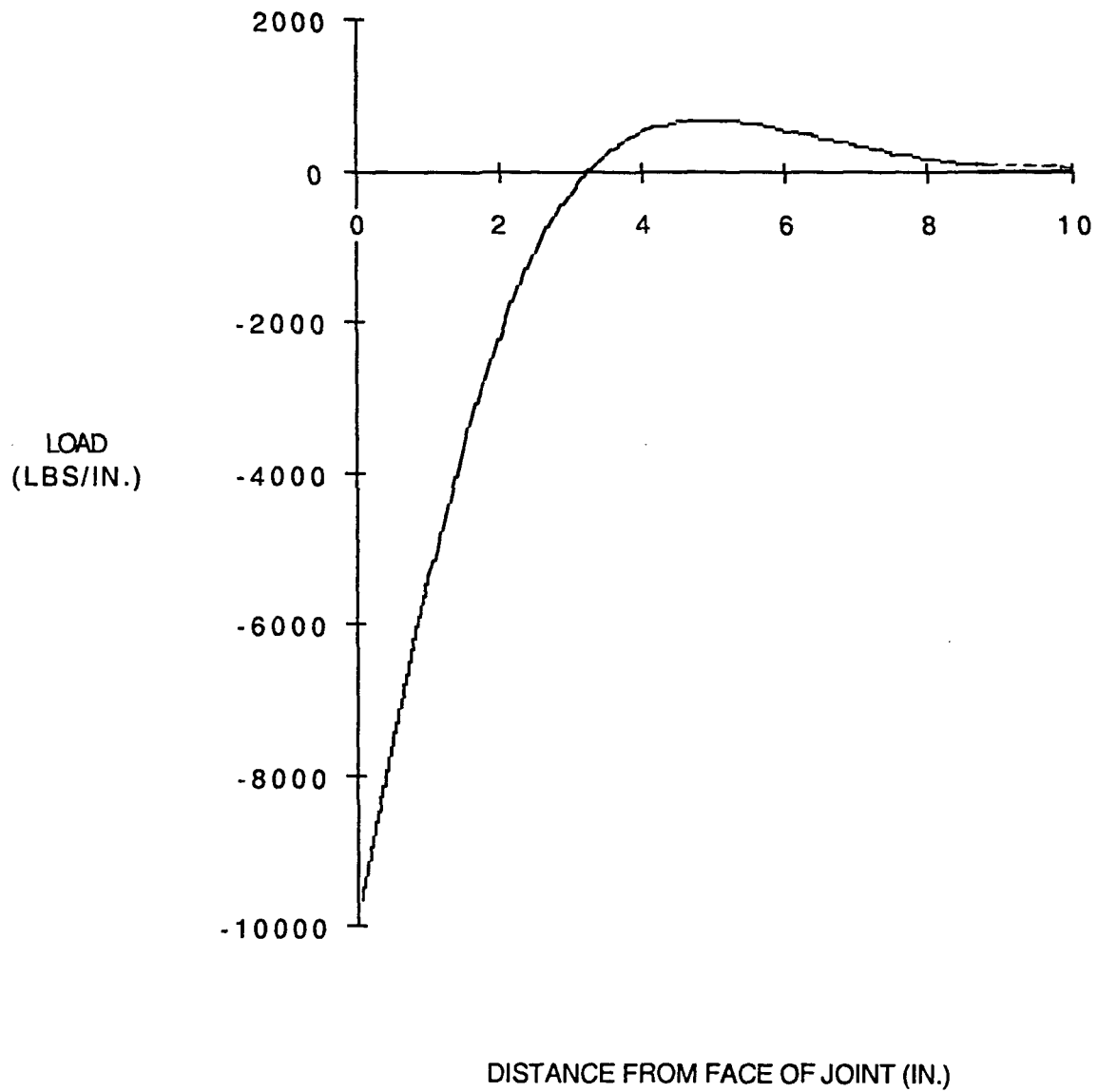
Figure 3.14. Load diagram for a 1.25-inch fibercomposite dowel of average stiffness of the specimens using the Timoshenko analysis method

Table 3.7. ß and ßL values

Specimen Type	k value (psi)	ß (in.$^{-1}$)	ßL
Steel Specimen of Average Stiffness	3,210,000	0.577	5.20
Fibercomposite Specimen of Average Stiffness	176,000	0.480	4.32

3.5   Finite-Length Beam on an Elastic Foundation

Previously, a solution to the beam on an elastic foundation assumed that the beam was semi-infinitely long, i.e., infinitely long from the face of the joint. For some situations, using a solution that assumes that the beam is semi-infinitely long or using a solution that takes into account the actual finite length of the beam will virtually make no difference in the accuracy of the results. For other situations, however, assuming that the beam is semi-infinitely long can yield incorrect results. The point at which this assumption gives accurate results is a function of ßL and is given in some references on beams on elastic foundations as 5 to 6 [13, 40]. However, the value of ßL at this point is not well defined for a pavement dowel bar situation [13]. Because the results of this research program generated ßL values that made the applicability of

the semi-infinitely long beam solution approach questionable, the finite-length beam solution approach was also investigated.

3.5.1   Finite-length beam solution approach

As discussed in Section 1.4.1.1, the general equation for the deflection of the dowel along its axis was determined by Timoshenko to be as follows[13]:

$$y = e^{\beta x}(A_t \cos \beta x + B_t \sin \beta x) + e^{-\beta x}(C_t \cos \beta x + D_t \sin \beta x)$$

$$(1.3)$$

The difference between the semi-infinitely long beam solution and the finite-length beam solution approaches lies in the boundary conditions assumed to solve this equation. The boundary conditions for the semi-infinitely long beam solution, which are discussed in Section 1.4.1.1, are that (1) the moment at the face of the joint is M_0, (2) the shear at the face of the joint is equal to P, and (3) the moment, and (4) the deflection at a distance of infinity away from the face of the joint both equal zero [13]. Assuming that the deflection and the moment equal zero at a distance of infinity away from the face of the joint, A and B will equal zero. For the finite-length beam solution approach, the four boundary conditions are that: (1) the moment at the face of the joint is M_0, (2) the shear at the face of the joint is P, (3) the moment at a distance of L from the

face of the joint is zero, and (4) the deflection at a distance of L from the face of the joint is zero.

Alternate boundary condition combinations are possible. For example, two other possible boundary conditions for (3) and/or (4) are that the shear at a distance L away from the face of the joint can be equal to either zero or the value of a point force existing at the end of the dowel. An alternate boundary condition was used in Ref. 42. Boundary condition (4) was that the shear at a distance of L away from the face of the joint is equal to zero. The difference in the results generated by these sets of boundary conditions was found to be insignificant.

The difference in the two solution approaches becomes evident when the last two boundary conditions for each approach are compared: the finite-length beam solution will have nonzero answers for all four constants, whereas the semi-infinitely long beam solution will have nonzero answers for only two of the constants. Because two additional boundary conditions must be determined, the finite-length beam solution approach is more complex to utilize.

3.5.2   Solution to the finite-length beam problem

The general equation for a finite-length beam on an elastic foundation is [13]:

$$y = e^{\beta x}(A_t \cos\beta x + B_t \sin\beta x) + e^{-\beta x}(C_t \cos\beta x + D_t \sin\beta x) \quad (1.3)$$

The boundary conditions used to solve for the constants A_t, B_t, C_t, and D_t are:

1) $y'' = -M_0/EI_z$ at the face of the joint (x=0)

2) $y''' = -V/EI_z$ at the face of the joint (x=0)

3) $y'' = 0$ at the end of the dowel (x=L)

4) $y = 0$ at the end of the dowel (x=L)

where:

M_0 = Bending moment in the dowel at the face of the joint (lb-in.) = $-PZ/2$

V = Shear force on a cross section (at the face of the joint) = $-P$

To arrive at the solution to this equation, the second and third derivatives of the general solution must be known. They are:

$$y'' = \beta^2 e^{\beta x}(-2A_t \sin\beta x + 2B_t \cos\beta x)$$
$$+ \beta^2 e^{-\beta x}(2C_t \sin\beta x - 2D_t \cos\beta x) \quad (3.2)$$

and

$$y''' = \beta^3 e^{\beta x}(-2A_t \cos\beta x - 2A_t \sin\beta x + 2B_t \cos\beta x - 2B_t \sin\beta x)$$
$$+ \beta^3 e^{-\beta x}(2C_t \cos\beta x - 2C_t \sin\beta x + 2D_t \cos\beta x + 2D_t \sin\beta x)$$

$$(3.3)$$

Simultaneously solving the four equations corresponding to the four boundary conditions results in the following solutions for the four constants $A_t, B_t, C_t,$ and D_t:

$$A_t = \frac{[-(con4 + con5)/con6]con1 + con2}{con3} \qquad (3.4)$$

$$B_t = \frac{PZ}{4\beta^2 EI_z} - \frac{(con4+con5)}{con6} \qquad (3.5)$$

$$C_t = \frac{P}{2\beta^3 EI_z} - \frac{PZ}{4\beta^2 EI_z} - \frac{[(con4+con5)/con6]con1 + con2}{con3}$$
$$+ \frac{2(con4+con5)}{con6} \qquad (3.6)$$

$$D_t = -(con4+con5)/con6 \qquad (3.7)$$

where:

$$con1 = 2e^{\beta L}\cos(\beta L) + e^{-\beta L}(-4\sin(\beta L) - 2\cos(\beta L)) \qquad (3.8)$$

$$con2 = e^{\beta L}[(PZ)/(2\beta^2 EI_z)]\cos(\beta L) + e^{-\beta L}[(P/\beta^3 EI_z) - (PZ/2\beta^2 EI_z)]\sin(\beta L) \qquad (3.9)$$

$$con3 = 2e^{\beta L}\sin(\beta L) - 2e^{-\beta L}\sin\beta L \qquad (3.10)$$

$$con4 = e^{\beta L}\cos(\beta L)(con2/con3) + e^{\beta L}\sin(\beta L)(PZ/4\beta^2 EI_z) \qquad (3.11)$$

$$con5 = e^{-\beta L}\cos(\beta L)[(P/2\beta^3 EI_z) - (PZ/4\beta^2 EI_z) + con2/con3] \qquad (3.12)$$

$$con6 = e^{\beta L}[(con1\cos(\beta L)/con3) + \sin(\beta L)]$$
$$+ e^{-\beta L}[\sin(\beta L) + \cos(\beta L)((con1/con3)-2)]$$

$$(3.13)$$

The finite-length beam solution is obviously more complicated to use than the semi-infinitely long beam length solution. However, the method used to calibrate the finite-length beam solution approach with the experimental results is exactly the same as the method used with the semi-infinite solution approach, which was described in Section 3.4.1.1

3.5.3 Comparison of finite-length beam and semi-infinitely long beam solutions

As described in the previous section, the semi-infinitely long beam solution is much easier to apply to a beam on an elastic foundation than the finite-length beam solution. As its name indicates, the semi-infinitely long beam solution theoretically only applies to semi-infinitely long beams--which could never occur. Therefore, what needs to be determined is: (1) when the semi-infinitely long beam solution approach can be applied to a finite-length beam, and (2) the difference between the two solution approaches. As described in Refs. 13 and 40, the applicability of the semi-infinitely long beam solution can be determined by comparing the βL of the finite-length beam to known limits of βL corresponding to the limit of the applicability of the semi-infinitely long beam solution approach. If the βL value for the actual beam is

greater than the ßL limit, the semi-infinitely long beam solution can be used to arrive at results with little or no error in comparison to the finite-length beam solution. The limiting ßL values given in Ref. 13 and 40 are not specifically intended for a pavement dowel situation; therefore, the limiting ßL value for the applicability of the semi-infinitely long beam solution approach was not known. To determine the limiting ßL value, analyses made at various ßL values for both the semi-infinitely long and finite-length beam solution approaches were compared. The comparisons of the results for the moment and deflection are shown in Figure 3.15 and given in Table 3.8. As indicated in Figure 3.15 and Table 3.8, there are virtually no differences in the results for the deflections and the moments between the two analysis approaches when ßL is greater that 2. At a ßL value of 2, the semi-infinitely long beam solution method has an error of 0.4 percent for the calculated deflection at the face of the joint and an error of 1.8 percent for the calculated maximum moment, as compared to the finite-length beam solution. This amount of error is certainly should be within the tolerances of accuracy.

3.5.4. Comparison of finite-length beam and semi-infinitely long beam solutions for the dowels of average stiffness in the research program

The fibercomposite dowel of average stiffness has a ßL value of 4.32, as given in Section 3.4.1.2. The steel dowel of average
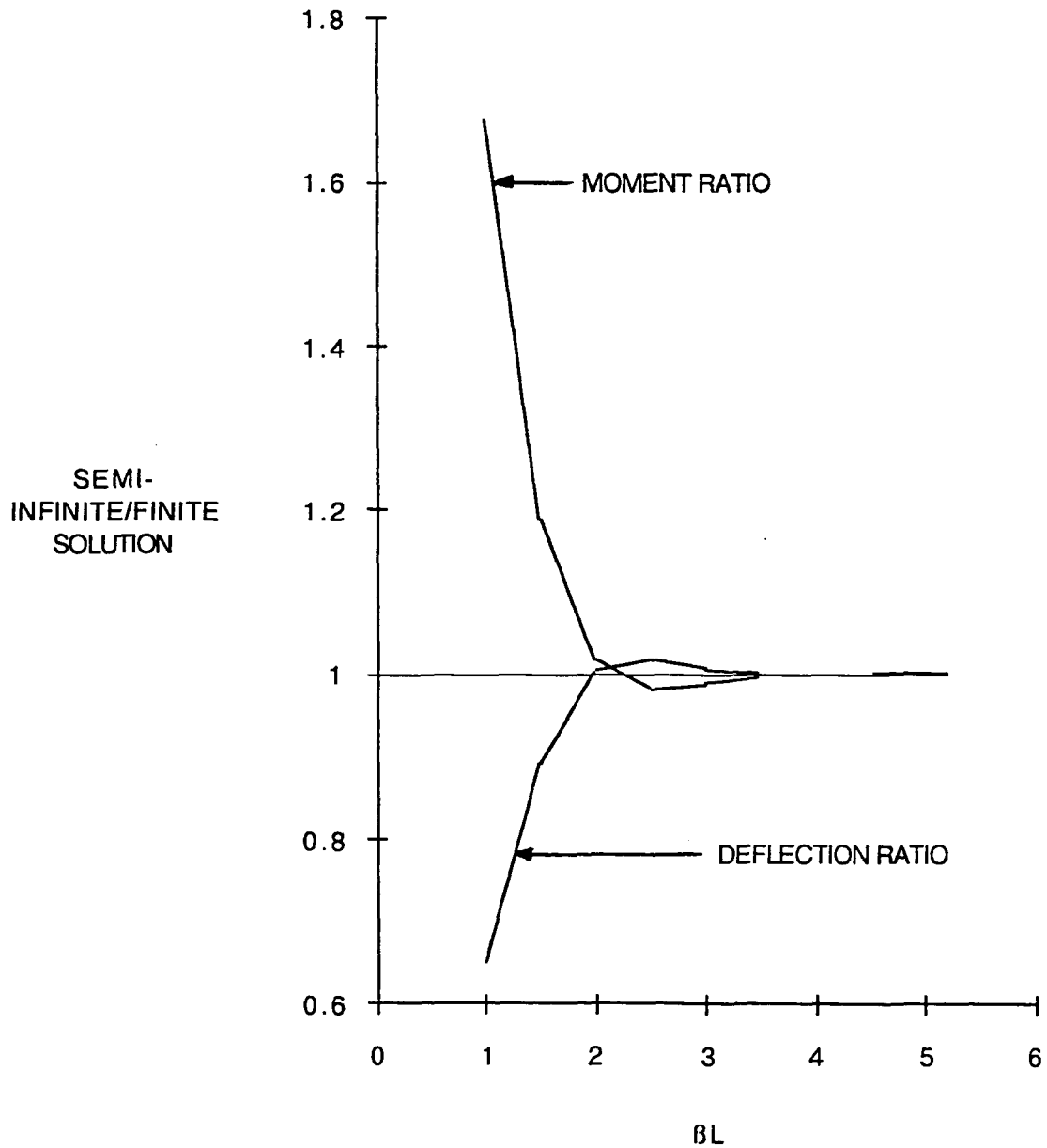
Figure 3.15. Comparison of moments and deflections at various ßL
values for the semi-infinitely long beam and finite-
length beam analysis approaches

Table 3.8. Comparisons of maximum moments and deflections for semi-infinitely long and finite-length beam solutions

βL	$\dfrac{\text{Semi-infinite Deflection}}{\text{Finite Deflection}}$	$\dfrac{\text{Semi-infinite Moment}}{\text{Finite Moment}}$
1.0	0.65	1.68
1.5	0.89	1.19
2.0	1.00	1.02
2.5	1.01	0.98
3.5	1.01	0.99
4.5	1.00	1.00
5.2	1.00	1.00

stiffness has a βL value of 5.2, as indicated in Section 3.4.1.2. Both of these βL values are far above the proposed minimum βL limit of 2.0 given in the previous section. Based on this information, the semi-infinitely long beam solution approach is applicable to the dowels of average stiffness that were used in this research program. According to the previous section, the error in using the semi-infinitely long beam solution approach versus the finite-length beam solution approach should be slight. For comparison purposes, the deflection, shear, moment and load diagrams are presented for both analyses for a fibercomposite dowel of average stiffness in Figures 3.16 through 3.19. Table 3.9 compares the maximum deflections, shears, moments, and load lengths of the steel and fibercomposite dowels of average stiffness for both the semi-infinitely long beam and finite-length beam solution approaches.
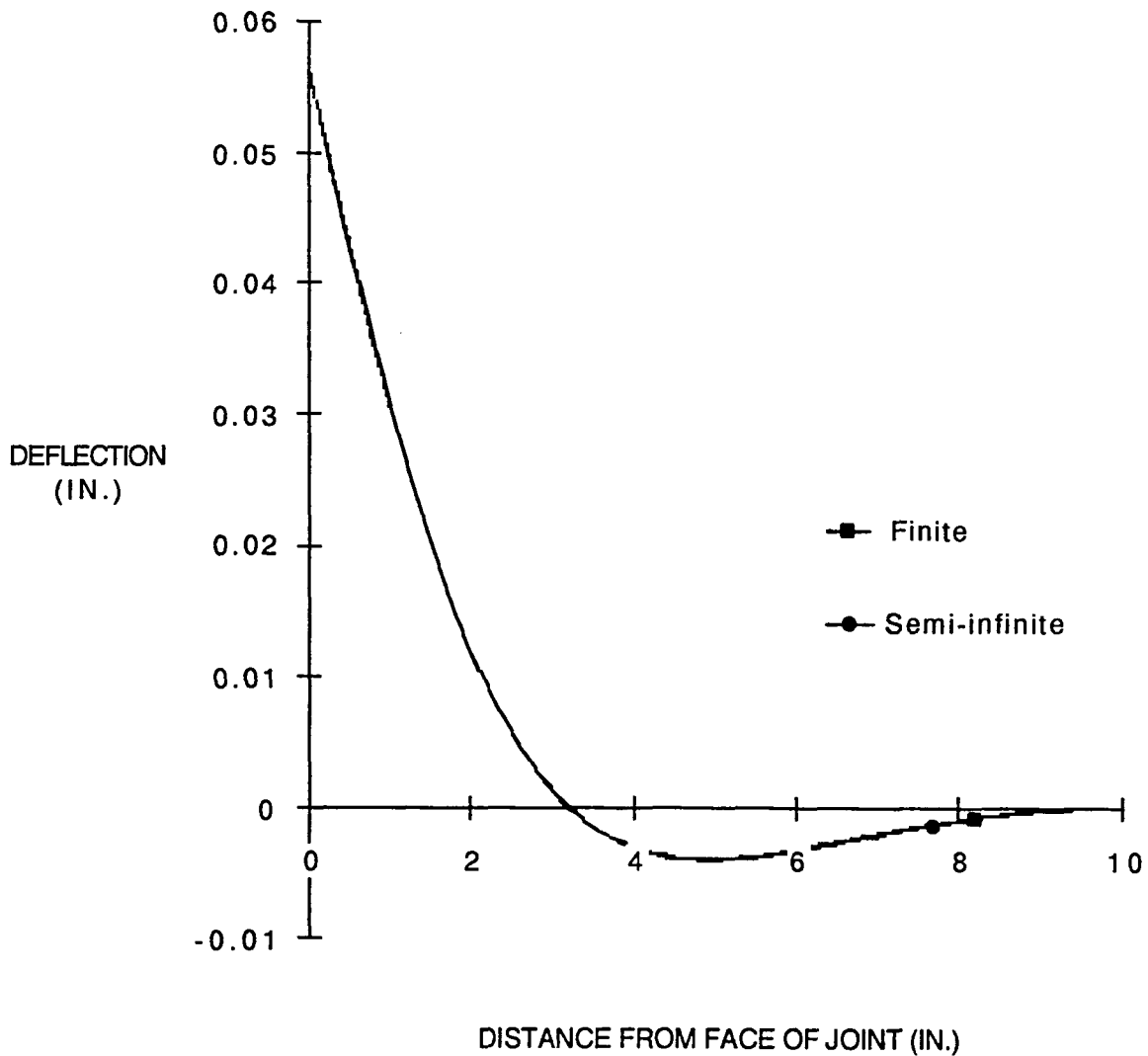
Figure 3.16. Deflection diagrams for 1.25-inch fibercomposite
dowel of average stiffness for semi-infinitely long
beam and finite-length beam analysis approaches

Figure 3.17. Moment diagrams for 1.25-inch fibercomposite dowel of average stiffness for semi-infinitely long beam and finite-length beam analysis approaches

Figure 3.18. Shear diagrams for 1.25-inch fibercomposite dowel of average stiffness for semi-infinitely long beam and finite-length beam analysis approaches
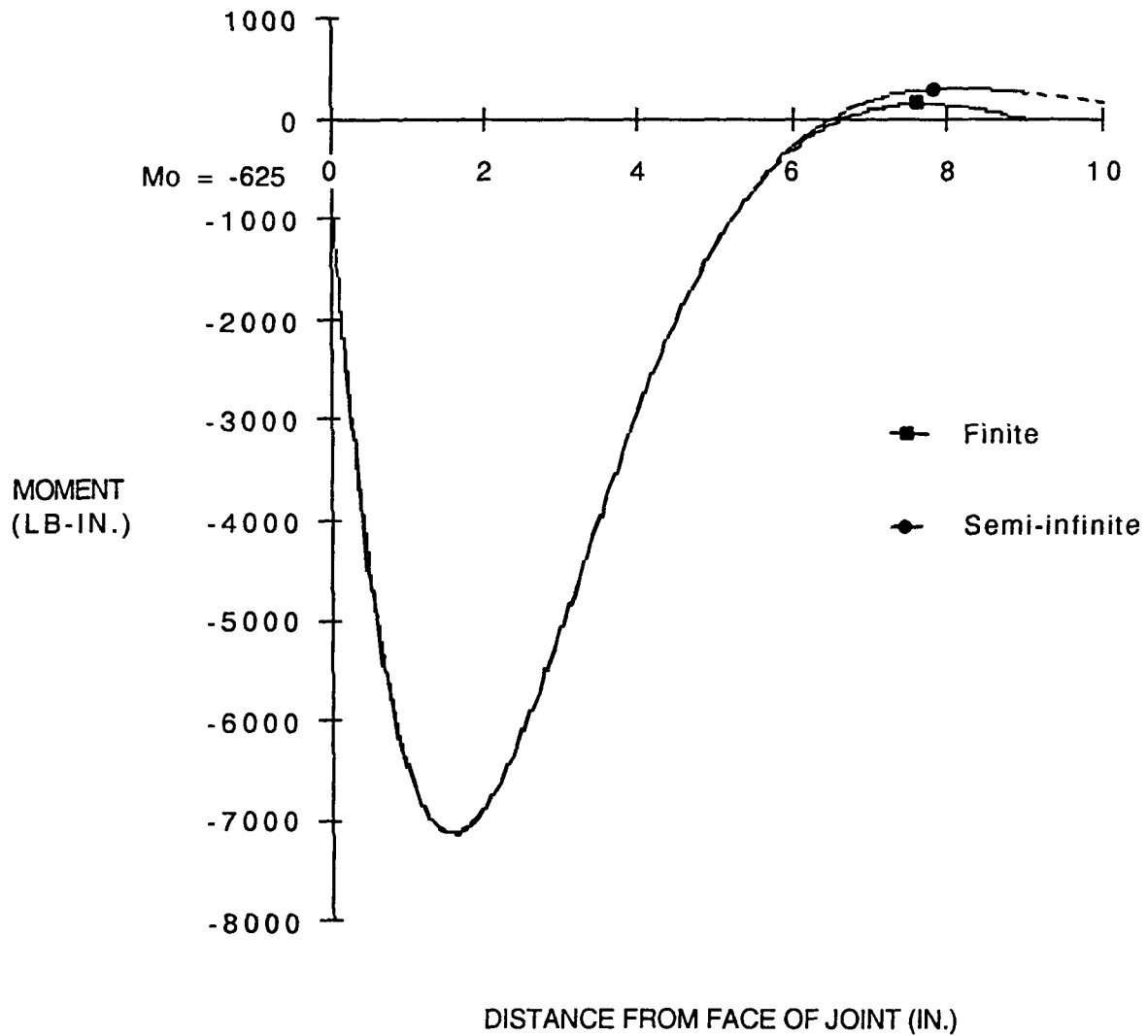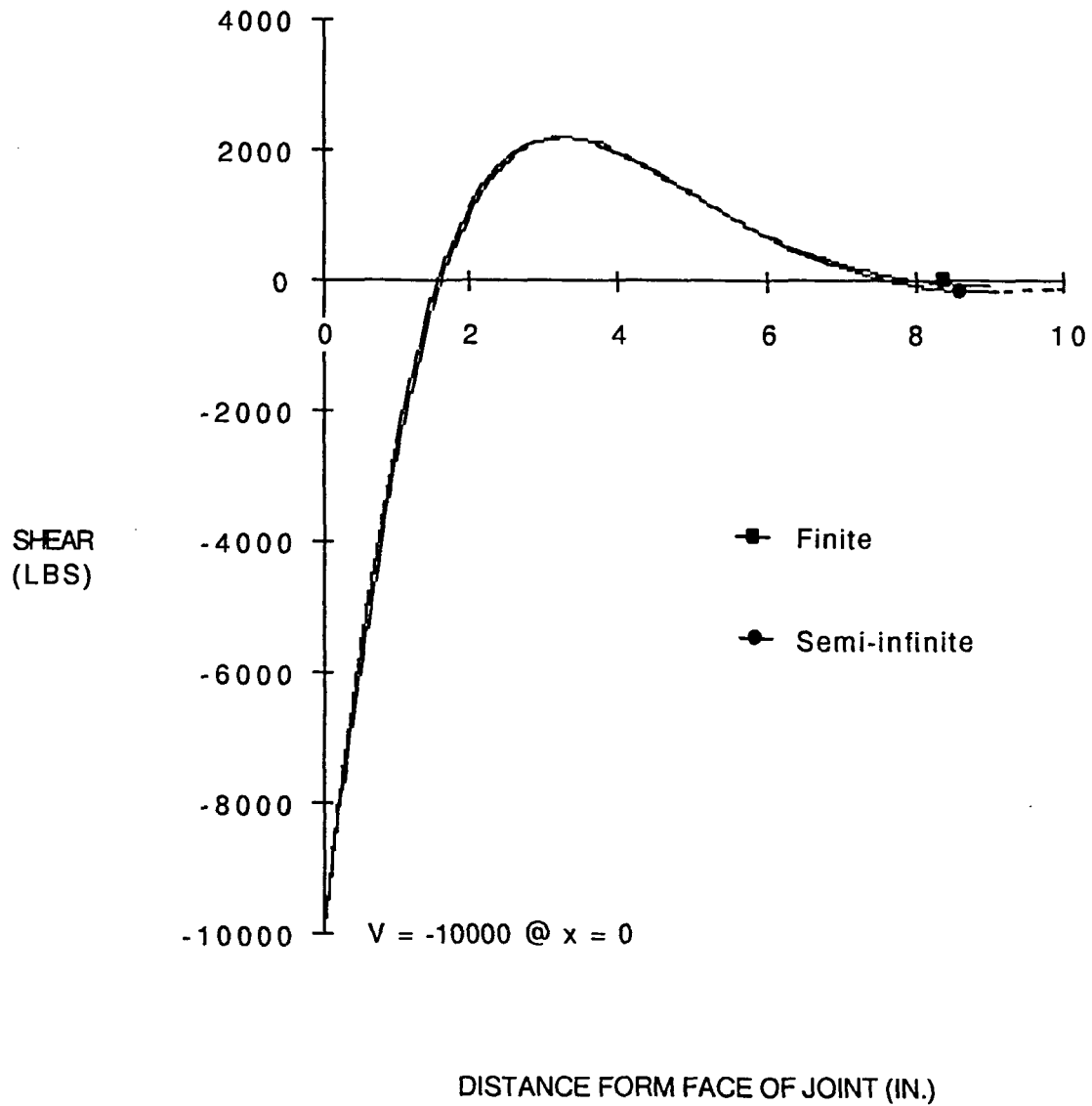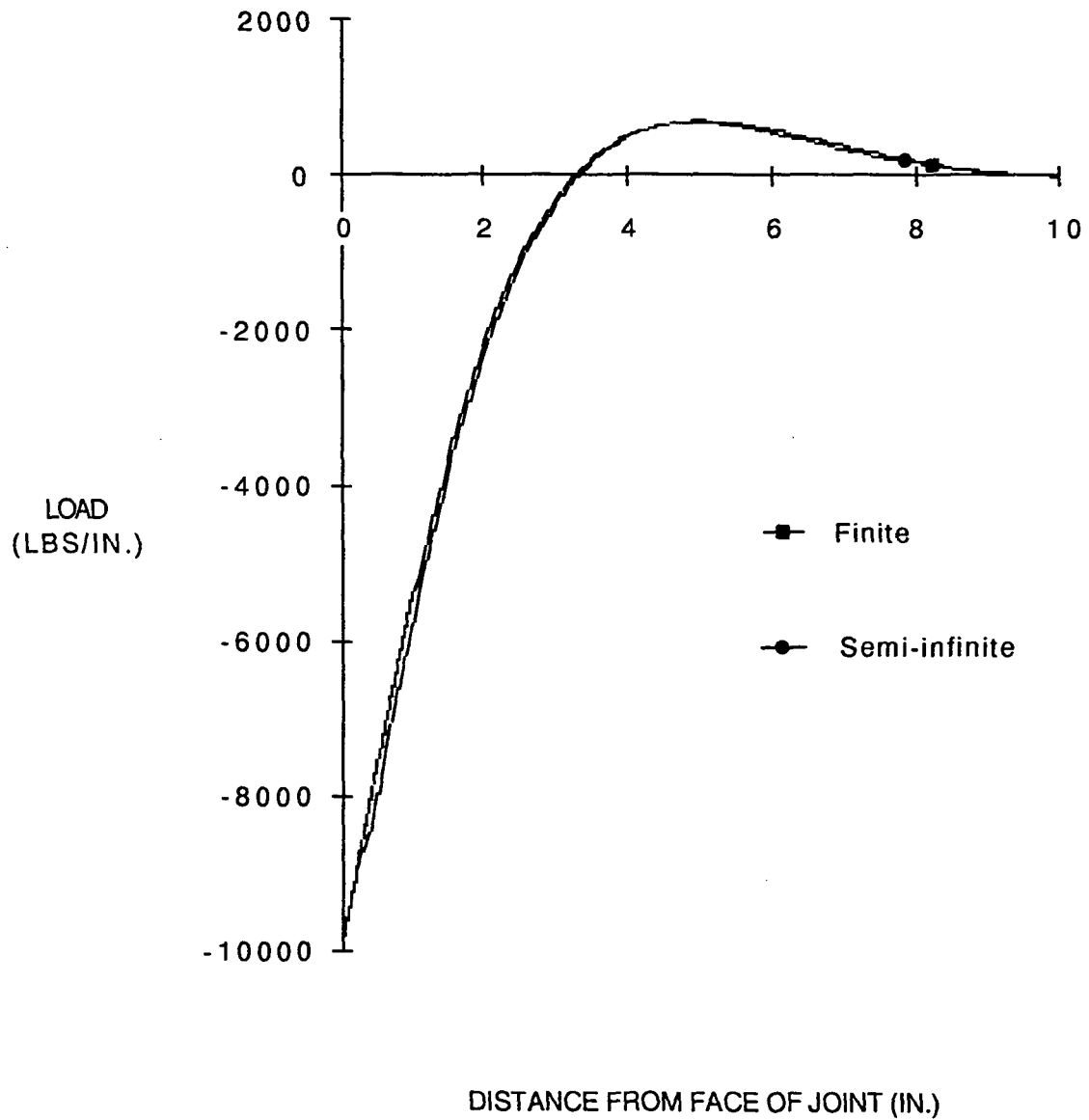
Figure 3.19. Load diagrams for 1.25-inch fibercomposite dowel of average stiffness for semi-infinitely long beam and finite-length beam analysis approaches

Table 3.9. k values, maximum deflections, shears, moments, and loads/lengths for steel and fibercomposite dowels for semi-infinitely long beam and finite-length beam solutions

	Fibercomposite		Steel	
	Semi-infinite	Finite	Semi-infinite	Finite
k value (psi)	176,000	176,000	3,210,000	3,210,000
Deflection (in.)	0.0563	0.0563	0.00373	0.00373
Shear (lbs)	10,000	10,000	10,000	10,000
Moment (lb-in.)	7,120	7,120	5,990	5,990
Load/ Length (lbs/in.)	9,860	9,880	12,200	12,000

3.6. Bearing Capacity of Concrete

Table 3.9 and Figures 3.16 through 3.19 show that the two solution approaches give virtually identical answers. The only differences between the two solution approaches lie in the results at the far end of the dowel bar. The semi-infinitely long beam solution approach results do not converge to zero at the far end of the dowel bar like the finite-length beam solution approach results do. This is of little or no significance because the values at the

www.manaraa.com

ends of the bar are small and have no affect on the design of the dowel bar. Therefore, as assumed in Section 3.4, that the semi-infinitely long beam solution approach is applicable for the dowels tested in this research program and that the results of using this analysis approach are nearly identical in all aspects to the results obtained using the finite-length beam solution approach. Because the finite-length beam solution approach is more complicated than the semi-infinitely long beam solution approach, and the accompanying difficulty in developing an understanding of the dowel behavior for the more complicated solution approach, the semi-infinitely long beam solution approach is a better and more practical analysis approach for the dowels in this research program.

Existing bearing capacity theories assume that a uniform pressure exists on the loading area [21-23]. In the case of the pavement dowel, the pressure can best be described as a three-dimensional, elliptical paraboloid that is defined by orthogonal parabolic lines [43]. Figure 3.20 illustrates the elliptical, paraboloid-shaped bearing stress distribution. The elliptical paraboloid pressure distribution has high pressures under the center of the dowel at the face of the joint and rapidly decreasing pressures away from the center of the dowel at the face of the joint. Very high bearing stresses occur under the centerline of the dowel at the face of the joint.

Previous studies of the bearing strength of concrete, masonry, and stone determined the bearing strength of the material at
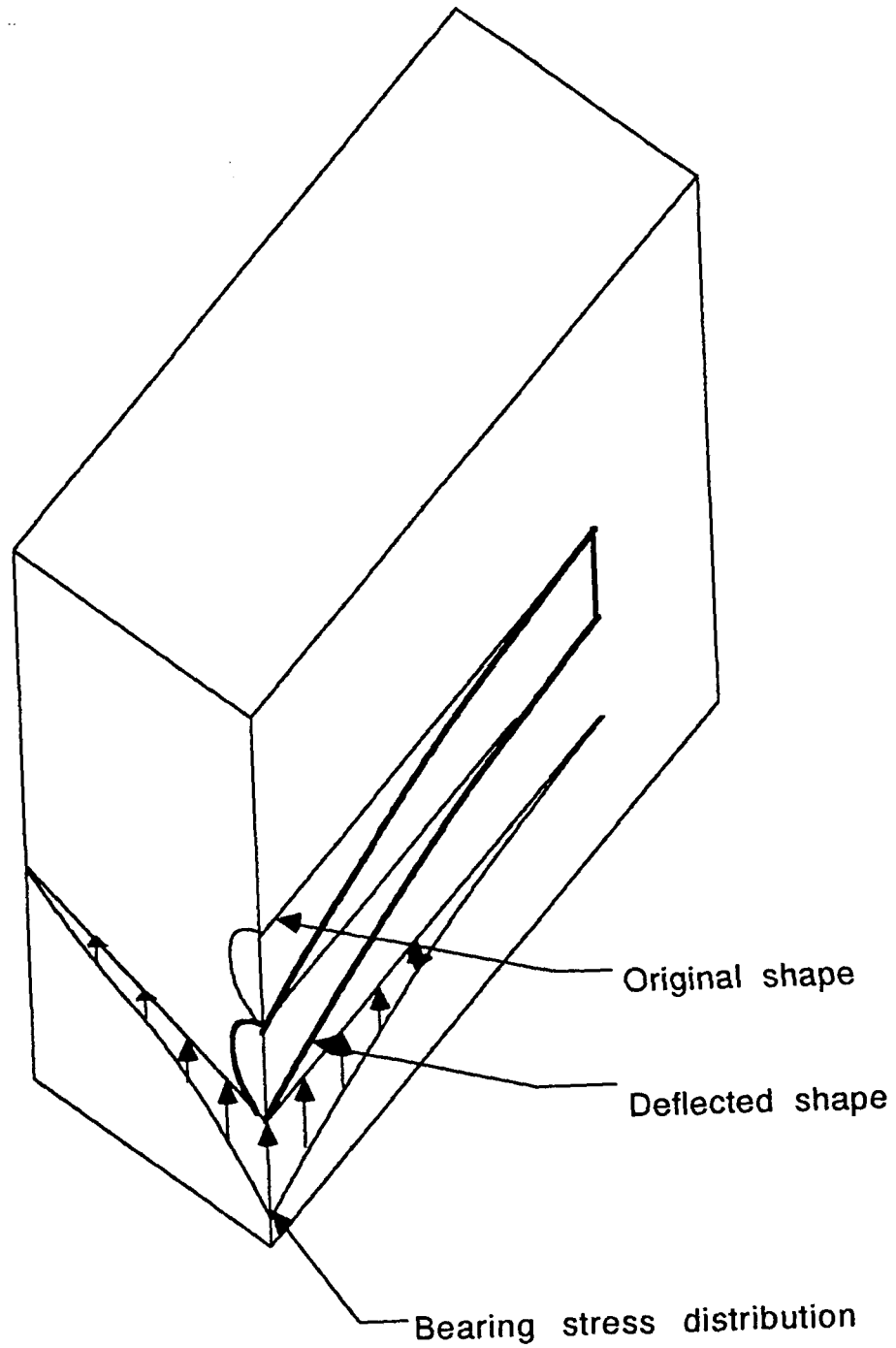
Figure 3.20. Elliptical paraboloid bearing stress distribution

different material strengths and/or at different ratios of bearing area to supporting area [18 to 23]. Literature dealing with the bearing strength of concrete under nonuniform loading conditions could not be found, so a subjective decision was made on which behavior models and analysis methods should be used in this situation.

Prior to analyzing the complex stress situation occurring in the concrete surrounding the pavement dowel, a decision was made to keep the information resulting from this research program in a simple format. Engineers designing joints should be able to utilize this information easily and receive a basic understanding of the behavior of the dowel joint system.

The most usable design process for bearing capacity was the process outlined in the ACI Code [44]. To be able to use the ACI method, two parameters had to be determined: an equivalent area to transfer the entire joint load, and the magnitude of the factor that takes into account the confinement effects of the concrete surrounding the loaded area [44]. Figure 3.21 shows the assumed bearing stress situation to be used in conjunction with the ACI Code.

For clarity, an equivalent area was determined in which the load being transferred across the joint distributes itself into the supporting concrete. The bearing capacity of the joint would then be the equivalent area times the compressive strength of the concrete times a factor accounting for the confinement effects. This method
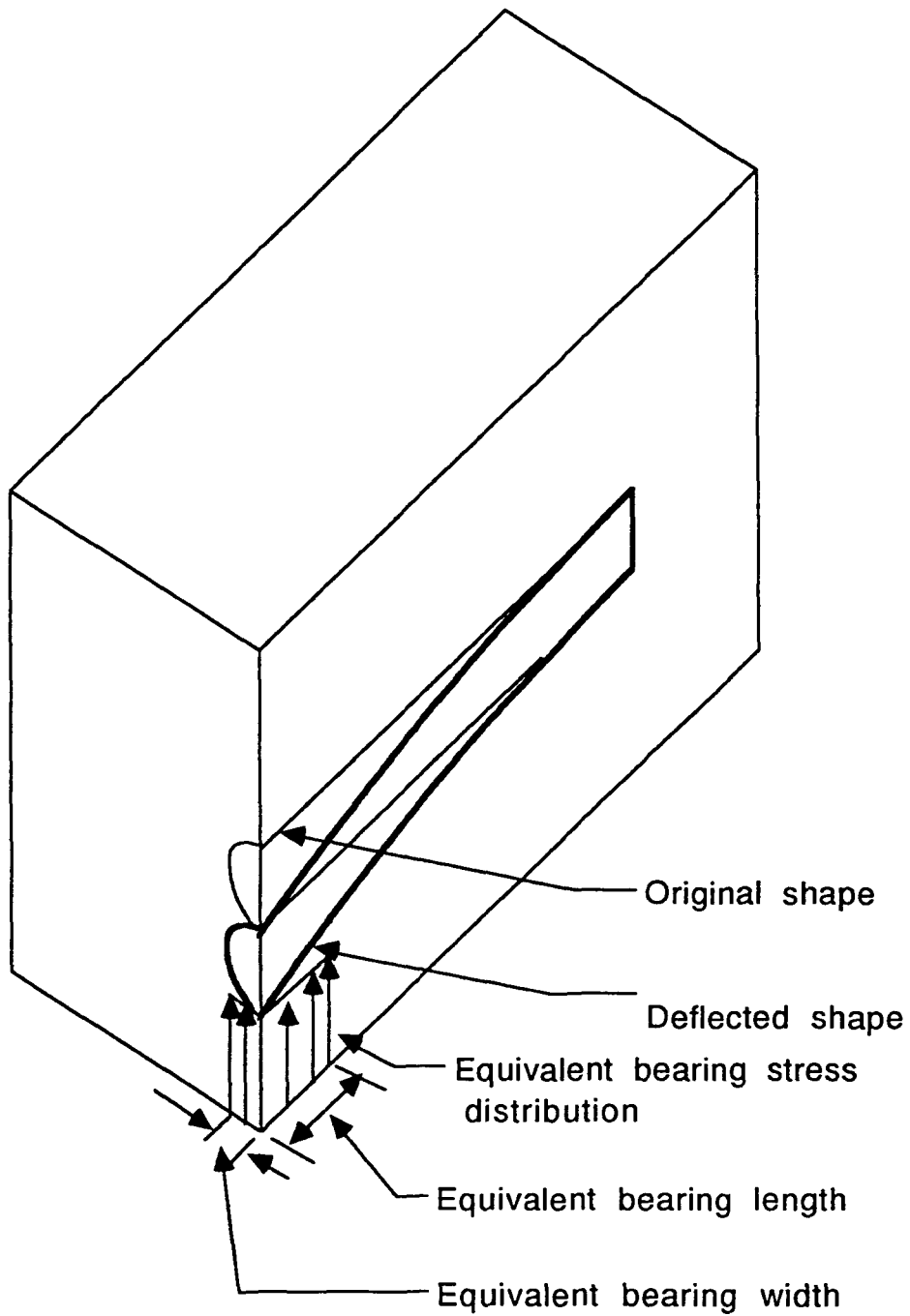
Figure 3.21.   Equivalent bearing area

would be similar to current methods used in the ACI Code for determining the bearing capacity of concrete [44].

The width of the equivalent area was chosen to be the diameter of the bar. The actual behavior of the distribution of stress in this direction is a logarithmic relationship [18]. The bearing stress reaches a high peak directly under the centerline of the bar, but the stress in the concrete diminishes away from the centerline of the dowel.

The length for the equivalent area was more difficult to determine. Figures 3.10 and 3.14 give the load diagrams for the steel and fibercomposite dowels of average stiffness. The figures show a nearly linear relationship from the face of the joint to the point where the load equals zero. The center of gravity of the load function over this distance would be approximately one-third of the distance from the face of the joint to the point where the load equals zero. By letting the center of gravity of the equivalent bearing length coincide with the center of gravity of this portion of the load, the equivalent bearing length would be two-thirds of the distance from the face of the joint to the point where the load function equals zero.

To find what the previous bearing capacity research programs would predict to be the bearing capacity of the dowels, the ratio of supporting area to bearing area must be known [21-23]. The ACI code specifies that the supporting area must be similar in shape with a center of the area coincident with the loading area. For the

case of the pavement dowel, where the load is being applied adjacent to an edge, the maximum similar shaped area for the supporting area would be the loading area. As a result, the ratio of the supporting area to the loading area is equal to one.

3.7   Shear Cone Capacity of Concrete

The shear cone capacity of concrete was discussed in Section 1.4.3. The shear cone capacity of the concrete can be determined according to the method outlined in the PCI Design Handbook. The values to use for x_{pci} and y_{pci} are the equivalent width and length as determined in Section 3.6.

4. DESIGN PROCESS FOR A DOWELED PAVEMENT JOINT

4.1. Introduction

The design of any structural system must address all of the parameters that can affect its behavior. In the design of a doweled pavement joint, there are several parameters that must be considered, including: the bearing capacity of the concrete supporting the dowel, the shear capacity of the dowel, the moment capacity of the dowel, the shear cone capacity of the concrete, and the load-deflection characteristics of the system.

This chapter of the research report is intended to give design engineers an empirical approach to the design of a doweled pavement joint based primarily on a simplified version of the Timoshenko analysis method. The design approach includes factors relating the analysis methods to the results obtained in the testing program. The first four sections of this chapter isolate individual parameters that must be considered in the design of a pavement dowel, and the final section of this chapter contains a summary of the design process and an example.

4.2. Theoretical Approach

The analysis method used was developed by Timoshenko. This method is Timoshenko's beam on an elastic foundation analysis

method. This analysis method is described more fully previously in Section 3.4.1.

This research determined the modulus of subgrade reaction, k, through comparisons with experimental data. The modulus of subgrade reaction is a property of the doweled joint system that is dependent upon the diameter of the dowel, the thickness of the concrete, the Young's modulus of the dowel, and the Young's modulus of the concrete. Presently, the k values must be determined experimentally for each unique combination of variables; in the future these values may be more readily available.

The analysis of the dowel can be completed after the k has been determined. After the analysis has been completed, all of the parameters that can affect the design of the dowel can be evaluated.

4.3. Bearing Strength of a Doweled Pavement Joint

The limiting factor in the strength of a pavement joint is usually the bearing capacity of the concrete supporting the pavement dowel. For fibercomposite dowel bars the shear capacity of the dowel or the shear cone capacity may govern in some situations.

The true bearing capacity of the doweled joint system can be determined only if the complex stress distribution existing around the pavement dowel is accounted for in the analysis process. In the case of the pavement dowel, the pressure can best be described as a

three-dimensional, elliptical paraboloid that is defined by orthogonal parabolic lines (see Section 3.5).

A simplification made was to approximate the elliptical paraboloid stress distribution shape with uniform stress distribution. The load being transferred across the joint is evenly distributed over a fairly small rectangular area, called the "equivalent" area (see Section 3.5). After the equivalent area has been determined, the method used to determine the bearing capacity of the system is similar to the method outlined in the ACI Code, Section 10.15 [44].

Table 4.1 shows the equivalent widths, lengths and resulting areas. The confinement factors for the dowel systems tested are also listed in Table 4.1. The equivalent widths and lengths shown were determined in Section 3.5.

Table 4.1. Equivalent widths, lengths, areas and confinement factors for steel and fibercomposite dowel systems

| Dowel System | Equivalent | | Area (in.^{2}) | Confinement Factor |
	Width (in.)	Bear. Length (in.)		
Fibercomposite	1.25	1.60	2.00	1.0
Steel	1.50	1.87	2.81	1.0

4.4. Shear Capacity of the Pavement Dowel

The capacity of the doweled joint system may be controlled by the shear capacity of the dowel itself. Although shear failures will generally not occur in steel dowels, they may occur in fibercomposite dowels.

The approach utilized determines the cross-shear capacity of the bar through the use of the equation:

$$V = t_s A \qquad (4.1)$$

where:

V = Shear force on a cross section (lbs)

t_s = Shear stress (psi)

A = Cross-section area (in.^{2})

When finding the ultimate shear capacity of a round dowel bar, Equation 4.1 reduces to:

$$V_{max} = t_{s\ max}\ \pi D^2/4 \qquad (4.2)$$

where:

V_{max} = Ultimate shear capacity of dowel bar (lbs)

$$t_{s\ max} = \text{Maximum shear stress of dowel bar}$$
$$(psi)$$

For the steel dowel bar, the maximum shear stress that can occur in the bar is 0.577 times the yield strength [13]. For this particular type of steel, the nominal design yield strength is 36,000 psi. This would result in a maximum shear stress of 20,800 psi. For the fibercomposite dowel bar, the maximum shear stress was elaborated on in Section 2.6. As discussed in that section, the maximum shear stress in the fibercomposite bar was determined to be 13,090 psi.

4.5. Moment Resistance of a Pavement Dowel Bar

The capacity of a doweled pavement joint may, in some instances, be controlled by the moment capacity of the dowel bar. The determination of the maximum moment existing in the dowel bar is a complex issue. The simplest way to determine the maximum moment existing in the dowel bar is through two numerical differentiations of the deflection function. The numerical differentiations of the equation for the deflection of the dowel are easily accomplished either with a spreadsheet program or with a computer program. For this research project, a spreadsheet program using a trapezoidal area approximation process was used to carry

out the numerical differentiation process. The function being differentiated was split into over 100 segments.

From the numerical differentiation, the maximum moment occurring in the bar can be determined either through inspection of the spreadsheet results or through the extrapolation of the resulting moment diagram determined with the spreadsheet.

The maximum moment existing in the dowel bar occurs inside the face of the joint. Typically, the distance to the maximum moment from the joint face is approximately one-tenth of the length of the dowel, according to Bradbury [14].

The elastic moment resistance capacity of a dowel bar is determined with the equation:

$$M_{max} = f I_z / c \qquad (4.3)$$

where:

M_{max} = Maximum moment resistance of the dowel (lb·in.)

f = Maximum fiber stress (psi)

c = Distance to extreme fiber from the centroidal axis of the member (in.)

I_z = Moment of inertia of beam about the z-axis (in.^{4})

For the steel dowel bar, the maximum fiber stress is equal to the nominal design yield stress of the steel, which was 36,000 psi. For the fibercomposite dowel bar, the maximum elastic fiber stress for bending given by the manufacturer is 100,000 psi [26].

4.6.   Load-deflection Characteristics of Doweled Pavement Joints

In the design of any structure, the load-deflection characteristics of the resulting design must be considered. This is especially true for pavements where deflections must be minimized so the rideability of the pavement can be kept at the highest level possible. Pavement joints can be problematic if joint deflections are not minimized. Relatively large deflections at pavement joints can significantly reduce the joints' fatigue behavior and increase the pavement's susceptibility to pumping [1]. Relatively large deflections can also cause an oblonging of the concrete surrounding the dowel, which leads to increased deflections of the joint [1]. These undesirable consequences of large deflections emphasize the importance of a design process that includes the calculation of the load-deflection characteristics of the doweled joint system. The magnitude of the maximum allowable deflection of a pavement joint is a relatively subjective parameter, but a typical range for the maximum deflection of the joint may be from 0.02 inches to 0.05 inches when a 9,000 pound load is applied to one side of the joint [1].

The deflection at the face of a doweled joint system can be directly determined using the equation for the deflection, with a predetermined relative stiffness parameter, k. The relative stiffness parameter for determining the deflection of the joint was determined experimentally for the specimens used in the Iowa State testing program. Variance from the stated variables that affects the performance of the doweled joint may significantly affect the relative stiffness parameter, k, of the dowel, and thus the accuracy of the analysis.

In this Iowa State testing program, 8,000 psi concrete was used for both the 1.5-inch steel dowels and the 1.25-inch fibercomposite dowels. For the 1.5-inch steel dowel specimens tested, the average k value was determined to be 3,210,000 psi. For the 1.25-inch fibercomposite dowel specimens, the average k value was determined to be 176,000 psi. These values were determined in Section 3.4.2.

4.7. Example of the Suggested Design Procedure for a Pavement Dowel

The following design problem is an example of how to use the suggested static design procedure for the determination of the expected capacity of a 1.25-inch diameter fibercomposite bar with the following given properties.

GIVEN:

Dowel Properties

1.25-inch diameter fibercomposite dowel bar 18 in. long

Elastic modulus of elasticity of the dowel bar = 6,900,000 psi

Maximum shear stress for dowel bar = 13,000 psi

Maximum fiber stress in bending = 100,000 psi

Strength design load factor = 1.7

ACI strength reduction factor for bearing capacity = 0.70 [44]

PCI strength reduction factor for shear cone capacity = 0.85 [44]

LRFD strength reduction factor for bending = 0.90 [45]

Concrete Properties

Depth of concrete = 10 in.

Strength of concrete = 8,000 psi

Width of joint = 1/8 in.

From numerical differentiation of deflection function

Maximum moment occurring in the bar with a 10,000-pound load being transferred across the joint = 7,120 lb-in. at 1.6 in. from face of joint

Deflection at the face of the joint that occurs with a 10,000-pound load being transferred across the joint = 0.056 in.

Distance from face of joint to the position along the dowel where the load/length is zero = 3.25 in.

Shear deflection = 0.0004 in.

Bearing strength capacity

Equivalent bearing width = 1.25 in. (diameter of dowel)

Equivalent bearing length = (3.25 in.) (2/3) = 2.17 in.

Equivalent bearing area = (1.25 in.)(2.17 in.) = 2.71 in.^{2}

Confinement factor = 1.0

Bearing

concrete strength = (cylinder compressive strength of concrete)(Equivalent bearing area)(Confinement factor)($\emptyset_{ACI}$ factor-strength reduction)

= (8,000 psi)(2.00 in.^{2})(1.0)(0.70)

= 11,200 lbs

Shear

dowel strength = $(\pi/4)(t_{max})(D^2)\emptyset_{ACI}$

= $(\pi/4)(13,000 \text{ psi})(1.25 \text{ in.})^2(0.85)$

= 13,600 lbs

Moment

dowel strength = (fl/c)$\emptyset_{LRFD}$

$$= \frac{(100,000 \ \text{psi})(\pi(1.25)^4(1/64))(0.9)}{(1.25/2)}$$

$$= 17,300 \ \text{lb-in.}$$

Load at which

maximum allowable

moment will occur at $= \dfrac{(17,300 \ \text{lb-in.})(10,000 \ \text{lbs})}{7,120 \ \text{lb-in.}}$

$$= 24,300 \ \text{lbs}$$

Shear cone

capacity strength $= \emptyset_{pci} A_o (2.8 \yen \sqrt{f'_c})$

where:

$\emptyset_{pci} =$ 0.85

$A_o = \sqrt{2}(l_e(2x_{pci} + y_{pci}) + 2l_e^2)$

where:

$x_{pci} =$ Equivalent bearing length

$=$ 1.60 in.

$y_{pci} =$ Equivalent bearing width

$=$ 1.25 in.

$l_e =$ Distance to free edge plane parallel to

the bearing surface plane

$=$ 4.375 in.

$$A_o = \sqrt{2}(4.375 \text{ in. } (2(1.60\text{in.}) + 1.25 \text{ in.}) +$$

$$2(4.295 \text{ in.})^2)$$

$$= 79.71 \text{ in}^2$$

Concrete shear cone

strength $\quad = \quad 0.85(79.71)(2.8(1.0)\sqrt{8,000})$

$\quad = \quad 17,000 \text{ lbs}$

Design strength $\quad = \quad$ minimum of all strengths

$\quad = \quad 11,200 \text{ lbs (based on bearing strength)}$

Maximum service level

load as determined by

strength capacity $\quad = \quad$ strength/load factor

$\quad = \quad 11,200 \text{ lbs}/1.7$

$\quad = \quad 6,600 \text{ lbs}$

Load-deflection characteristics

Suggested maximum allowable deflection at the face joint of the dowel as determined by rideability = 0.04 in. [1]

Maximum allowable deflection of the dowel at the centerline of the specimen = 1/2 total deflection = 0.5(0.04 in.) = 0.02 in.

Shear deflection = 0.0004 in.

Load at which

maximum allowable

deflection would be

expected to occur at: = $\frac{(0.02 \text{ in})(10,000 \text{ lbs})}{0.056 \text{ in}}$

                          =   3,600 lbs

The predicted service level capacity of the joint equals the minimum of the service level load as determined from strength and serviceability standpoints. For this example, the maximum service level load equals 3,600 lbs (limited by load-deflection).

The capacity for this example is controlled by the characteristics of the system. This example did not consider the fatigue behavior of the dowel because this factor is beyond the scope of this research project. However, in the design of an actual dowel, the fatigue behavior must be considered.

Research work is being continued at Iowa State concerning the fatigue behavior of pavement dowels.

5. COMPARISONS AND CONCLUSIONS

In Chapter 3, it was determined that the 1.5-inch steel dowel had an average deflection at the face of the joint of 0.0075-inch at 10,000 pounds; the 1.25-inch fibercomposite dowel had an average deflection of 0.113 inch at 10,000 pounds. The deflection at 4,500 pounds was 0.0034 inch for the steel dowel and 0.0509 inch for the fibercomposite dowel.

The results of the testing program show that both dowel systems had static deflections under 0.13 inch at 4,500 pounds, the maximum deflection recommended according to the FHWA report [1]. Both dowel systems reached relatively high loads as compared to the maximum service load that a dowel could expect--4,500 pounds. The steel dowels had an average maximum load of 18,300 pounds, and the fibercomposite dowels had an average maximum load of 13,900 pounds. This results in factors of safety against failure of 4.1 for the steel dowel and 3.1 for the fibercomposite dowel.

An analysis method was developed for the pavement dowels based on the existing Timoshenko analysis method. The constants required for the analysis methods were determined based on the experimental results. The constants developed are only accurate for the systems tested. Both of the dowel systems used 8,010 psi concrete. One dowel system used 1.5-inch steel dowels with a modulus of elasticity of 29,000,000 psi, and the other system used

1.25-inch fibercomposite dowels with a modulus of elasticity of 6,900,000 psi.

Further testing is strongly recommended for other dowel systems using ranges of concrete strengths, dowel types, and dowel sizes. If further testing is done, the analysis technique may be generalized to include all types of dowel systems. A general analysis procedure can give design engineers an improved understanding of the behavior of the doweled pavement joints. With an improved understanding, better designs can result.

WORKS CITED

★1. Snyder, Mark B., Michael J. Reiter, Kathleen T. Hall, and Michael I. Darter, <u>Rehabilitation of Concrete Pavements, Volume I: Repair Rehabilitation Techniques FHWA-RD-88-071</u>. McLean, VA: Research, Development, and Technology Turner-Fairbank Highway Research Center, 1989.

2. Babaei, Khossrow, and Neil M. Hawkins. <u>Evaluation of Bridge Deck Protective Strategies-NCHRP Report 297</u>. Washington, D.C.: Transportation Research Board, September 1987.

3. Popovics, Sandor, Y. Simeonov, G. Bozhinov, and N. Barovsky. "Durability of Reinforced Concrete in Sea Water." <u>Corrosion of Reinforcement in Concrete Construction.</u> London: Ellis Horwood Limited, 1983.

4. Corbo, Vincent. "Advanced Materials Geared for the 90s." <u>Design News</u> (22 January 1990): 69-70.

5. Brown, Gordon. "Fiber Glass Scores with Designers." <u>Design News</u> (21 November 1988): 258-262.

6. Pittsburgh Paint and Glass. <u>Fiber Glass Reinforced Plastics... By Design.</u> Pittsburgh, PA: PPG Fiber Glass Reinforcements Market Series, 1981.

7. Plecnik, J.M., and S. H. Ahmad, "Transfer of Composite Technology to Design and Construction of Bridges." Interim Report prepared for U.S. Department of Transportation. Raleigh, NC: North Carolina State University, 1985.

8. Bakeri, P.A. "Analysis and Design of Polymer Composite Bridge Decks." Master's Thesis. Massachusetts Institute of Technology, Cambridge, MA, 1989.

9. Long, Bob. Personal Interviews. Ames, Iowa: Composite Technologies Corporation, 1990-1991.

10. Composite Technologies Corporation. Advertising Brochure on Fibresteel. Ames, Iowa: Composite Technologies Corporation, 1990.

11. Morrison Molded Fiber Glass Company. <u>Extren Fiberglass Structural Shapes</u>. Bristol, VA: Morrison Molded Fiber Glass Company.

12. Wade, G.T., M. L. Porter, and D. R. Jacobs. <u>Glass Fiber Composite Connectors for Insulated Concrete Sandwich Walls</u>. Ames, IA: Iowa State University Engineering Research Institute, March 1988.

13. Timoshenko, S. <u>Strength of Materials. Part II: Advanced Theory and Problems</u>. Princeton, NJ: D. Van Nostrand Company, Inc., 1956.   Part 2, ch 1

14. Bradbury, R. D. "Design of Joints in Concrete Pavements." <u>Proc. of the 12th Annual Meeting of the Highway Research Board in Washington D.C.</u> Baltimore, MD: Highway Research Board, 1933: 105-136.

15. Friberg, B.F. "Load and Deflection Characteristics of Dowels in Transverse Joints of Concrete Pavements." <u>Proc., 18th Annual Meeting of the Highway Research Board.</u> Washington, D.C.: Highway Research Board, 1930: 140-144.

16. Westergaard, H.M. "Stresses in Concrete Pavement Computed by Theoretical Analysis." <u>Public Roads</u> 7.2 (1926): 25-35.

17. McWaters, Bryan. Personal Interview. Ames, IA: Iowa Department of Transportation, September 1991.

18. Douglas, D.J., and N.S. Trahair. "An Examination of the Stresses in the Anchorage Zone of a Post-tensioned Prestressed Concrete Beam." <u>Magazine of Concrete Research</u> 12.34 (1990): 9-18.

19. Middendorf, K.H. "Practical Aspects of End Zone Bearing of Post-Tensioning Tendons." <u>PCI Journal</u> (August 1963): 57-62.

20. Cowan, Henry J. "The Strength of Plain, Reinforced and Prestressed Concrete Under the Action of Combined Stresses, With Particular Reference to the Combined Bending and Torsion of Rectangular Sections." Magazine of Concrete Research (December 1953): 75-86.

21. Au, Tung, and Donald L. Baird. "Bearing Capacity of Concrete Blocks." Journal of the American Concrete Institute (March 1960): 869-880.

22. Meyerhof, G.G. "The Bearing Capacity of Concrete and Rock." Magazine of Concrete Research (London) 4.11 (1953): 107-116.

23. Shelson, William. "Bearing Capacity of Concrete." ACI Journal 29.5, (1957): 405-413.

24. Prestressed Concrete Institute. PCI Design Handbook 3rd edition. Chicago, IL: Prestressed Concrete Institute, 1985.

25. Beyond 2000. Discovery Channel (television). February 1, 1991.

26. Marshall Vega Corporation. Brochure on Fiberglass Reinforcement Bar. Harrison, AR: Marshall Vega Corporation. 1989.

27. Tsai, Stephen W., and Edward M. Wu. "A General Theory of Strength for Anisotropic Materials." Journal of Composite Materials. 5.1 (1971): 58-80.

28. Barnes, Bruce A. "Bond and Low Cycle Fatigue Behavior of Thermoset Composite Reinforcing for the Concrete Industry." Master's Thesis. Iowa State University, Ames, Iowa, 1990.

29. Whitney, J.M., and C.E. Browning. "On Short-Beam Shear Tests for Composite Materials." Experimental Mechanics (September 1985): 294-300.

30. American Society for Testing and Materials. Annual Book of ASTM Standards. Philadelphia, PA: ASTM, 1984.

31. Adams, Donald F., and Rodney L. Thomas. "The Solid-Rod Torsion Test for the Determination of Unidirectional Composite Shear Properties." Textile Research Journal (April 1969): 339-345.

32. Walrath, D.E., and D.F. Adams. "The Iosipescu Shear Test as Applied to Composite Materials." Experimental Mechanics (March 1983): 105-110.

33. Hurwitz, Frances I., and Donald R. Behrendt. "Application of Iosipescu Specimen Geometry to Determination of Shear Strength in Unidirectional Composites." 16th National SAMPE Technical Conference. Hi-tech Review. Covina, CA: Society for the Advancement of Material and Process Engineering, 1984: 609-618.

34. Adams, Donald F., and David E. Walrath. "In-Plane and Interlaminar Iosipescu Shear Properties of Various Graphite Fabric/Epoxy Laminates." Journal of Composites Technology & Research 9.3 (1987): 88-94.

35. Rosen, B. Walter. "A Simple Procedure for Experimental Determination of the Longitudinal Shear Modulus of Unidirectional Composites." Journal of Composite Materials 6.10 (1972): 552-554.

36. Lenoe, Edward M. "Testing and Design of Advanced Composite Materials." Journal of the Engineering Mechanics Division of the American Society of Civil Engineers Annual Meeting and National Meeting on Structural Engineering Proceedings (Pittsburgh, PA). New York, NY: American Society of Civil Engineers, 1970: 809-823

37. American Concrete Institute Subcommittee III, ACI Committee 325. "Structural Design Considerations for Pavement Joints." Journal of the American Concrete Institute. (July 1956): 1-26.

38. Portland Cement Association. "Joint Design for Concrete Pavements." Brochure. Skokie, IL: Portland Cement Association, 1961.

39. Teller, Leslie W., and Harry D. Cashell. "Performance of Doweled Joints Under Repetitive Loading." Public Roads 30.1 (1958): 1-15.

40. Young, Warren C. Roark's Formulas for Stress & Strain. Sixth Edition. New York, NY: McGraw-Hill Book Company, 1989.

41. Porter, Max L., Eric A. Lorenz, Bruce A. Barnes, and Kasi P. Viswanath. "Thermoset Composite Concrete Reinforcement. Part 2." Final Report prepared for the Iowa Department of Transportation and Iowa Highway Research Board. Ames, Iowa: Engineering Research Institute, Iowa State University, October 1992.

42. Porter, Max L., Eric A. Lorenz, Kasi P. Viswanath, Bruce A. Barnes, and Michael D. Albertson. "Thermoset Composite Concrete Reinforcement. Part 1." Final Report prepared for the Iowa Department of Transportation and Iowa Highway Research Board. Ames, Iowa: Engineering Research Institute, Iowa State University, May 1992.

43. Swokowski, Earl W. Calculus with Analytic Geometry. Alternate Edition. Boston, MA: Prindle, Weber, & Schmidt, 1983.

44. American Concrete Institute. American Concrete Institute Building Code Requirements for Reinforced Concrete (ACI 318-89) and Commentary - ACI 318R-89. Detroit, MI: American Concrete Institute, 1989.

45. American Institute of Steel Construction. Load and Resistance Factor Design Specification for Structural Steel Buildings. Chicago, IL: American Institute of Steel Construction, September1986.

ACKNOWLEDGEMENTS

APPENDIX
LOAD VERSUS DEFLECTION CURVES FOR THE
INDIVIDUAL SPECIMENS

The graphs on the following pages are the load versus deflection curves for the individual specimens. The first five graphs are for the fibercomposite dowel specimens, and the final five graphs are for the steel dowel specimens.
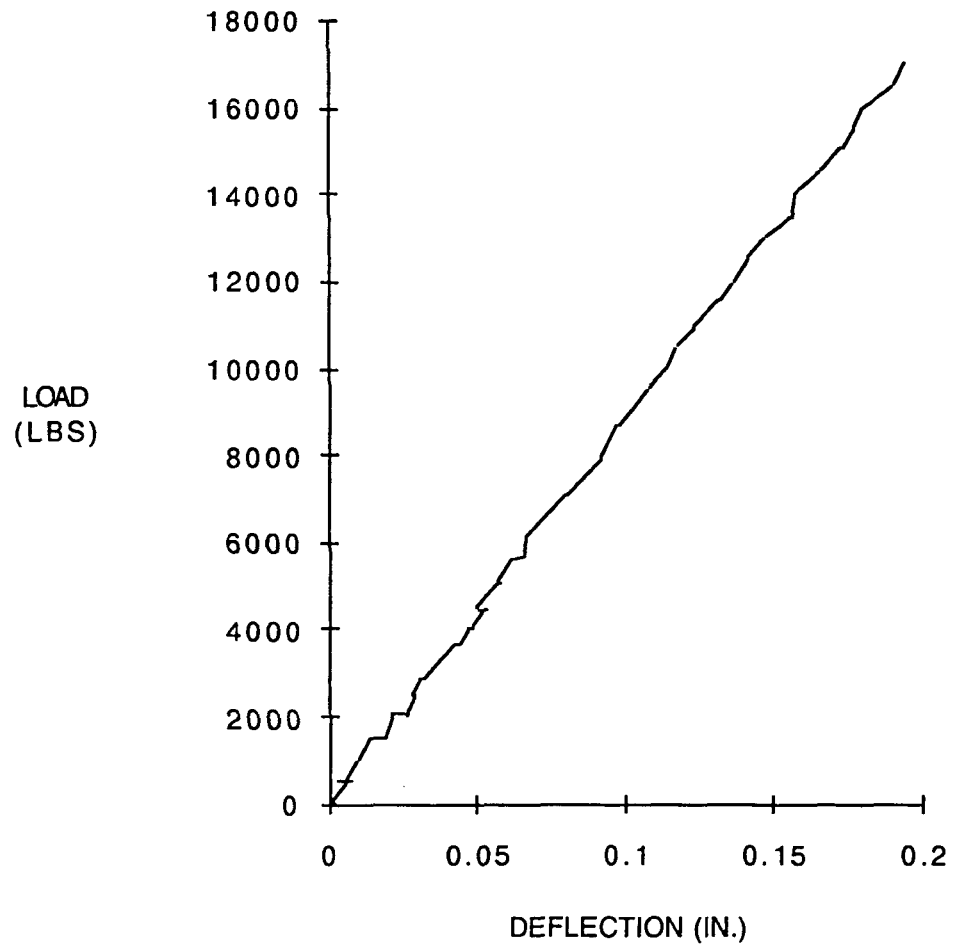
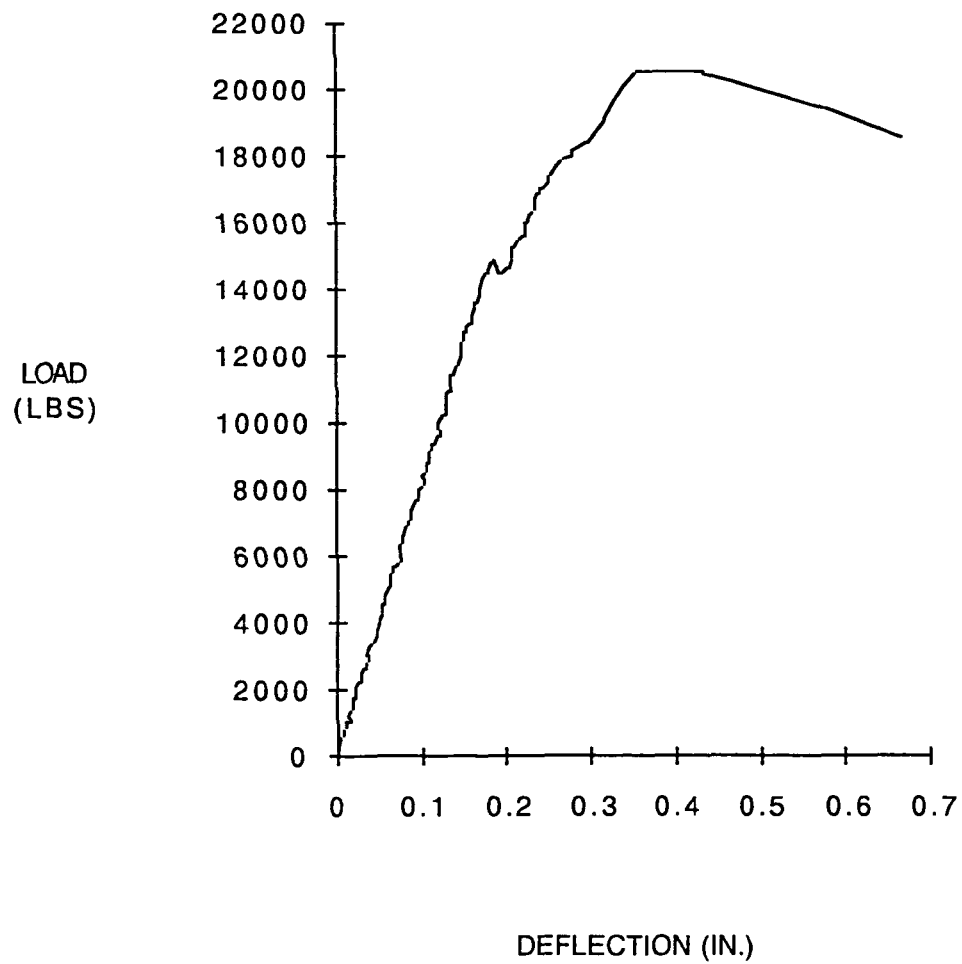Figure A.1. Load versus deflection for fibercomposite Specimen 1

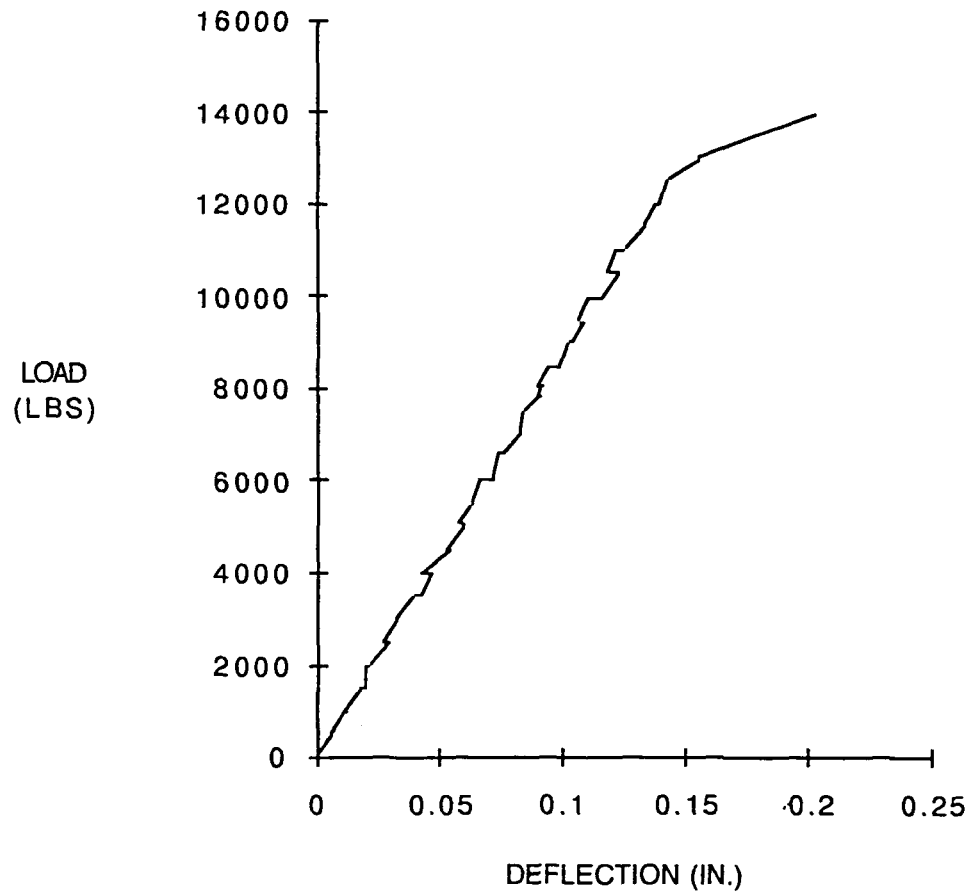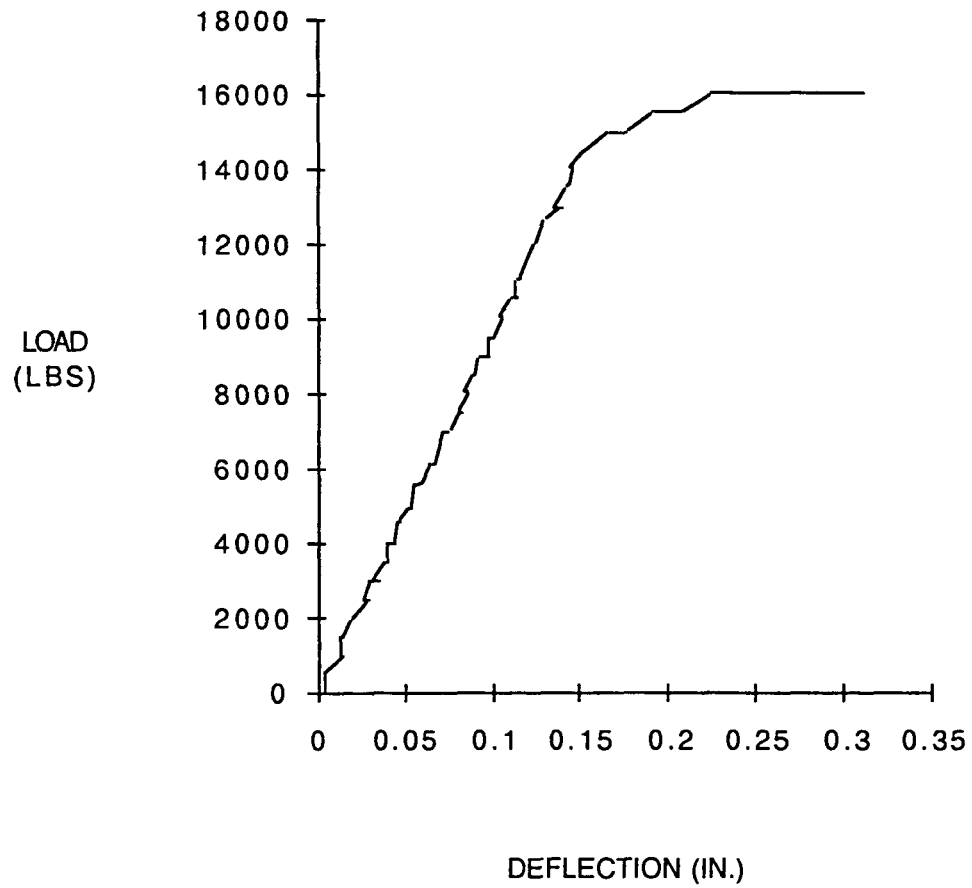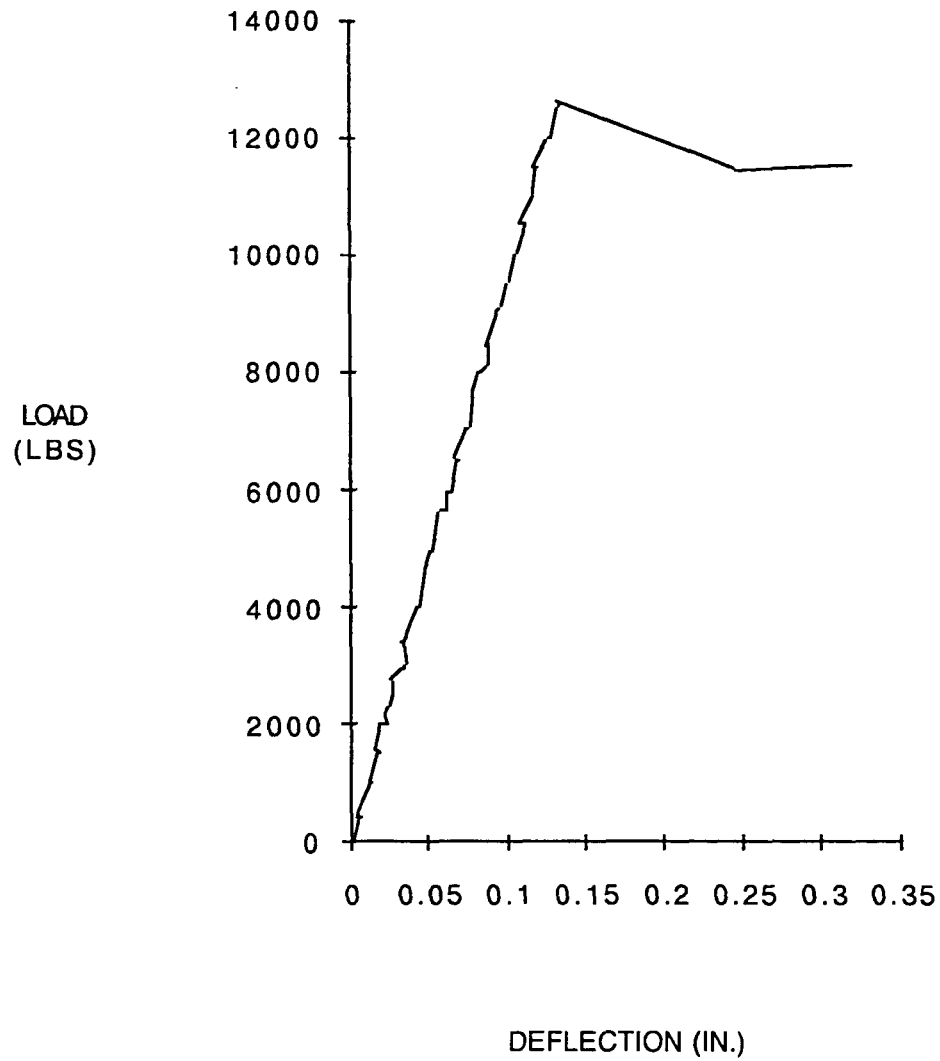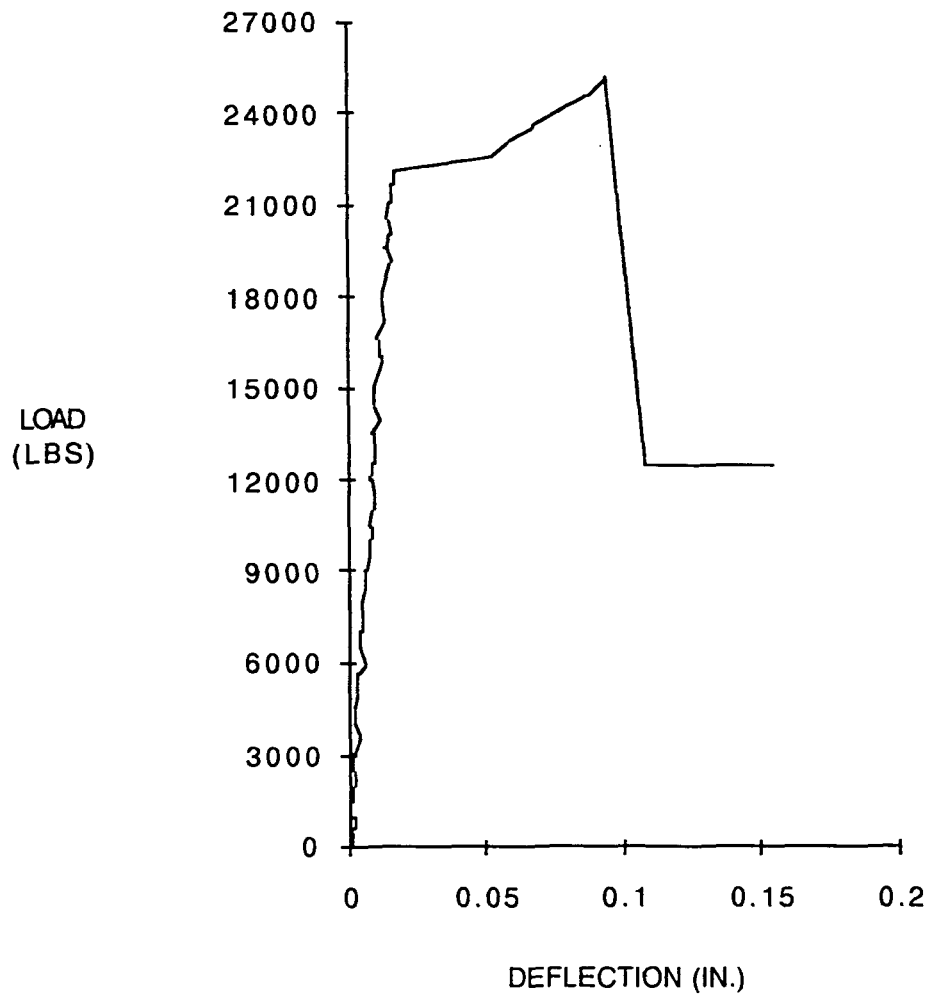Figure A.2. Load versus deflection for fibercomposite Specimen 2

Figure A.3. Load versus deflection for fibercomposite Specimen 3

Figure A.4. Load versus deflection for fibercomposite Specimen 4

Figure A.5.   Load versus deflection for fibercomposite Specimen 5

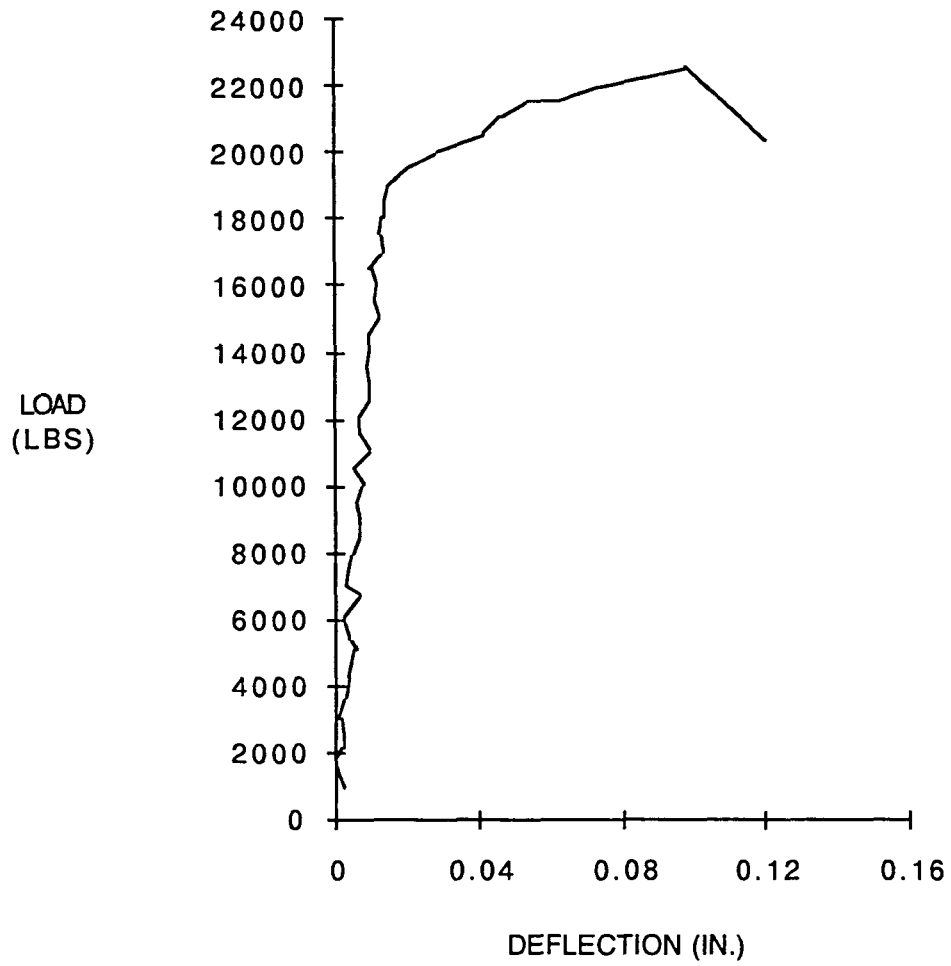Figure A.6. Load versus deflection for steel Specimen 1

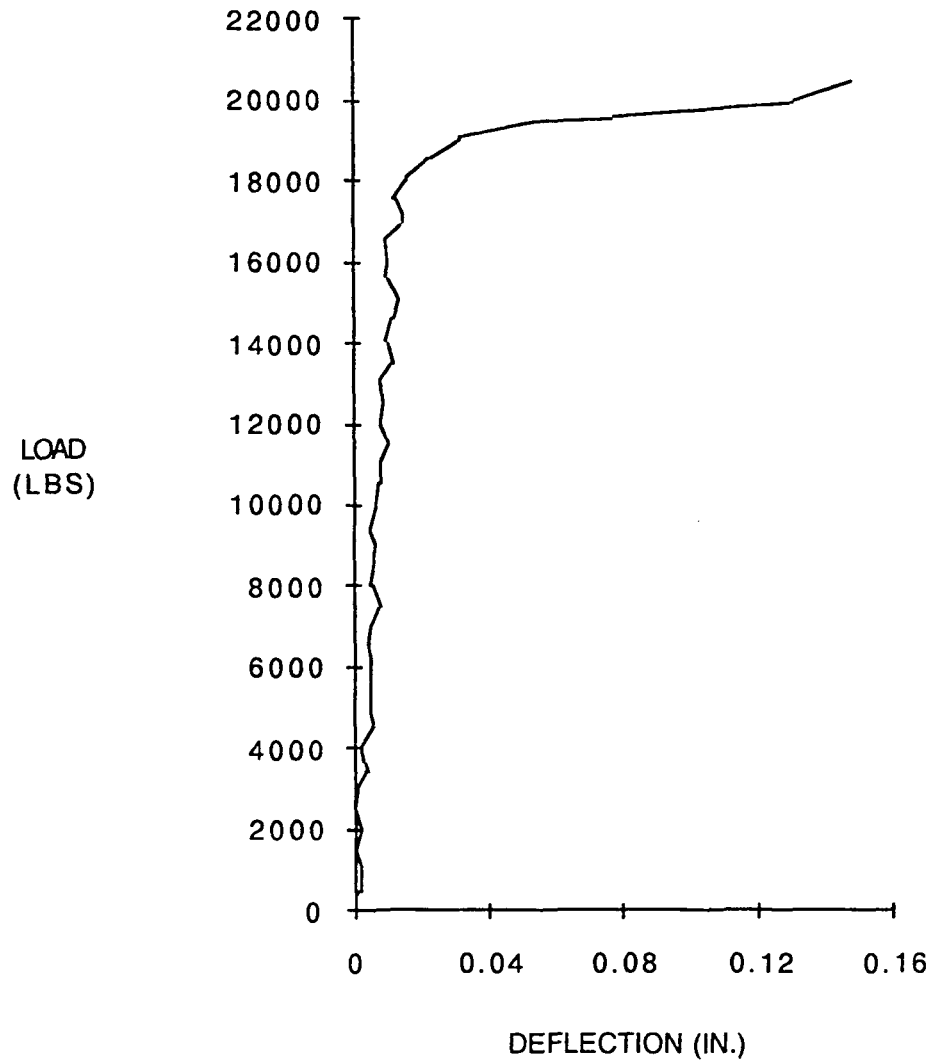Figure A.7. Load versus deflection for steel Specimen 2

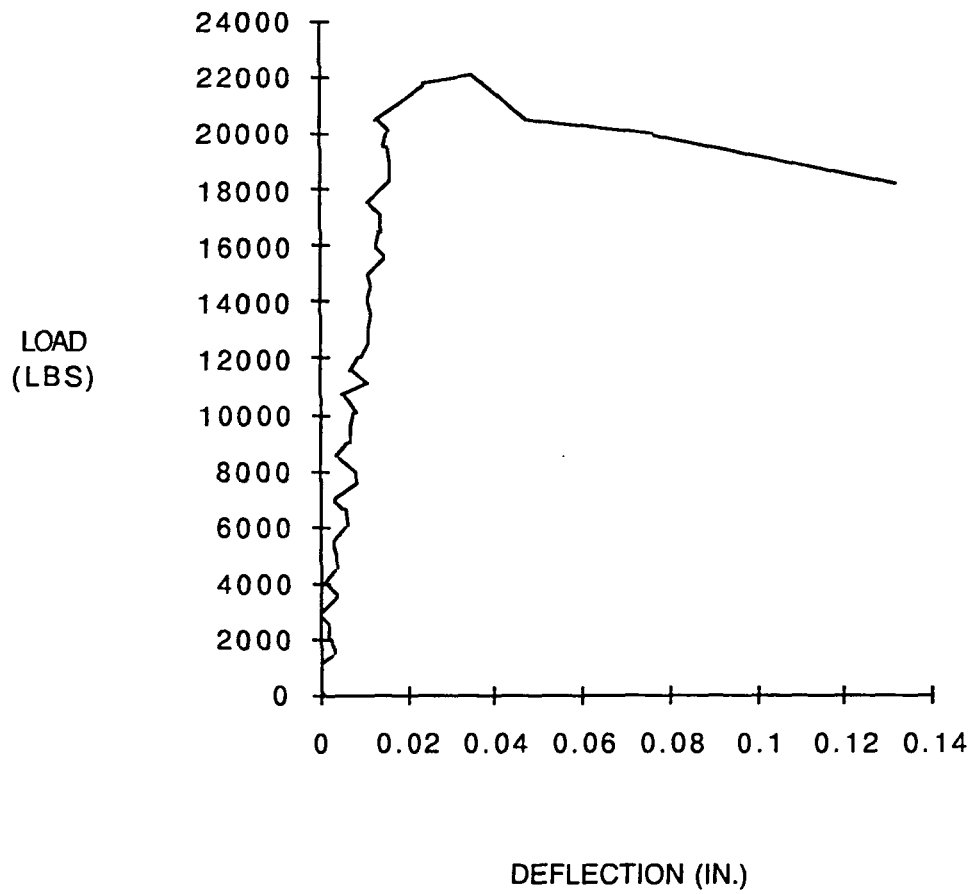Figure A.8. Load versus deflection for steel Specimen 3
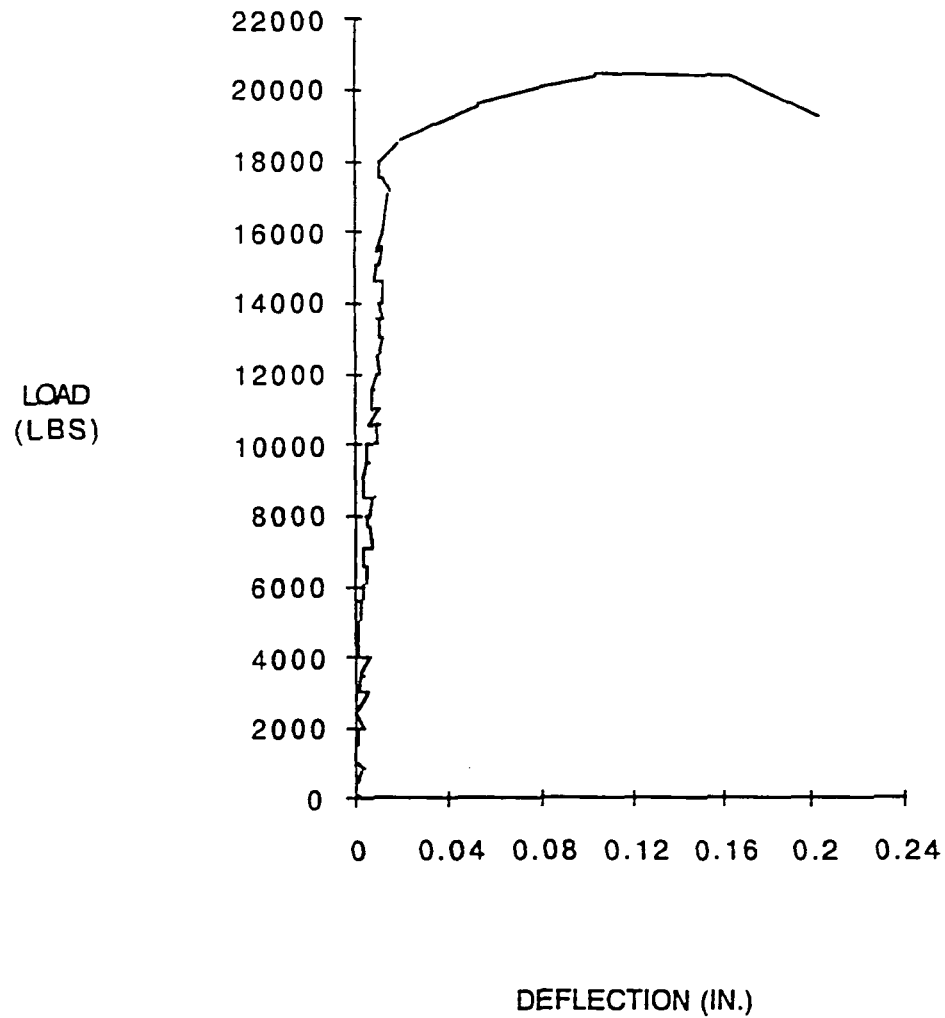
Figure A.9. Load versus deflection for steel Specimen 4

Figure A.10. Load versus deflection for steel Specimen 5